Supporting Information

Mechanistic analysis of the biosynthesis of the aspartimidylated graspetide amycolimiditide

Brian Choi[†], Hader E. Elashal[†], Li Cao[†], A. James Link[†,‡,§,*]

[†]Department of Chemical and Biological Engineering, Princeton University, Princeton, NJ 08544, United States
[‡]Department of Chemistry, Princeton University, Princeton, NJ 08544, United States
[§]Department of Molecular Biology, Princeton University, Princeton, NJ 08544, United States
*Corresponding Author: ajlink@princeton.edu

Table of Contents

Supplementary Materials and Methods

Comparative sequence analysis of AmdA homologs

BLASTP was performed on AmdA (WP_141997876.1) in January 2022, using the Non-redundant protein sequences (nr) database (National Center for Biotechnology Information, NCBI). Of the resulting 33 hits, 3 AmdA homologs from *Salinispora cortesiana* (WP_025618767.1), *Cryptosporangium phraense* (WP_142707138.1), and *Cryptosporangium arvum* (WP_035858693.1) were removed as outliers after manual inspection of their amino acid sequences. Using the resulting list of 30 sequences, WebLogo was used to generate the sequence logos for sites aligning with residues 2-10 and 21-29 of the AmdA core peptide.[1]

Plasmid Construction

General Methodology

Plasmids were constructed by using Golden Gate Assembly on DNA fragments or ligating them after restriction digestion. DNA fragments to be assembled were prepared by PCR, oligonucleotide annealing, or digesting a plasmid with restriction enzymes. After the assembly, *E. coli* transformation was performed for selection and propagation. Plasmids were prepared with Qiaprep Spin Miniprep Kit (Qiagen), and the insert sequences were confirmed by Sanger sequencing (Azenta/Genewiz). All oligonucleotides used and plasmids generated in this study are listed in **Table S2 and S3**, respectively. **Table S4** specifies the construction methodology of all plasmids generated in this study.

Strains and Reagents

The genomic DNA of *Amycolatopsis cihanbeyliensis* (DSM 45679) was obtained from the German Collection of Microorganisms and Cell Cultures (DSMZ). PCR amplification was performed with dNTP and Q5 High Fidelity DNA polymerase purchased from New England Biolabs (NEB), and oligonucleotide primers from Integrated DNA Technologies (IDT). Oligonucleotide annealing was performed with T4 polynucleotide kinase (T4 PNK) purchased from NEB. Golden gate assembly, restriction digestion, and ligation were performed with restriction enzymes and T4 DNA ligase purchased from NEB. Chemically competent *Escherichia coli* XL1-Blue (Stratagene) was prepared with *Mix & Go E. coli* Transformation Kit and Buffer Set (Zymo Research). For *E. coli* growth, sterile lysogeny broth (LB) medium (5 g L^{-1} yeast extract, 10 g L^{-1} tryptone, 10 g L^{-1} sodium chloride) containing 100 µg mL^{-1} ampicillin (Amp) or 50 µg mL^{-1} kanamycin (Kan) was used. For growth on solid LB medium, 15 g L^{-1} agar was added.

Oligonucleotide Annealing

10 μM of each oligonucleotide was treated with T4 PNK in 1X T4 DNA Ligase Buffer (NEB) for 1 hour at 37 °C. Then, the phosphorylated oligonucleotides were combined and diluted 20-fold in ultrapure water. The diluted oligonucleotide mixture was then heated to 96 °C for 6 minutes and slowly cooled down to 23 °C at a rate of -0.1 °C s^{-1}.

Golden Gate Assembly (GGA)

DNA fragments to be assembled were mixed with T4 DNA Ligase and *Bsa*I-HFv2. Thermal cycling was performed according to the manufacturer's protocol with the following modifications. The first 37 °C step was done for 1 minute, the second 16 °C step was done for 30 seconds, the first and second steps were cycled 25 times in total, and an additional 85 °C step was done at the end for 5 minutes.

Construction of the Plasmid for Expressing *amdABM*

The amycolimiditide biosynthetic gene cluster *amdABM* was PCR-amplified from *A. cihanbeyliensis* genomic DNA with oBC026 and oBC031. The backbone of pQE-80 was purified after restriction digestion with *Bam*HI and *Hin*dIII. The PCR product and the pQE-80 backbone were assembled by Golden Gate Assembly, creating the plasmid pBC011.

Construction of the Golden Gate Assembly-Enabled pQE-80-Based Vectors

For more efficient and convenient plasmid construction, we decided to generate a pQE-80-like cloning vector designed to accommodate green fluorescence screening and Golden Gate Assembly. First, we constructed pBC022, in which the *Bsa*I recognition site in AmpR is ablated with a silence mutation and the multicloning site (MCS) of pQE-80L is replaced with the GFP constitutive expression cassette flanked by *Bsa*I recognition sites that generate *Bam*HI and *Hin*dIII sticky ends upon digestion. The GFP constitutive expression cassette contains the coding sequence of sfGFP (avGFP S30R Y39N F64L S65T Q80R F99S N105T Y145F M153T V163A I171V A206V) under the control of PglpT promoter (Part: jtk2821; BBa_J72163 from iGEM Registry of Standard Biological Parts). Then, we constructed pBC043, in which the arginine residue of the His_6-tag was mutated to serine to suppress the background methylation of the N-terminus in *E. coli*.[2] Then, we constructed pBC108, in which the sfGFP was replaced with ffGFP (avGFP S2R S30R Y39N F64L S65T S72A F99S N105T Y145F M153T V163A I171V A206V), which is visibly more fluorescent than sfGFP. Similarly, we constructed pBC052 and pBC133 as entry vectors for *amdABM* and *amdAB* expression, respectively, for *amdA* mutants. In these constructs, the AmdA CDS was replaced with the PglpT-ffGFP constitutive expression cassettes flanked by *Bsa*I recognition sites, with SUMO-AmdB and AmdM coding sequences placed downstream of the second *Bsa*I site.

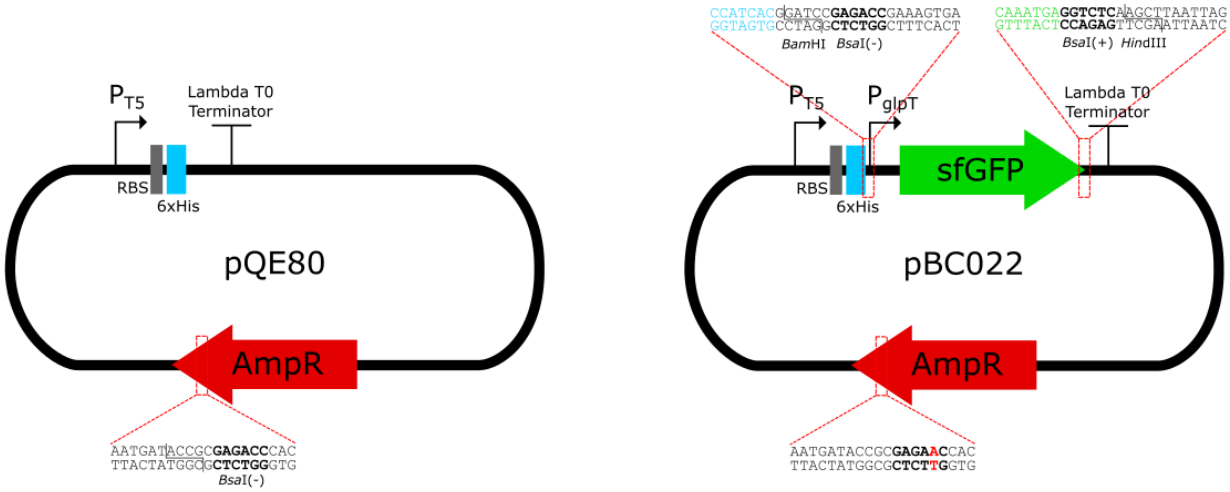

Here, we describe the construction methodology of pBC022. The construction methodology of pBC043, pBC052, pBC108, and pBC133 are outlined in **Table S4**. The PglpT promoter fragment was obtained by overlap-amplifying the primers oBC047, oBC055, oBC056, and oBC057. The superfolder-GFP (sfGFP) fragment was amplified from pWC108 with oBC058 and oBC050. PglpT and sfGFP fragments were overlapped and PCR-amplified with oBC047 and oBC050. The resulting amplicon (*Bam*HI-PglpT-sfGFP-*Hin*dIII) was digested with *Bam*HI and *Hin*dIII. The primer pairs oBC043/oBC044 and oBC045/oBC046 were used to PCR-amplify a part of pQE-80 backbone with AmpR G239G. The two amplicons were then overlapped and PCR-amplified with oBC043 and oBC046. The resulting amplicon (*Nde*I-pQE-80-AmpR_G239G-*Bam*HI) was digested with *Nde*I and *Bam*HI. The rest of the pQE-80 backbone was obtained by restriction digestion with *Nde*I and *Hin*dIII (*Hin*dIII-pQE-80-*Nde*I). The purified fragments *Nde*I-pQE-80-AmpR_G239G-*Bam*HI, *Bam*HI-PglpT-sfGFP-*Hin*dIII, and *Hin*dIII-pQE-80-*Nde*I were ligated together.

Gene Expression in *E. coli*

E. coli BL21 (DE3) Δ*slyD* was electroporated with a plasmid containing the gene(s) to be expressed. The transformants were grown overnight at 37 °C on the solid LB agar medium containing Amp/Kan. A single colony was grown overnight at 37 °C in the liquid LB+Amp/Kan medium with shaking at 250 rpm. Then, the starter culture was added to a larger liquid LB+Amp/Kan medium so that OD_{600} = 0.02. The cells were grown at 37 °C with 250 rpm shaking until OD_{600} = 0.5, and expression was induced by adding IPTG to 1 mM concentration. Afterwards, the culture was transferred to a benchtop shaker and continued to grow at room temperature (20-22 °C) with 250 rpm shaking for 20 hours. For the co-expression AmdA or its variant with SUMO-AmdB and AmdM, the cells were grown for 24 hours after the IPTG induction.

Protein Native Purification

The culture grown for SUMO-AmdB or AmdM purification was centrifuged at 4,000 x g for 15 min. Per 500 mL culture, the cell pellet was resuspended in 10 mL 50 mM NaH_2PO_4, 300 mM NaCl, 10 mM imidazole, pH 8.0. 1 mg/mL lysozyme was added to the resuspended cells, followed by incubation while rotating at 4 °C for 20 min. The cells were lysed by sonication on ice for 12 cycles (10 s on, 20 s off). The lysate was centrifuged at 12,000 x g for at least 30 minutes. The clarified lysate was mixed with 1 mL Ni-NTA resin (Qiagen) and incubated while rotating at 4 °C for 1 hour. The mixture was passed through an empty gravity column, followed by the first wash with 10 mL 50 mM NaH_2PO_4, 300 mM NaCl, 20 mM imidazole, pH 8.0, the second wash with 10 mL 50 mM NaH_2PO_4, 300 mM NaCl, 35 mM imidazole, pH 8.0, and the third wash with 10 mL 50 mM NaH_2PO_4, 300 mM NaCl, 50 mM imidazole, pH 8.0. Then, the protein was eluted with a total of 8 mL 50 mM NaH_2PO_4, 300 mM NaCl, 250 mM imidazole, pH 8.0, collecting 1 mL fraction at a time. After analyzing the fractions with SDS-PAGE, the clean elution fractions were pooled, buffer exchanged into 1X PBS, pH 7.4 containing 10% glycerol, and concentrated using a 30 kDa Amicon concentrator. The purified proteins were stored at -80 °C.

Protein Denaturing Purification

The culture grown for purifying AmdA or its variants was centrifuged at 4,000 x g for 15 min. Per 500 mL culture, the cell pellet was resuspended in 10 mL 100 mM NaH_2PO_4, 10 mM Tris, 8 M urea, pH 8.0. After freezing at -80 °C and thawing at room temperature in water bath, the cell lysate was centrifuged at 12,000 x g for at least 30 minutes. The clarified lysate was mixed with 1 mL Ni-NTA resin (Qiagen) and incubated while rotating at 4 °C for 1 hour. The mixture was passed through an empty gravity column, followed by the first wash with 10 mL 100 mM NaH_2PO_4, 10 mM Tris, 8 M urea, pH 6.3, and the second wash with 10 mL 100 mM NaH_2PO_4, 10 mM Tris, 8 M urea, pH 5.9. Then, the protein was eluted with a total of 8 mL 100 mM NaH_2PO_4, 10 mM Tris, 8 M urea, pH 4.5, collecting 1 mL fraction at a time. After analyzing the fractions with SDS-PAGE, the clean elution fractions were pooled, buffer exchanged into 1X PBS, pH 7.4, and concentrated using a 10 kDa Amicon concentrator. The purified proteins were stored at -80 °C.

Trypsin Digestion

AmdA or its variant was digested with trypsin to cleave the leader peptide. The purified protein was mixed with sequence grade trypsin (Promega) at a 100:1 w/w protein:trypsin ratio in 50 mM NH_4HCO_3. For the preparation of the amycolimiditide NMR sample, 500:1 w/w protein:trypsin ratio was used. For proteins expected to contain an aspartimide, the NH_4HCO_3 buffer was acidified to pH 7 with HCl prior to mixing with the protein and trypsin. The digestion was done at 37 °C for 30 min and then quenched by adding 1% formic acid.

Peptide purification by HPLC

Semi-preparative reverse-phase HPLC was performed on trypsin-digested AmdA or AmdA variant to purify its putative core peptide. An Agilent 1200 series instrument equipped with a Zorbax 300SB-C18 (9.4 mm x 250 mm, 5 µm) column and a 215 nm UV detector was used. The elution gradient with a mixture of water and acetonitrile with 0.1% trifluoroacetic acid flowing at a rate of 4 mL/min was used. The following linear gradients were used: 10% acetonitrile for 1 min, 10-75% acetonitrile over 19 min, 75-90% acetonitrile over 5 min, 90% acetonitrile for 5 min, and 90-10% acetonitrile over 2 min. The peak corresponding to the desired peptide was collected, frozen at -80 °C, lyophilized (Labconco FreeZone Freeze Dry System), and resuspended in ultrapure water for subsequent studies.

Mass spectrometry

All protein and peptide mass spectra were acquired using electrospray ionization (ESI) on an Agilent 6530 QTOF equipped with an Agilent 1260 LC system. Peptides from digested proteins or purified from HPLC were chromatographed on a Zorbax 300SB-C18 (2.1 mm x 50 mm, 3.5 µm particle size), and intact proteins were chromatographed on an XBridge Protein BEH C4 (Waters, 2.1 mm x 50 mm, 3.5 µm particle size). The elution gradient with a mixture of water and acetonitrile with 0.1% formic acid flowing at a rate of 0.5 mL/min was used. For peptides, the following linear gradients were used: 5% acetonitrile for 1 min, 5-45% acetonitrile over 20 min, 45-90% acetonitrile over 5 min, and 90% acetonitrile for 5 min. For intact proteins, the following linear gradients were used: 10% acetonitrile for 1 min, 10-50% acetonitrile over 20 min, 50-90% acetonitrile over 5 min, and 90% acetonitrile for 5 min. The instrument was calibrated using “Mass Calibration/Check” daily. Data were analyzed using MassHunter (Agilent). For MS/MS, the instrument was calibrated using “Standard Tune” prior to mass spectra acquisition. Data were analyzed using MassHunter and mMass.

Amycolimiditide NMR

amdABM (pBC105) was expressed in *E. coli* BL21 (DE3) Δ*slyD* using 16 L of LB+Amp medium. mAmdA^{BM} was purified in denaturing conditions and digested with trypsin as described above. Amycolimiditide was purified from the trypsinized mAmdA^{BM} by HPLC. 3.8 mM amycolimiditide was prepared in 95/5 H_2O/D_2O. 2D NMR spectra (TOCSY, NOESY, ^{1}H-^{13}C HSQC, ^{1}H-^{13}C HMBC) of amycolimiditide were collected on a Bruker Avance III 800 MHz spectrometer at 293 K. The mixing time for the TOCSY was 80 ms while two NOESY spectra were acquired with 150 ms and 700 ms mixing times. HMBC was acquired targeting 10 Hz proton-carbon coupling. The acquired spectra were processed and analyzed using MestReNova. Proton and carbon resonances were assigned to the structure manually (**Table S6**). The NOESY spectrum acquired with 150 ms mixing time was used to determine through space distance restraints, which was used to build the amycolimiditide structural model in CYANA 2.1. Additional geometric restraints corresponding to the ω-esters and the aspartimide were added to CYANA 2.1.

The top 20 structures were energy-minimized using Avogadro's MMFF94 forcefield. The coordinates for amycolimiditide have been deposited in PDB (8DYM) and BMRB (31036).

Circular Dichroism (CD)

CD was performed on the following three samples: The unmodified AmdA core peptide, pre-amycolimiditide, and amycolimiditide. For the unmodified AmdA core peptide, the unmodified AmdA protein was purified under denaturing conditions after expressing *amdA* from pBC054. The purified protein was trypsinized, and the resulting C-terminal 29-aa fragment was purified by HPLC. Pre-amycolimiditide was prepared similarly after expressing *amdAB* from pBC045, and amycolimiditide was prepared similarly after expressing *amdABM* from pBC051. After freeze-drying, all three peptides were individually reconstituted in ultrapure water at 0.1 mg/ml concentration, as determined by A_{280} measurements. The Applied Photophysics Chirascan instrument was used to collect the CD spectra of the three peptide samples, scanning from 180-280 nm in a 1 mm pathlength cuvette (Hellma Analytics).

Hydrazinolysis

4 M hydrazine was prepared in 1X PBS buffer at pH 5.0. Per 25 µL of this hydrazine solution, 1 µL of 6 M HCl was added to bring the pH to about 7-8. This solution was mixed with a sample of HPLC-purified peptide in a 1:1 volumetric ratio. The mixture was incubated at 55 °C for 45 min and immediately subjected to mass spectrometry.

***In vitro* reconstitution of enzymatic reactions**

For the *in vitro* ω-ester crosslinking with the ATP-grasp enzyme, the reaction mixture contained the following: 10 µM His_6-AmdA (or variant), 1 µM His_6-SUMO-AmdB, 10 mM ATP (Sigma-Aldrich, A2383), and 10 mM $MgCl_2$ in 1X PBS, pH 7.4. Prior to adding ATP to the reaction mixture, 100 mM ATP solution was prepared in water and brought to pH 7, as indicated by a Fisherbrand pH indicator strip, with NaOH. For the *in vitro* aspartimidylation with the *O*-methyltransferase, the reaction mixture contained the following: 10 µM substrate (His_6-mAmdA^B, pre-amycolimiditide, iso pre-amycolimiditide, or a variant), 1 µM His_6-AmdM, and 400 µM SAM in 1X PBS, pH 7.4. For any reaction with AmdA variants containing a disulfide bond, 10 mM DTT was added to the reaction mixture if the reduction of the disulfide bond was desired. All reactions were performed at room temperature. For time course studies, a fraction of the reaction mixture was mixed with 1% formic acid to quench the reaction. The reactions were analyzed by mass spectrometry. For the time course *in vitro* aspartimidylation reactions, EICs for the pre-aspartimidylated, methylated, and aspartimidylated states were obtained, and the peaks-of-interest were integrated. The percentage of each species was calculated as the ratio of the peak area of the species-of-interest to the sum of all three peak areas.

Then, the ratio was multiplied by the concentration of the pre-aspartimidylated species at t = 0 (10 μM) to obtained the concentration of each species at a given time.

Supplementary Information on Refactoring Amycolimiditide Biosynthetic Gene Cluster (BGC)

Initially, we expressed *amdA*, *amdAB*, and *amdABM* from the pQE-80L vector, placing the AmdA coding sequence downstream of the His_6-tag, MRGSHHHHHHGS, and using the native coding sequences of AmdB and AmdM. The *amdA* expression resulted in the purified AmdA protein with two masses, 13,712 Da and 13,726 Da, corresponding to the unmodified AmdA and one-fold methylated AmdA, respectively (Fig. S3A). Expressing *amdAB* resulted in the purified $mAmdA^B$ protein with several masses, seemingly corresponding to AmdA with 0-4-fold dehydrations and 0-1-fold methylation (Fig. S3B). Similarly, expressing *amdABM* resulted in the purified $mAmdA^{BM}$ protein with mass profiles corresponding to AmdA with 0-5-fold dehydrations and 0-1-fold methylation (Fig. S3C). For $mAmdA^B$ and $mAmdA^{BM}$, the masses of the intermediates deviate slightly from the expected masses of 1-3-fold and 1-4-fold dehydrated AmdA, respectively, probably due to the presence of the methylated species that further complicate the mass distributions of AmdA species. For example, the third rightmost mass peak (13,691 Da) for $mAmdA^B$ from *amdAB* expression from pQE-80L (Fig. S3B) is probably averaged by the 1-fold dehydrated AmdA and the 2-fold dehydrated and methylated AmdA.

The significant amounts of intermediates resulting from *amdAB* and *amdABM* expressions suggest that AmdB cannot efficiently modify AmdA to completion, leading us to suspect that His_6-AmdB is unstable *in cellulo*. We natively purified His_6-AmdB, and the protein precipitated within a few hours during storage at 4 °C. We circumvented this problem by immediately buffer-exchanging the eluted protein in 1X PBS, pH 7.4 with 10% glycerol. The protein was not precipitated by the time it transferred to the -80 °C freezer for storage. However, upon thawing for usage in the *in vitro* AmdA modification experiments, AmdB precipitated out. As such, it seems that His_6-AmdB is especially prone to aggregation *in vitro*, and this behavior may carry over *in vivo*. Following this observation, we predicted that improving the solubility/stability of AmdB would enhance the efficiency of AmdB activity in *E. coli*. To do so, we fused AmdB with an N-terminal SUMO-tag, which is known to enhance the solubility of the fused protein.[3] Indeed, expressing *amdAB* and *amdABM* with SUMO-AmdB resulted in significant improvements in the conversion to 4-fold dehydrated $mAmdA^B$ and 5-fold dehydrated $mAmdA^{BM}$, as indicated by the absence of intermediate peaks (Fig. S3D, E). However, most products remained methylated.

Even with the significant improvement in the AmdB activity, the methylation still complicates our analysis of the mass spectrometry data. For example, the 13,635 Da peak from AmdA co-expression with SUMO-AmdB and AmdM (Fig. S3E) is likely to be an average of 5-fold dehydrated and methylated AmdA and 4-fold dehydrated AmdA,

and it is difficult to distinguish between those two species by mass spectrometry. Therefore, we sought to eliminate the methylation on AmdA to improve the interpretability of the mass spectrometry data. According to the literature, a group of proteins containing IF-3, L33, L11, and rMalarial antigen with Lys or Arg as the second residue become methylated, and arginine as the second residue of a protein is known to block the N-terminal methionine excision activity of methionine aminopeptidase (MAP). [2, 4] Our observations with the original AmdA constructs are consistent with these findings from the literature: The second residue of the N-terminal His_6-tag for AmdA is arginine, and the N-terminal methionine is not cleaved. Suspecting the N-terminus of AmdA is methylated, we substituted the second residue of the N-terminal His_6-tag into Ser. In the new AmdA constructs with the modified His_6-tag, the N-terminal methionine was excised, and no methylation was observed (refer to Fig. 2A in the main text).

For the final *amdABM* expression construct, we changed the start codon of *amdM* into atg (originally gtg). While 20 hours of *amdAB* expression was sufficient for complete conversion to $mAmdA^{B}$, 24 hours of *amdABM* expression was required for complete conversion to $mAmdA^{BM}$.

Supplementary Figures

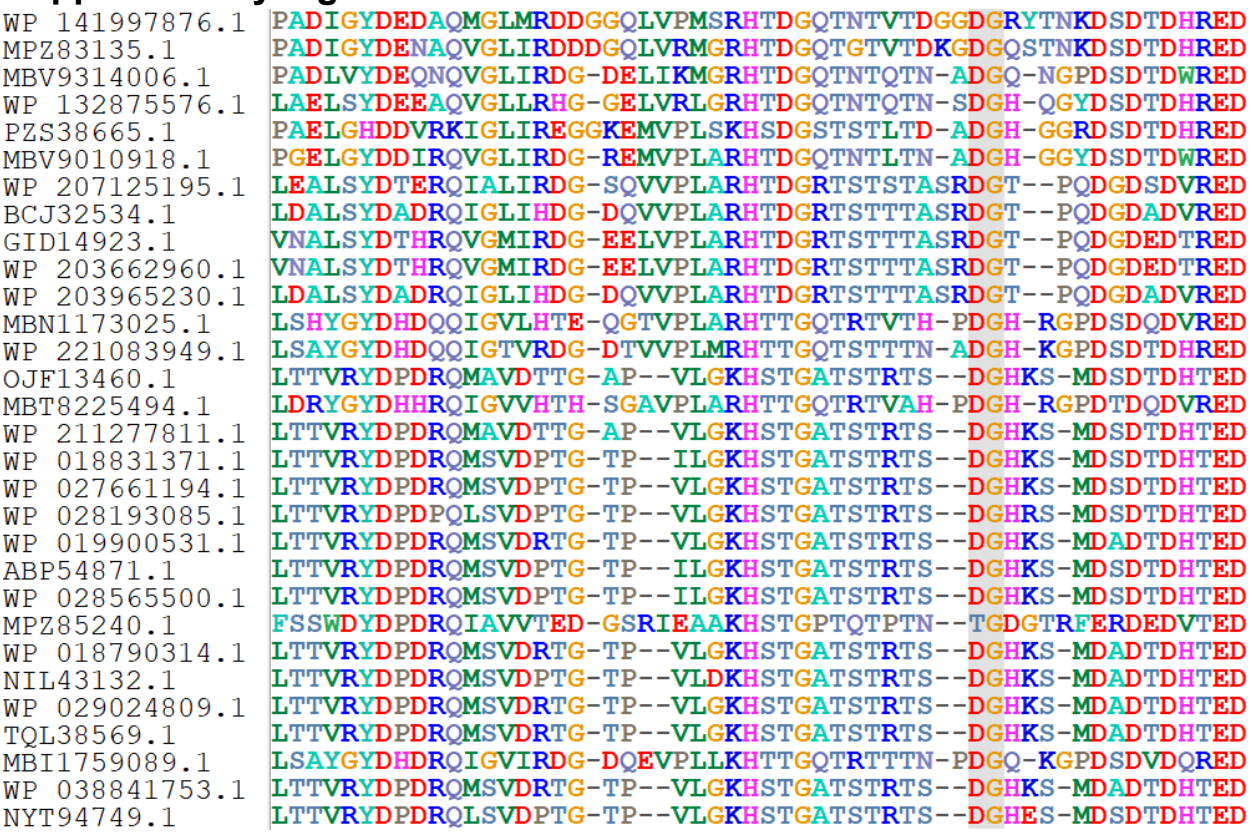

Figure S1: ClustalW alignment of AmdA and its 29 homologs. Left: The protein accession numbers. The first row represents AmdA (WP 141997876.1);right: the C-terminal ends of the corresponding sequences. The shaded region represents the DG that is conserved amongst the precursors and is likely to be an aspartimidylation site.

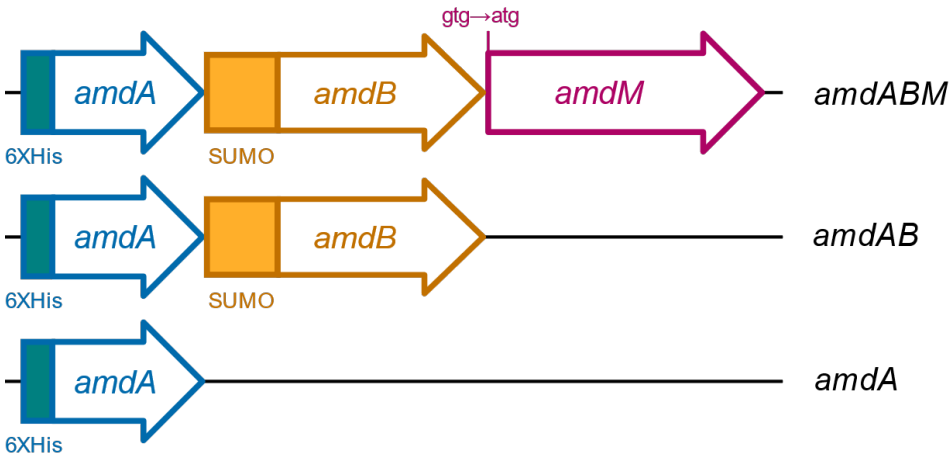

Figure S2: The architecture of the modified *amdABM*, *amdAB*, and *amdA* BGCs used for heterologous expression in *E. coli*. The His_6-tag (MSGSHHHHHHGS) is fused upstream to the coding sequence of AmdA. The SUMO-tag is fused upstream to the coding sequence of AmdB. The start codon of *amdM* was modified from gtg to atg.

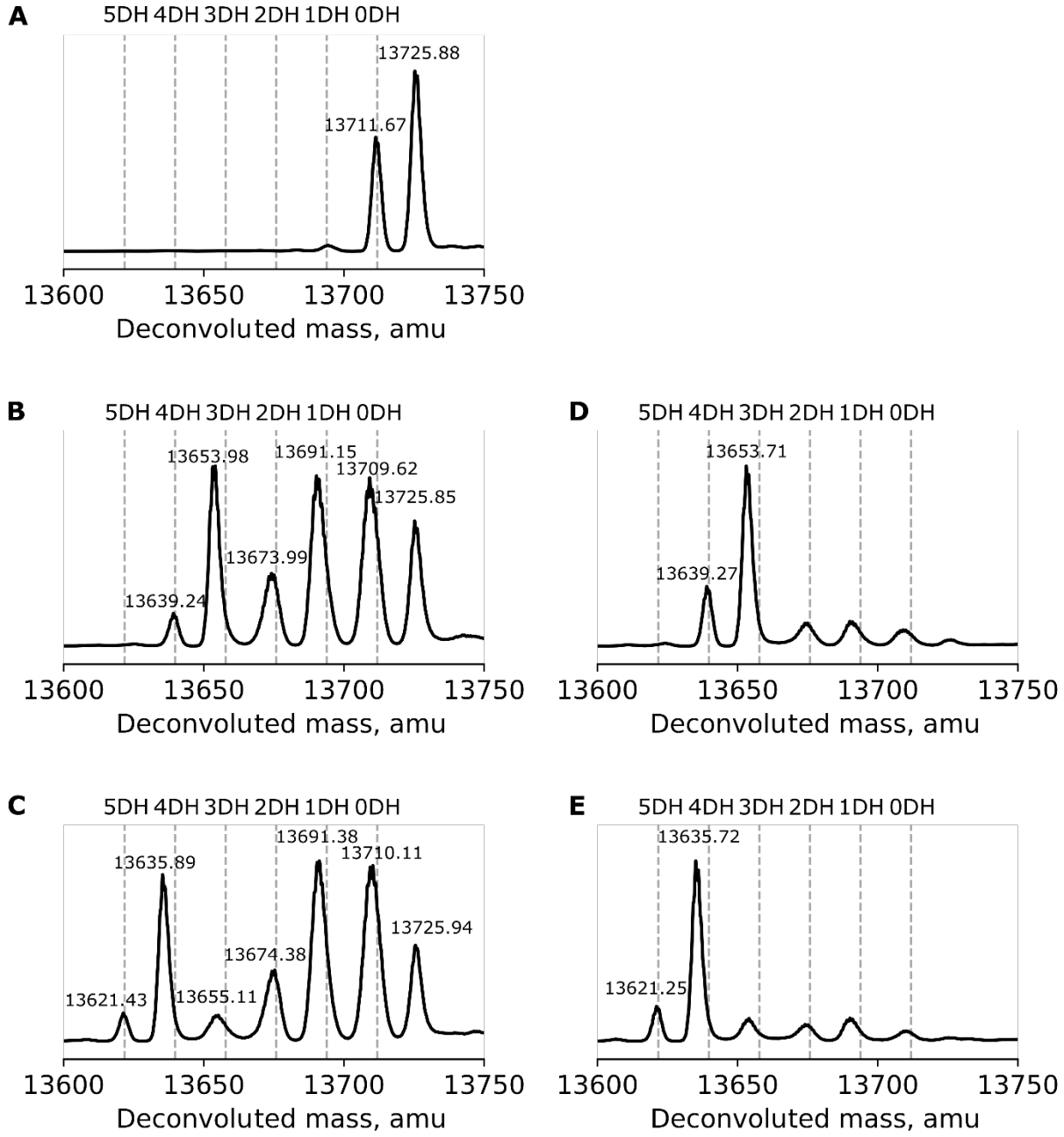

Figure S3: Deconvoluted mass spectra of the purified AmdA proteins with the original His_6-tag (MRGSHHHHHHGS). The grey dotted lines represent the theoretical average masses of the unmodified AmdA (0DH) and AmdA 1-5-fold dehydrated (1-5DH). **(A)** The unmodified AmdA; **(B)** $mAmdA^{B}$ from AmdA co-expressed with AmdB; **(C)** $mAmdA^{BM}$ from AmdA co-expressed with AmdB and AmdM; **(D)** $mAmdA^{B}$ from AmdA co-expressed with SUMO-AmdB; **(E)** $mAmdA^{BM}$ from AmdA co-expressed with SUMO-AmdB and AmdM. Co-expressing AmdA with SUMO-AmdB noticeably improves the yield of the completely modified AmdA. Most species of AmdA appear to contain nonspecific methylation.

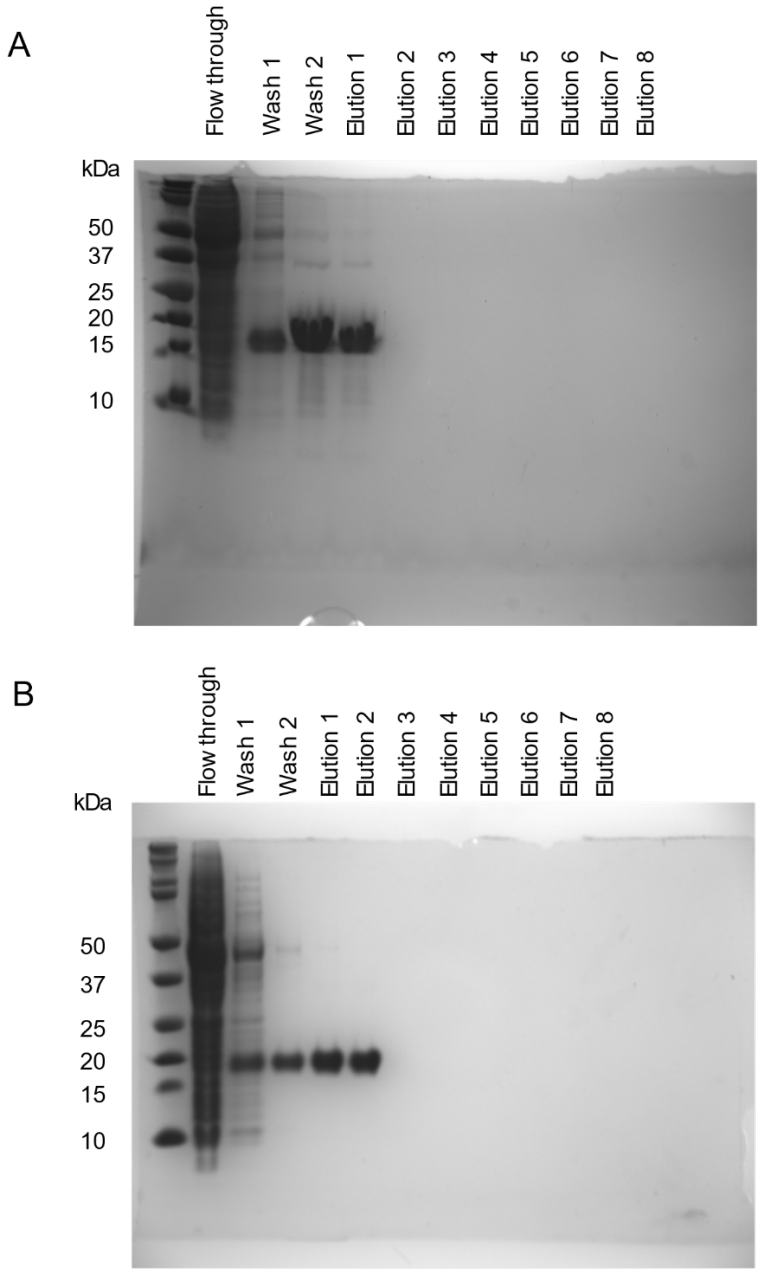

Figure S4: SDS-PAGE analysis of Ni-NTA urea-denaturing purification of **(A)** mAmdA^{B} and **(B)** mAmdA^{BM}. Flow through lane corresponds to *E. coli* cell lysate flow through after 1 hr incubation with Ni resin. Wash 1 corresponds to the first 10 mL wash of the resin with 8 M urea buffer, pH 6.3. Wash 2 corresponds to the second wash (10 mL) with 8 M urea buffer, pH 5.9. Each elution lane corresponds to 1 mL fractions eluted with 8 M urea buffer, pH 4.5.

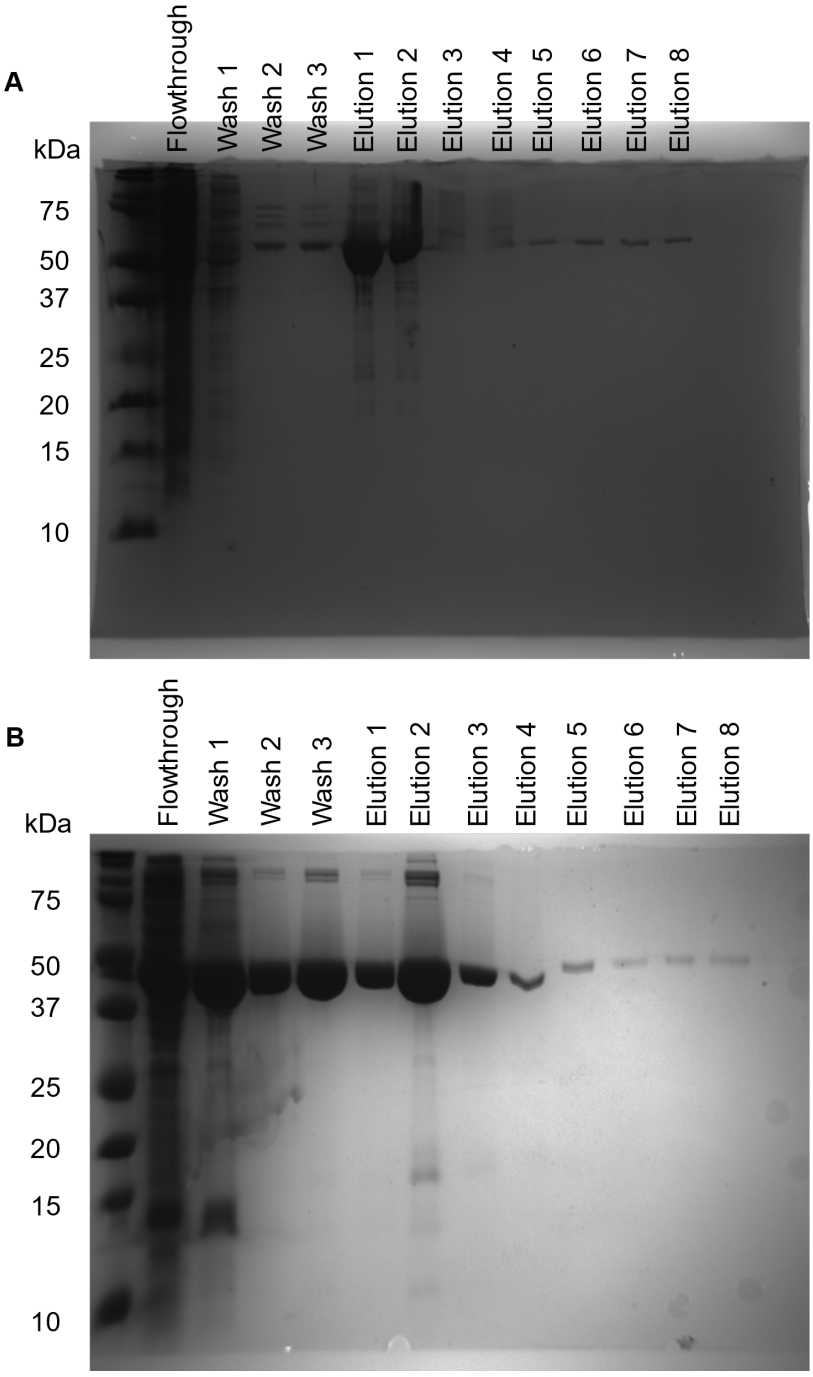

Figure S5: SDS-PAGE analysis of Ni-NTA native purification of **(A)** His_6-SUMO-AmdB and **(B)** His_6-AmdM. Flow through lane corresponds to *E. coli* cell lysate flow through after 1 hr incubation with Ni-NTA resin. Wash 1, 2, 3 corresponds to the 10 mL washes of the resin with buffer at pH 8.0 containing 50 mM NaH_2PO_4, 300 mM NaCl, and 20 mM, 35 mM, and 50 mM imidazole, respectively. Each elution lane corresponds to 1 mL fractions eluted with the same buffer containing 250 mM imidazole.

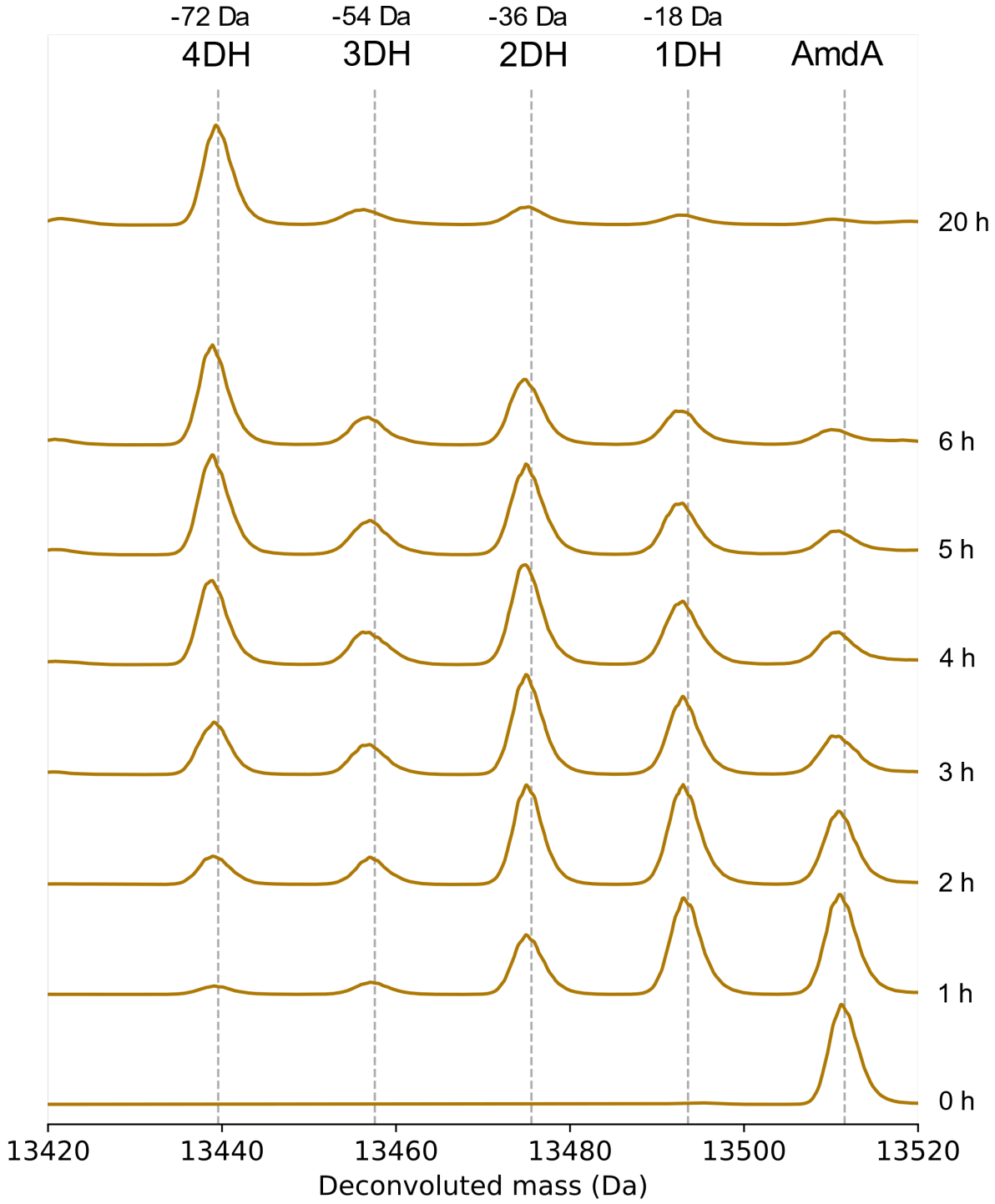

Figure S6: *In vitro* His_6-SUMO-AmdB-modification of AmdA. Over the course of 20 hours at room temperature, almost all AmdA becomes quadruply dehydrated, showing a near-complete conversion into $mAmdA^B$.

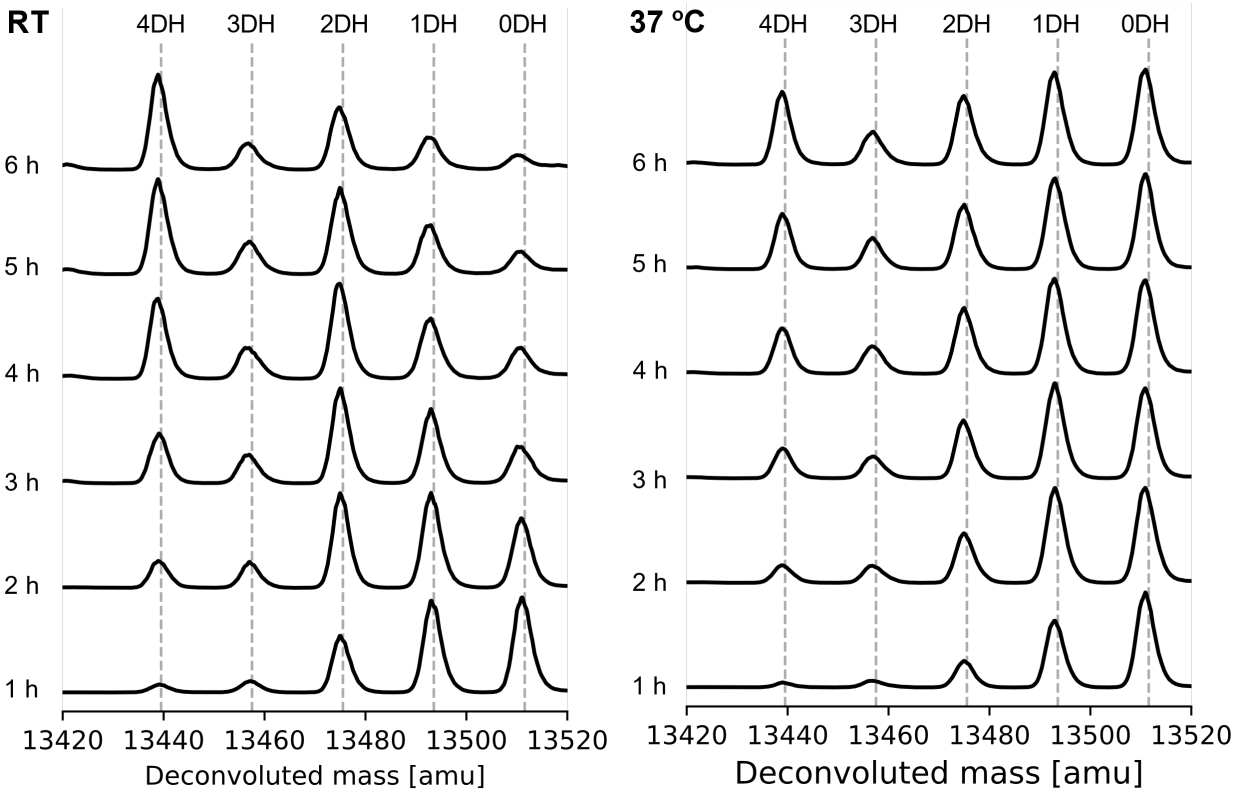

Figure S7: Comparison of *in vitro* His_6-SUMO-AmdB modification of AmdA at **(A)** room temperature (same experimental result as shown in Fig. S6) and **(B)** 37 °C. The reaction is significantly slower at 37 °C than at room temperature.

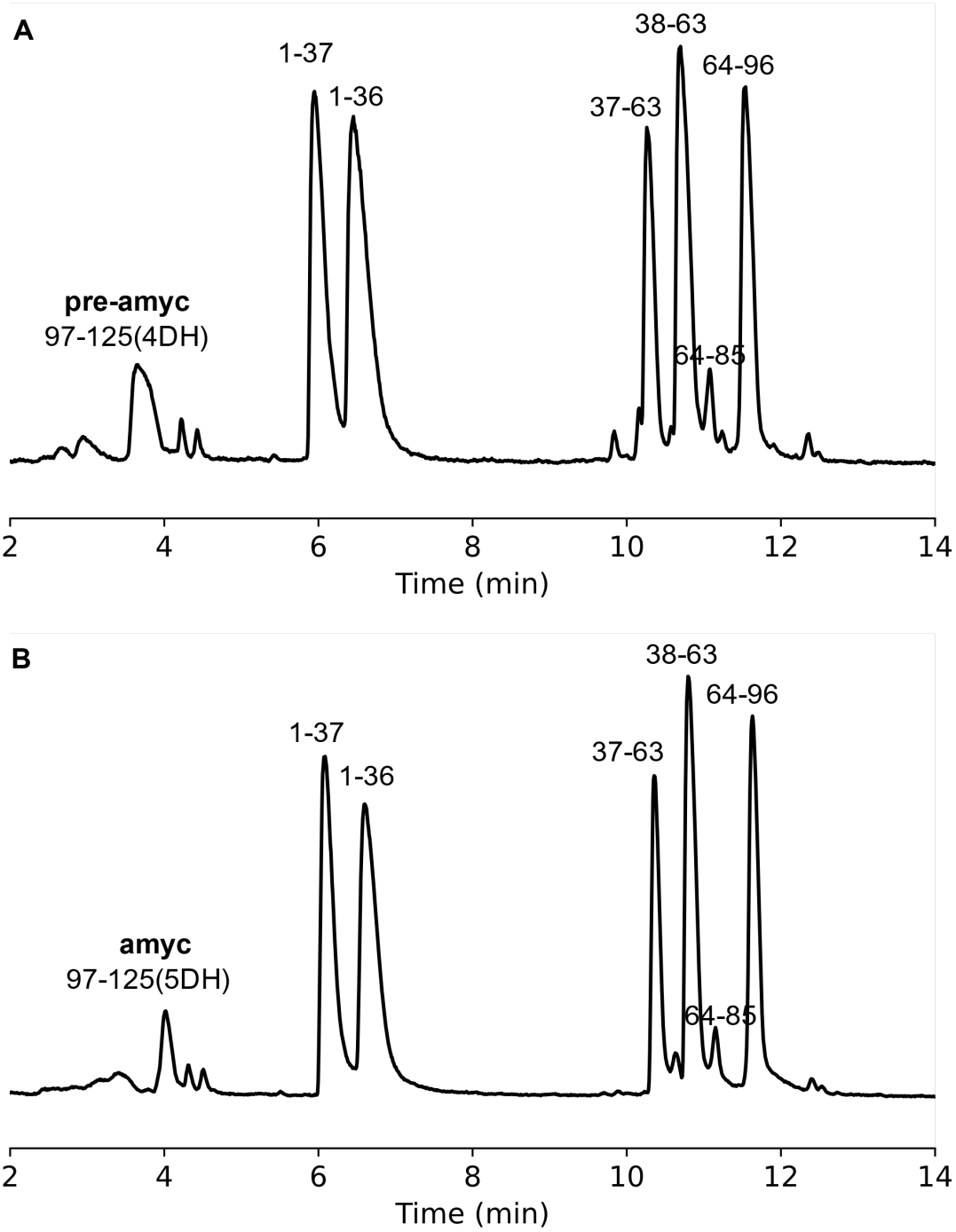

Figure S8: Total ion current chromatograms of trypsin-digested **(A)** mAmdA^{B} and **(B)** mAmdA^{BM}. The numbers above the peaks correspond to the specific peptide within mAmdA^{B} or mAmdA^{BM}. While the leader peptides (residues 1-96) fragment and chromatograph similarly, pre-amycolimiditide and amycolimiditide (residues 97-125) chromatograph at different retention times, at 3.6 min and 4.0 min, respectively.

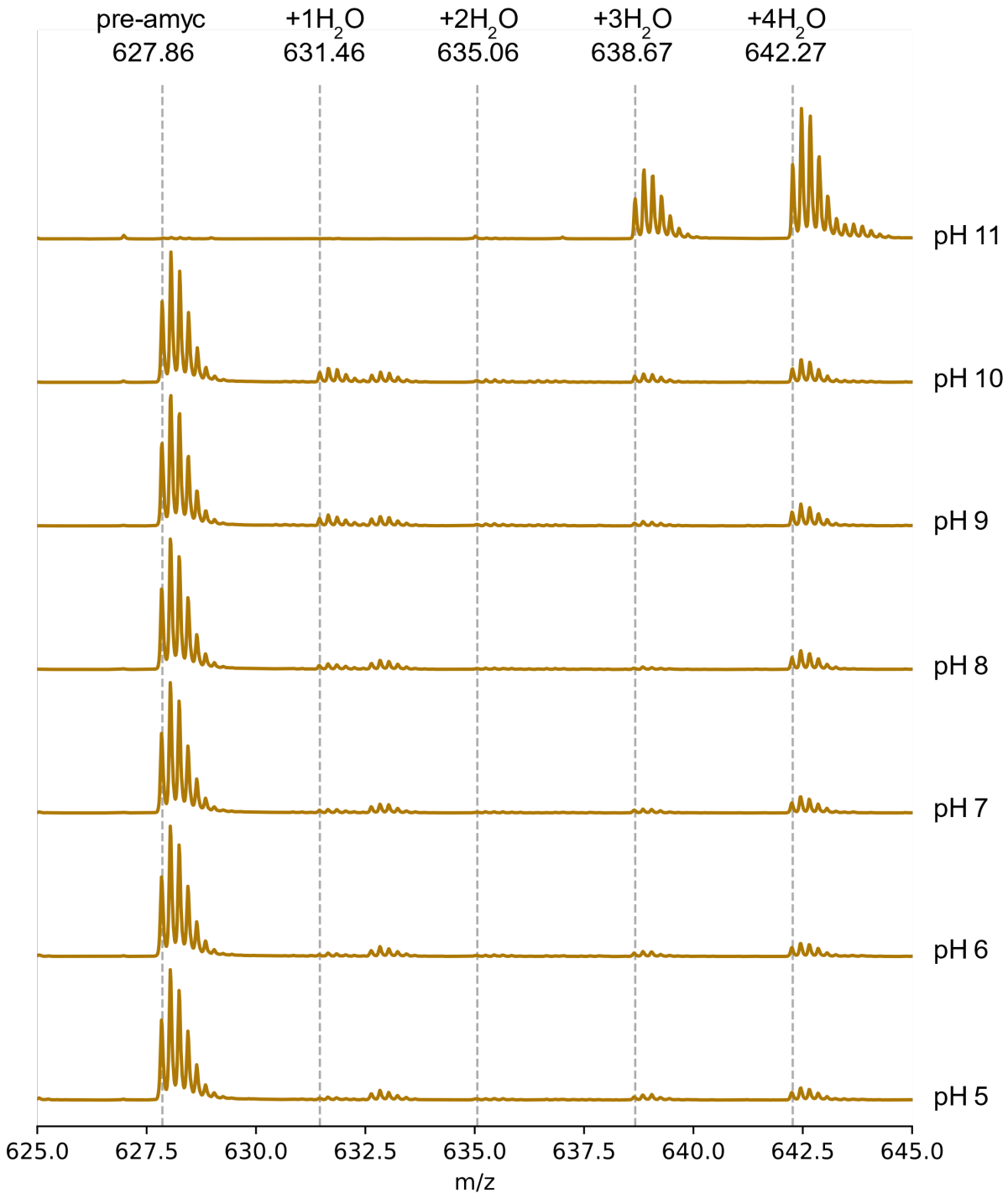

Figure S9: Hydrolysis of pre-amycolimiditide at various pH values. The +5 charge state is shown. 10 μM peptide was incubated in a 1X PBS buffer at room temperature for 30 hours. HCl or NaOH was used to change the pH of the buffer. All four dehydrations of pre-amycolimiditide installed by AmdB are undone at pH 11, suggesting the presence of four ester linkages and no amide crosslink.

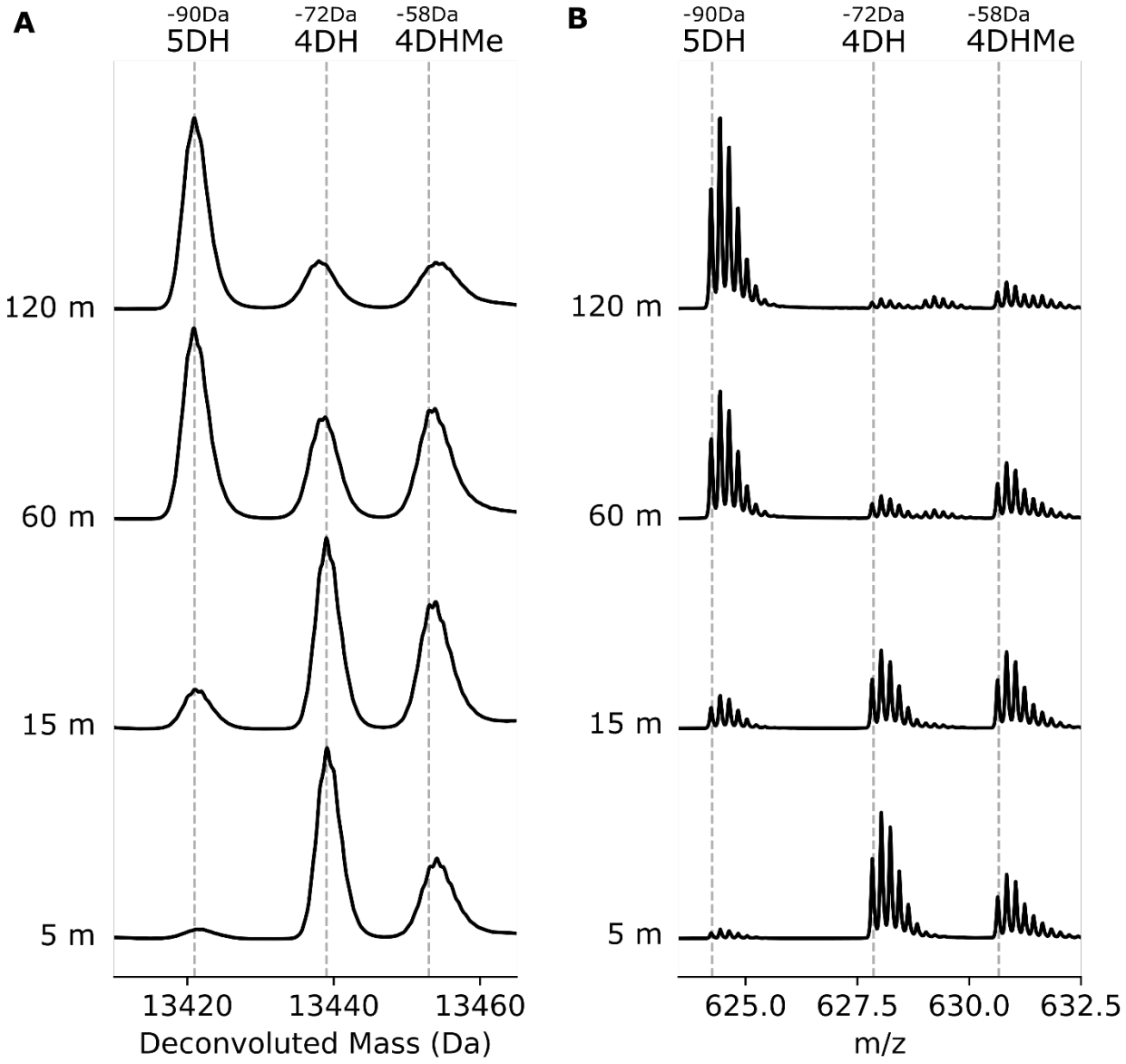

Figure S10: Comparison of the *in vitro* aspartimidylation of **(A)** mAmdA^{B} and **(B)** pre-amycolimiditide over time. 5DH/4DH indicates species with 5 or 4 dehydrations respectively while 4DHMe is a species with four dehydrations and one Asp methylation. Both reactions progress at a similar rate.

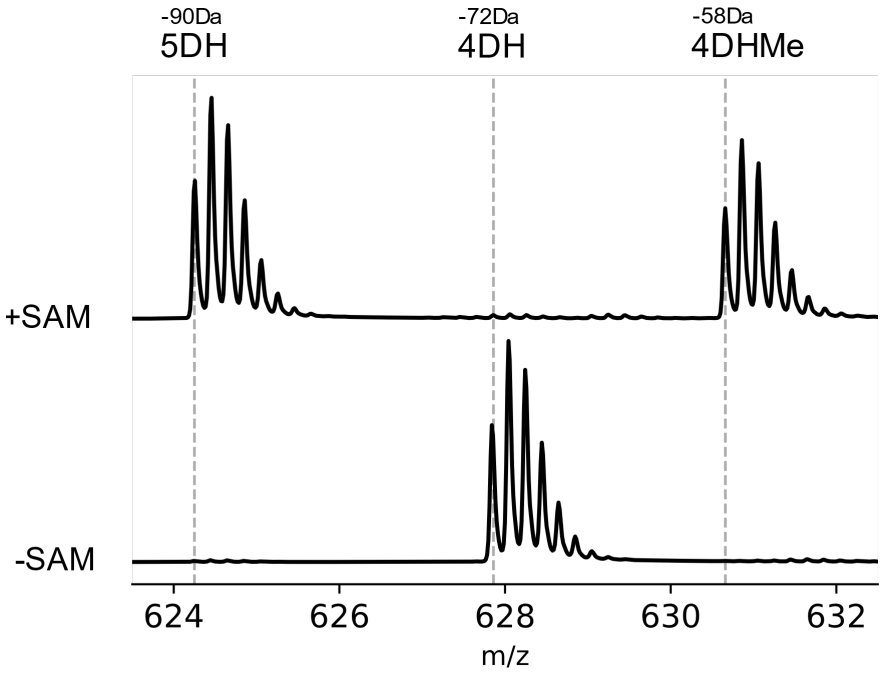

Figure S11: Comparison of the *in vitro* aspartimidylation of iso pre-amycolimiditide (top) with and (bottom) without *S*-adenosylmethionine (SAM). 5DH/4DH indicates species with 5 or 4 dehydrations respectively while 4DHMe is a species with four dehydrations and one Asp methylation. The reactions were done at 28 °C for 1 hour. Without SAM, the reaction does not proceed.

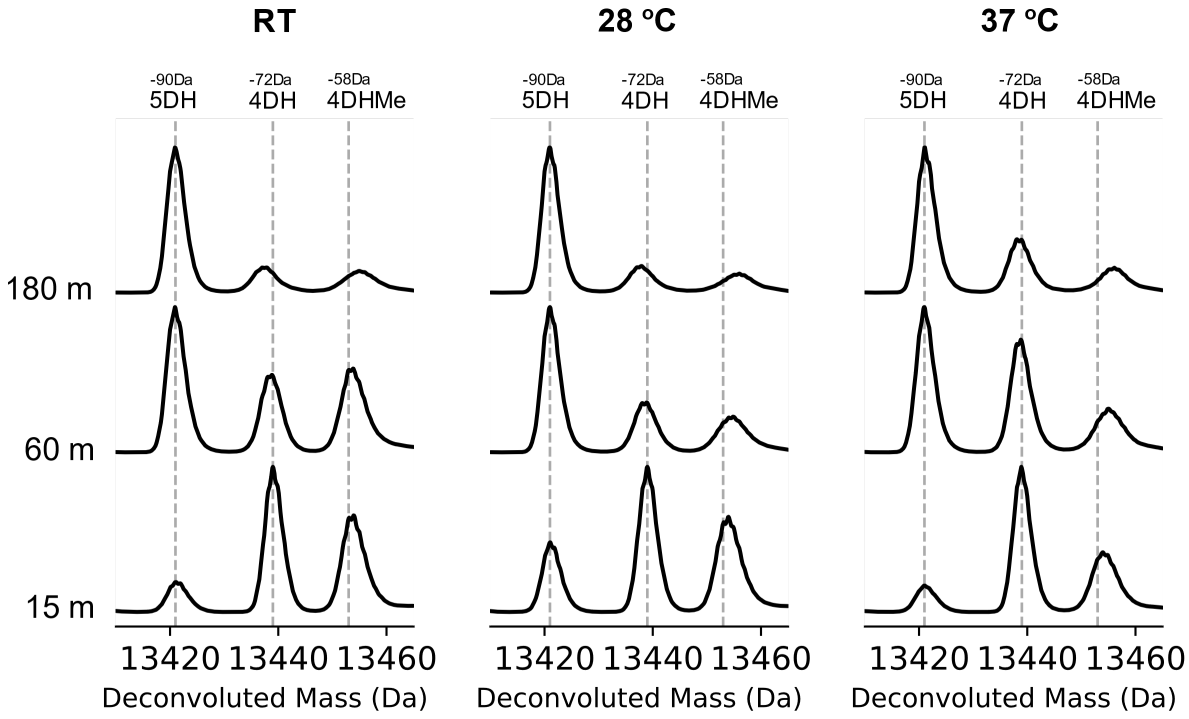

Figure S12: Comparison of the *in vitro* aspartimidylation of mAmdA^{B} at (left) room temperature, (middle) 28 °C, and (right) 37 °C. 5DH/4DH indicates species with 5 or 4 dehydrations respectively while 4DHMe is a species with four dehydrations and one Asp methylation. Reactions at all three temperatures proceed at a similar rate.

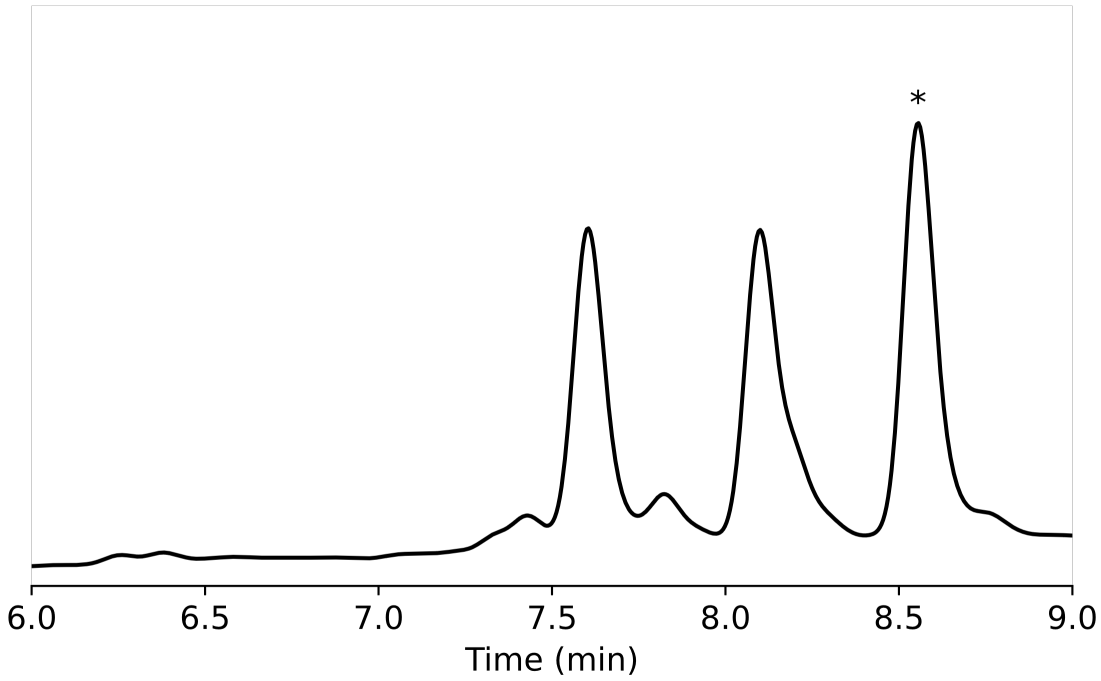

Figure S13: HPLC purification (absorbance at 215 nm) of methylated pre-amycolimiditide. The asterisk (*) indicates the peak that was purified.

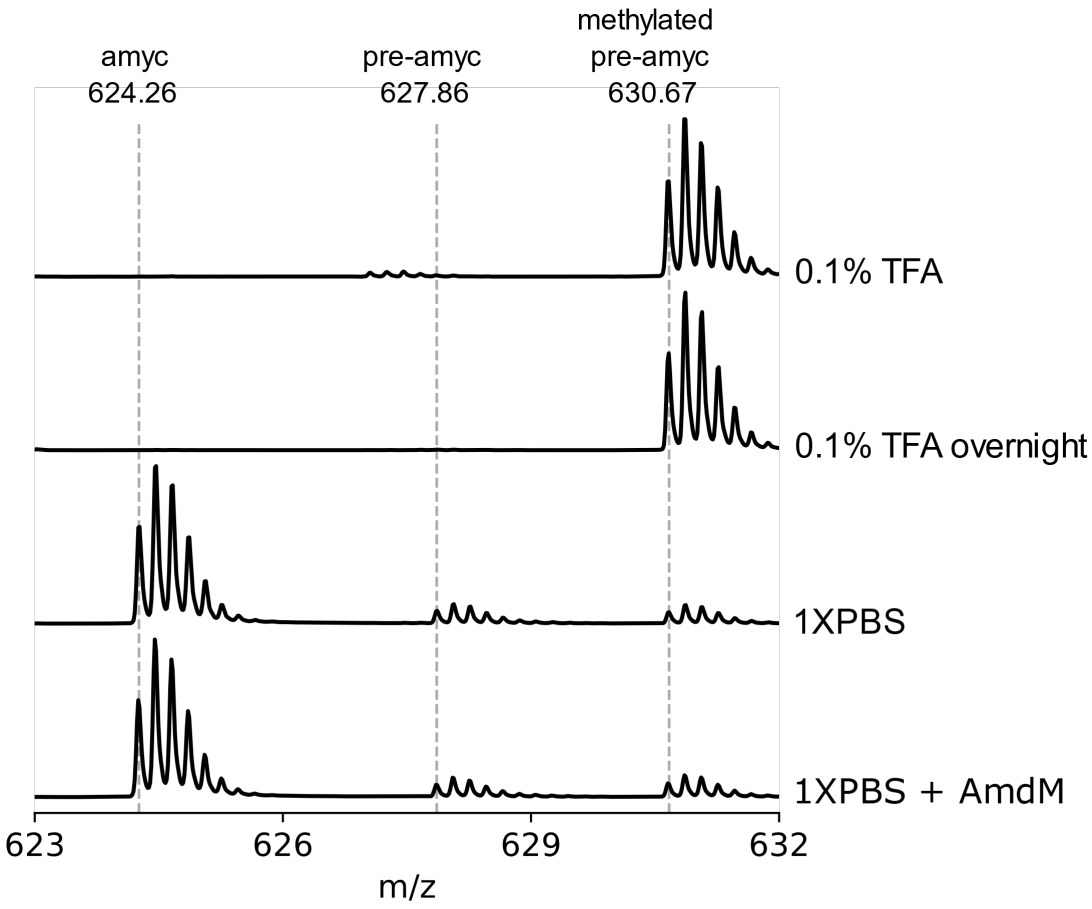

Figure S14: MS scan for monitoring the backbone cyclization after the HPLC-purification of methylated pre-amycolimiditide. 0.1% TFA: MS acquired immediately after the HPLC collection of the methylated pre-amycolimiditide. 0.1% TFA overnight: Methylated pre-amycolimiditide incubated in 0.1% TFA overnight. The backbone cyclization does not occur at a low pH. 1XPBS: The purified peptide was lyophilized and then resuspended in 1X PBS, pH 7.4 buffer and allowed to react for 30 min. 1XPBS + AmdM: 1 µM His_6-AmdM was added to the peptide and buffer and was allowed to react for 30 min. Conversion of the methyl ester to aspartimide occurs efficiently in the absence of AmdM.

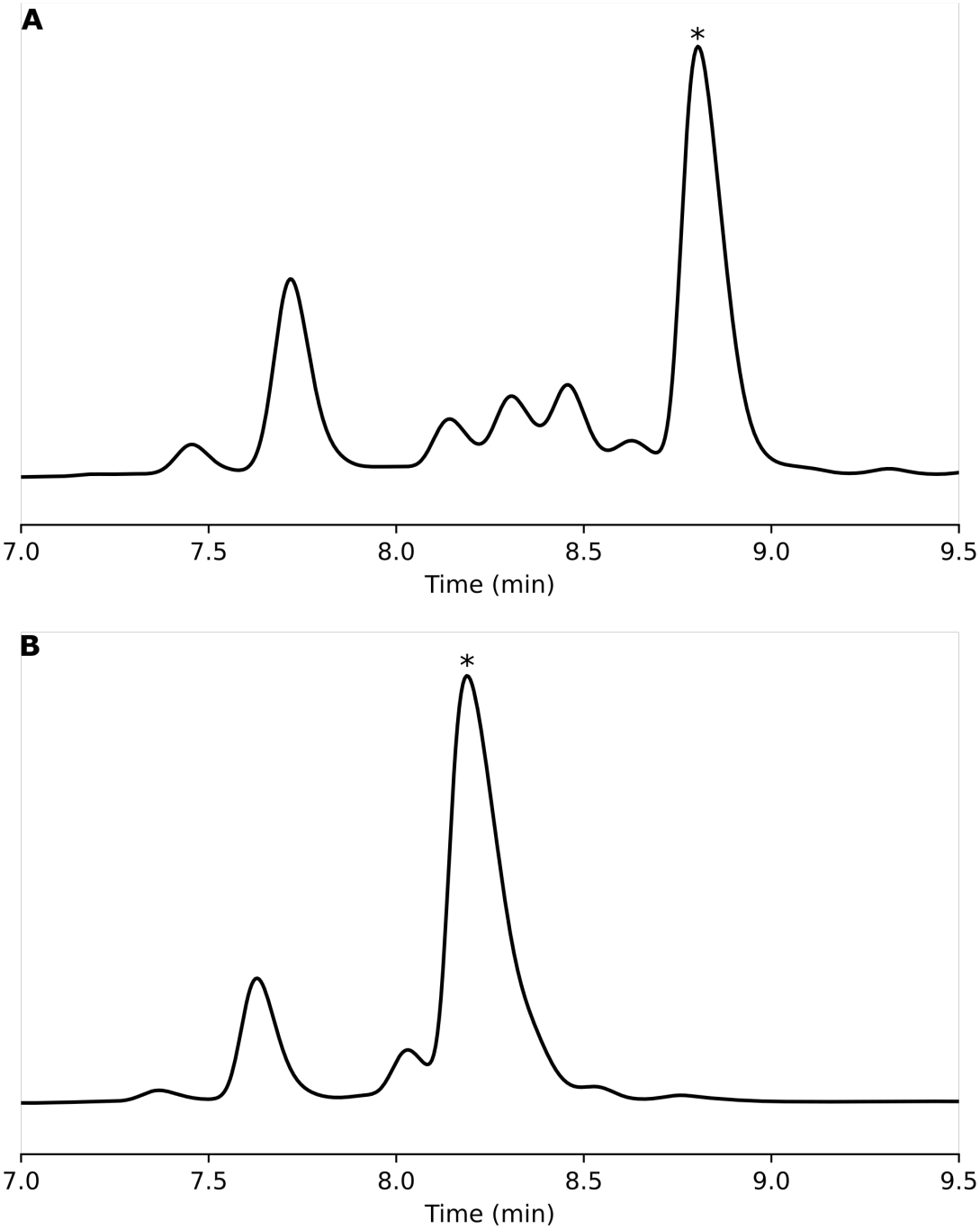

Figure S15: HPLC purification (absorbance at 215 nm) of **(A)** amycolimiditide, trypsin-digested from mAmdA^{BM}, and **(B)** pre-amycolimiditide, trypsin-digested from mAmdA^{B}. The asterisks (*) indicate the peaks that were purified.

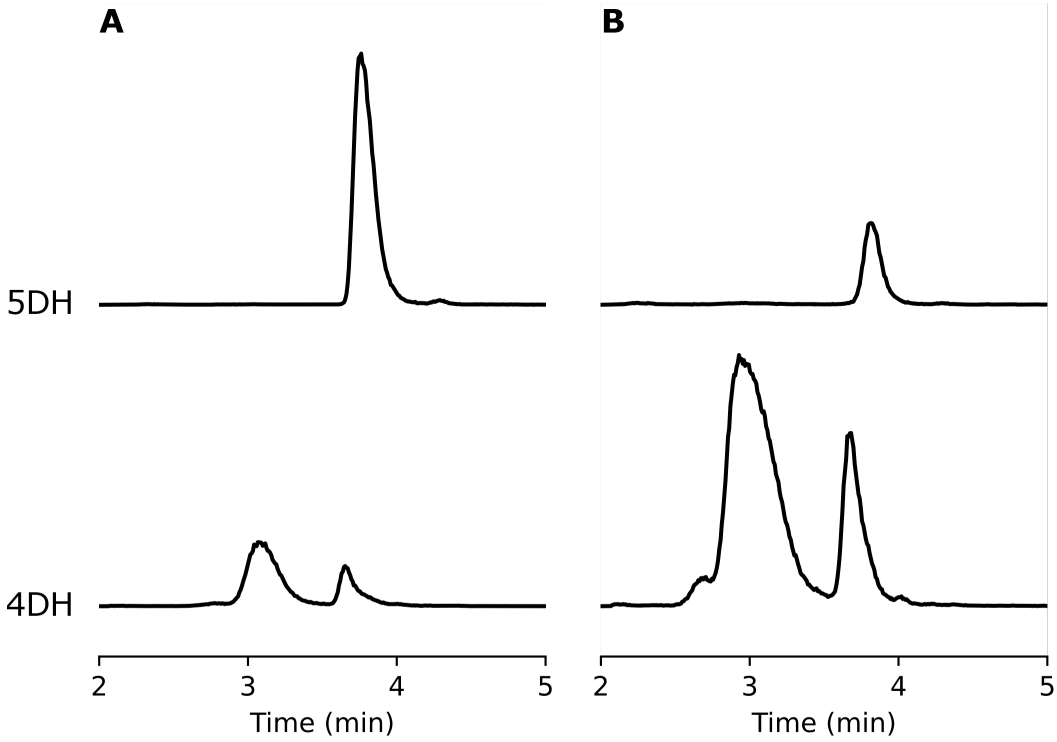

Figure S16: Extracted ion current chromatograms (EICs) of aspartimide hydrolysis in amycolimiditide. The top trace represents the EIC for the five-fold dehydrated core peptide (i.e. four esters and one aspartimide), and the bottom trace represents the EIC for the four-fold dehydrated core peptide (only four esters). The y-axes of the traces are normalized to the highest peak height across both EICs. **(A)** Amycolimiditide hydrolyzed at pH 7 for 12 h. **(B)** Amycolimiditide hydrolyzed at pH 8 for 12 h. Hydrolysis happens more rapidly at pH 8, with most of the amycolimiditide hydrolyzed to two isobaric species of pre-amycolimiditide.

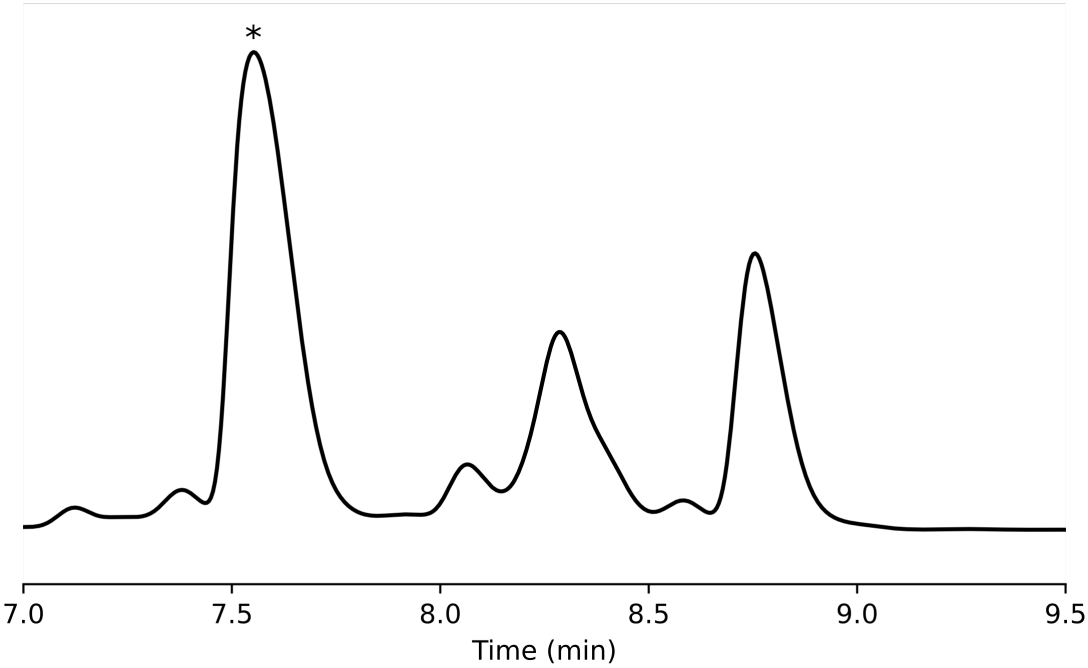

Figure S17: HPLC purification (absorbance at 215 nm) of iso pre-amycolimiditide, trypsin-digested from mAmdA^{BM} for 2 hours. The asterisk (*) indicates the peak that was purified.

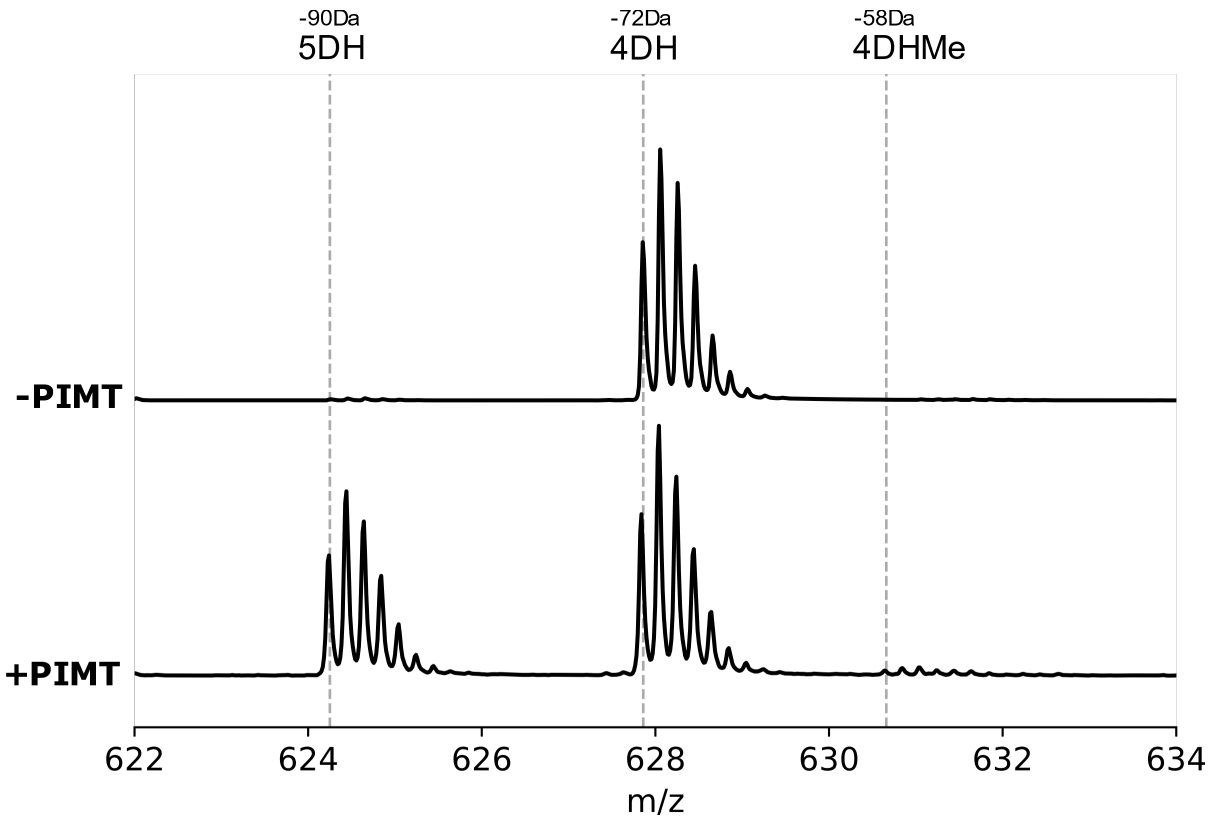

Figure S18: MS scan of the major species of amycolimiditide hydrolysate (iso pre-amycolimiditide) modified by the human PIMT. (top) No PIMT control. (bottom) PIMT modification for 3 h. A significant portion of the material is converted to the aspartimide.

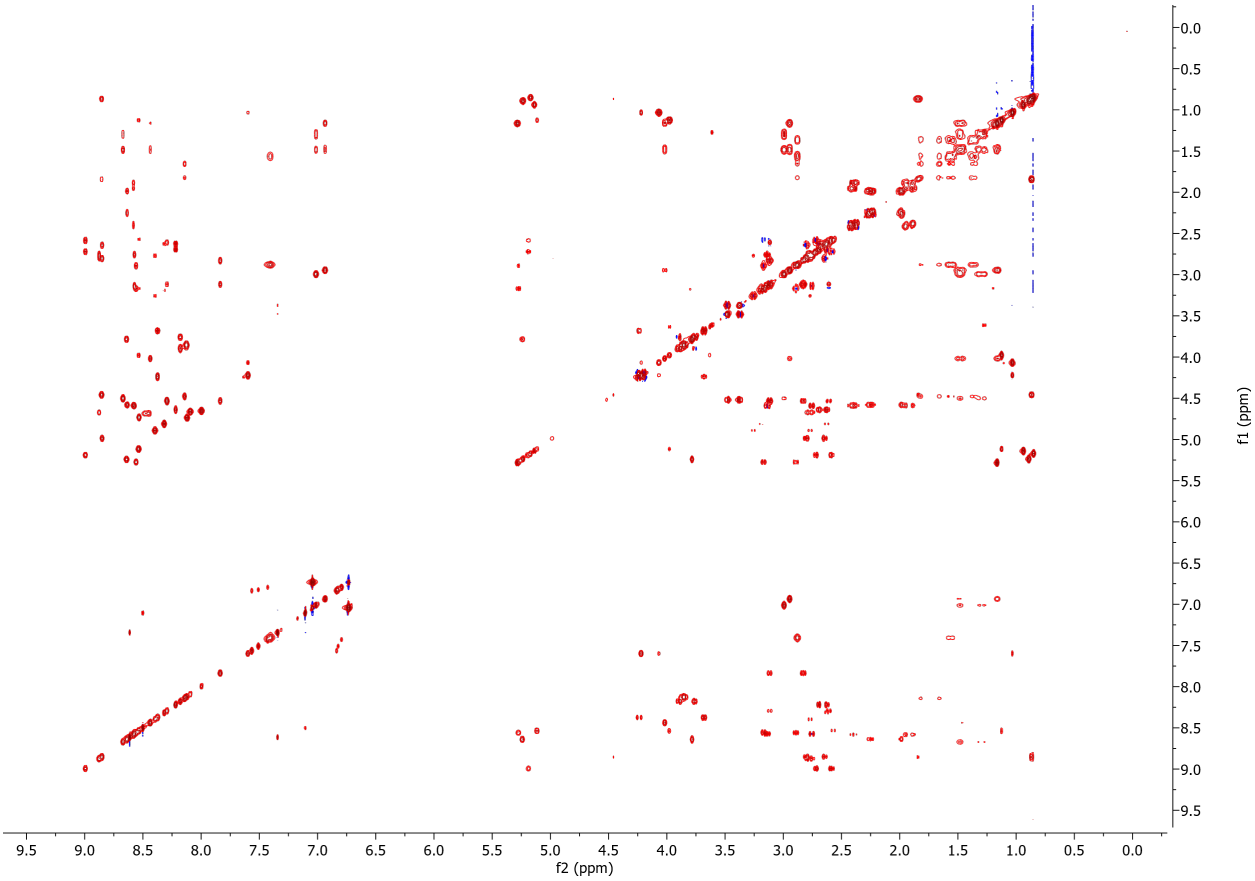

Figure S19: TOCSY spectrum of amycolimiditide. The peak assignments are listed in Table S6.

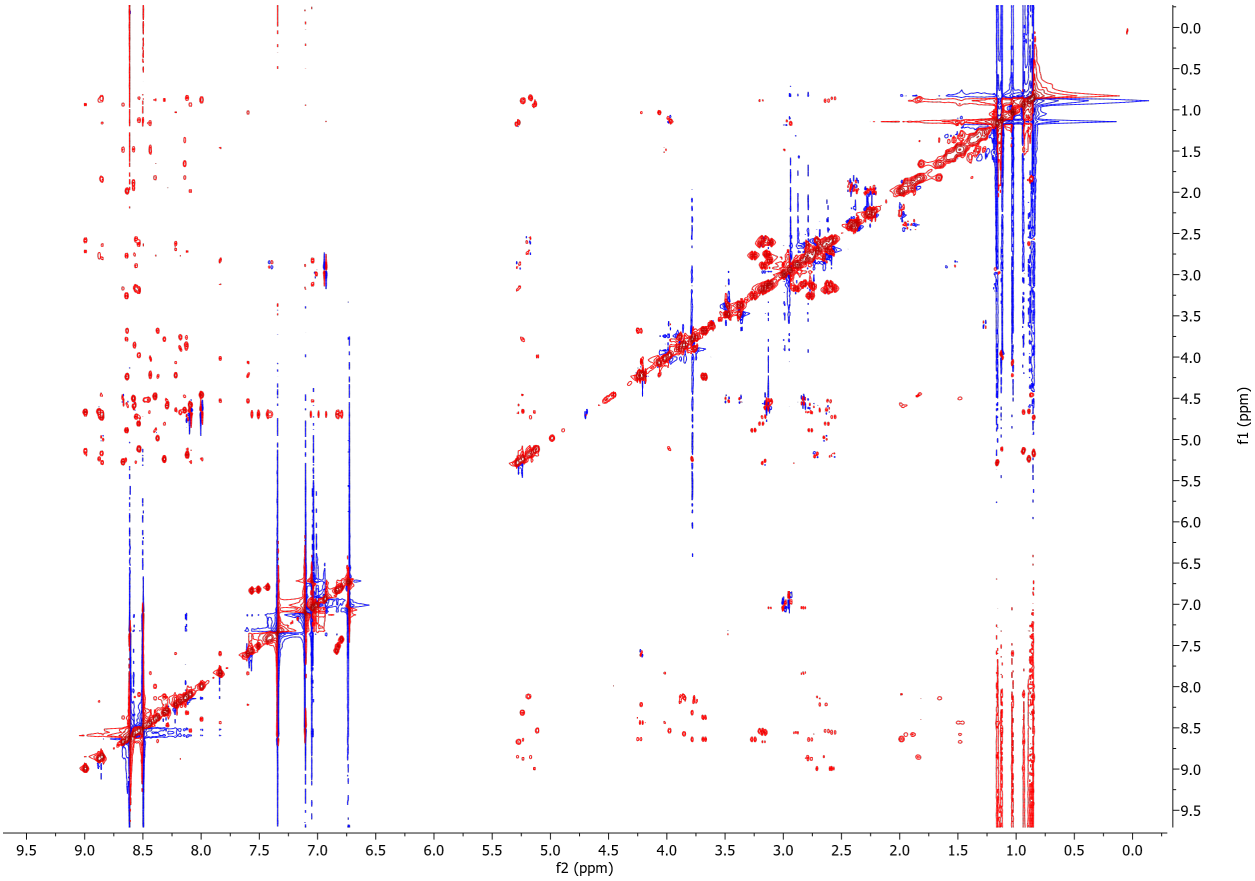

Figure S20: NOESY spectrum of amycolimiditide with a mixing time of 150 ms. This spectrum was integrated to determine distance constraints.

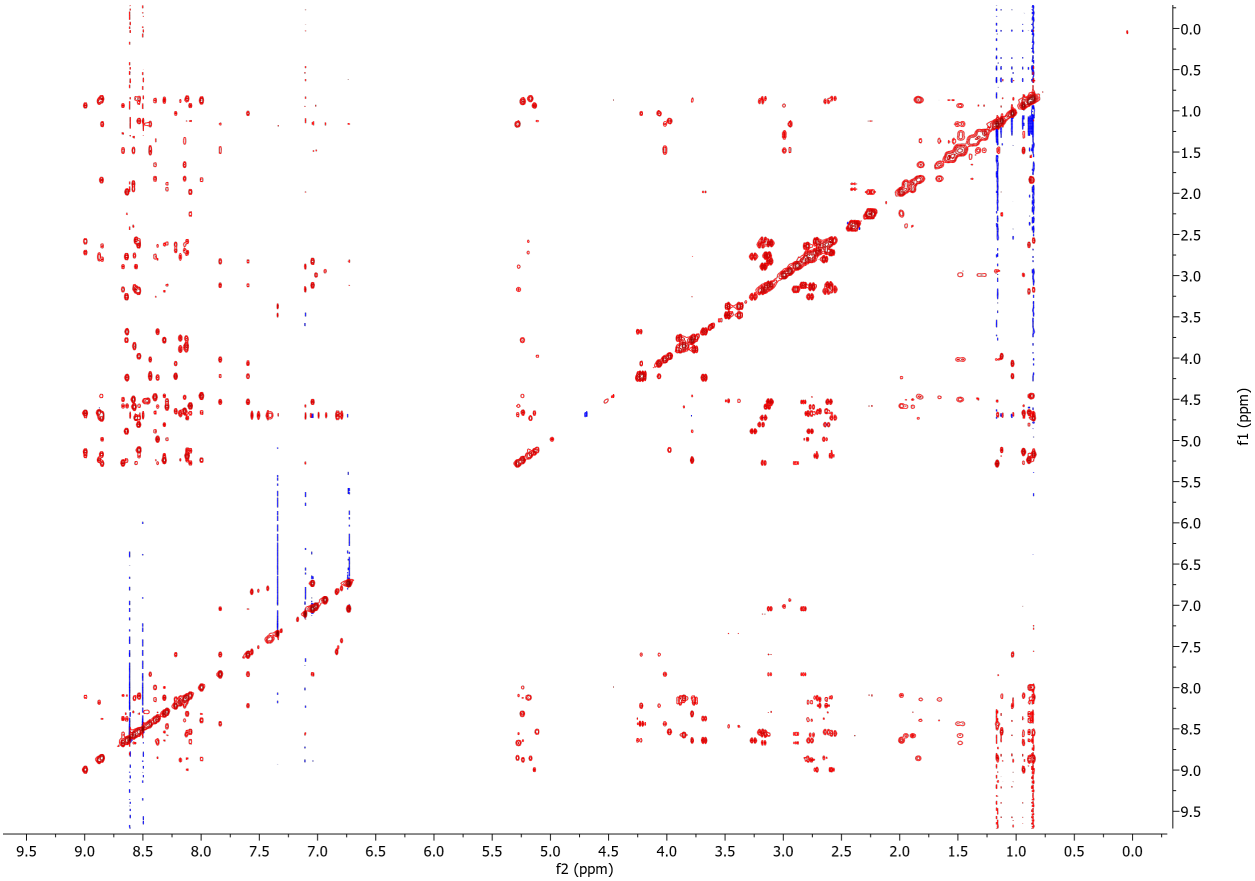

Figure S21: NOESY spectrum of amycolimiditide with a mixing time of 700 ms. The peak assignments are listed in Table S6.

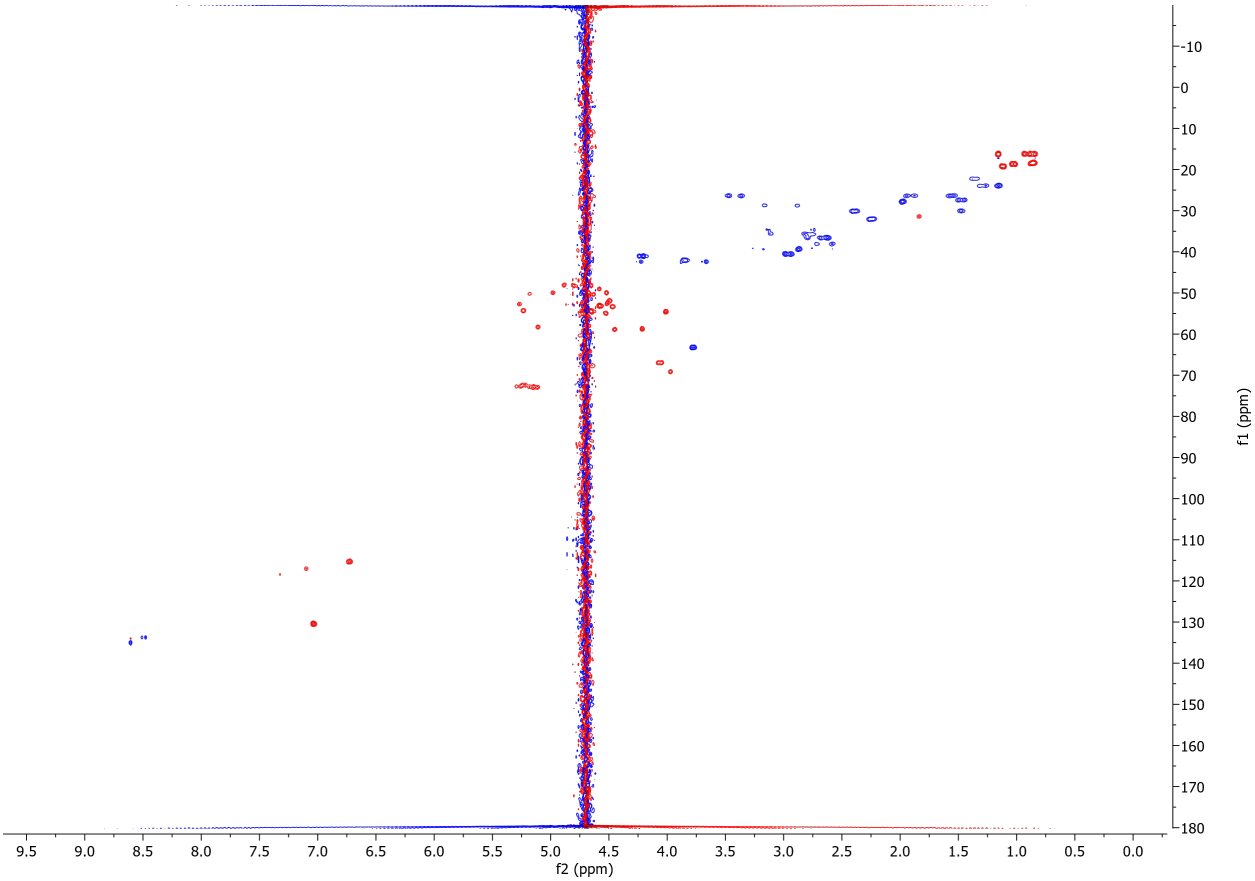

Figure S22: ^{1}H-^{13}C HSQC spectrum of amycolimiditide. The peak assignments are listed in Table S6.

Figure S23: ^{1}H-^{13}C HMBC spectrum of amycolimiditide, optimized for 10 Hz couplings. The peak assignments are listed in Table S6.

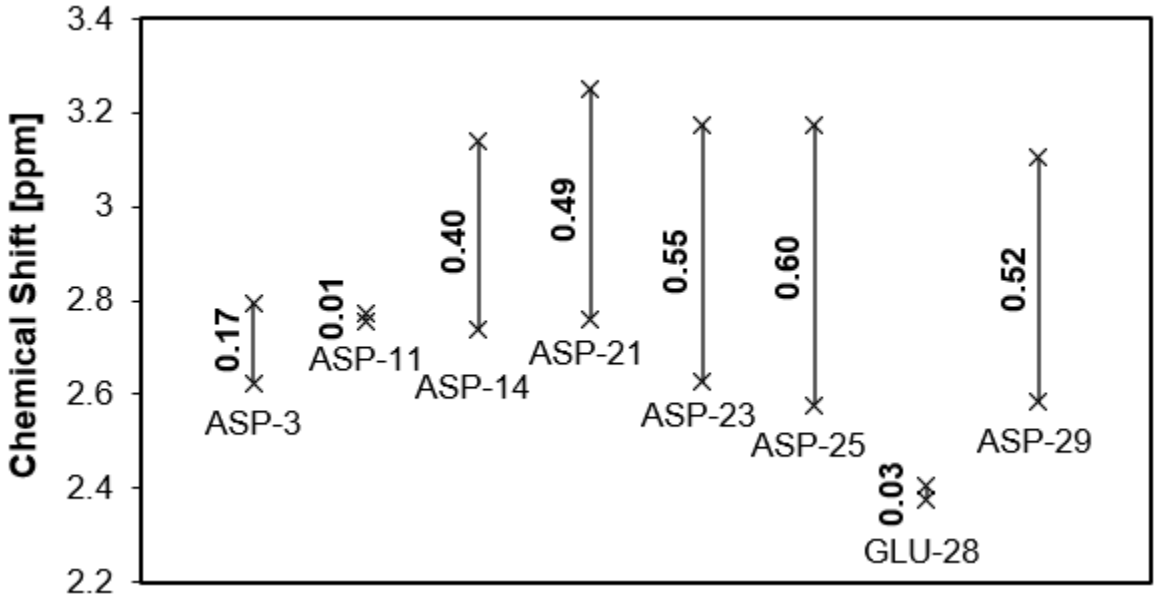

Figure S24: The chemical shifts of the β-protons of Asp and the γ-protons of Glu from amycolimiditide. The numbers adjacent to the vertical line segments indicate the difference between the chemical shifts of the two protons. The differences between the chemical shifts of the two β-protons of Asp-14, Asp-21, Asp-23, Asp-25, and Asp-29 are significantly larger than the others.

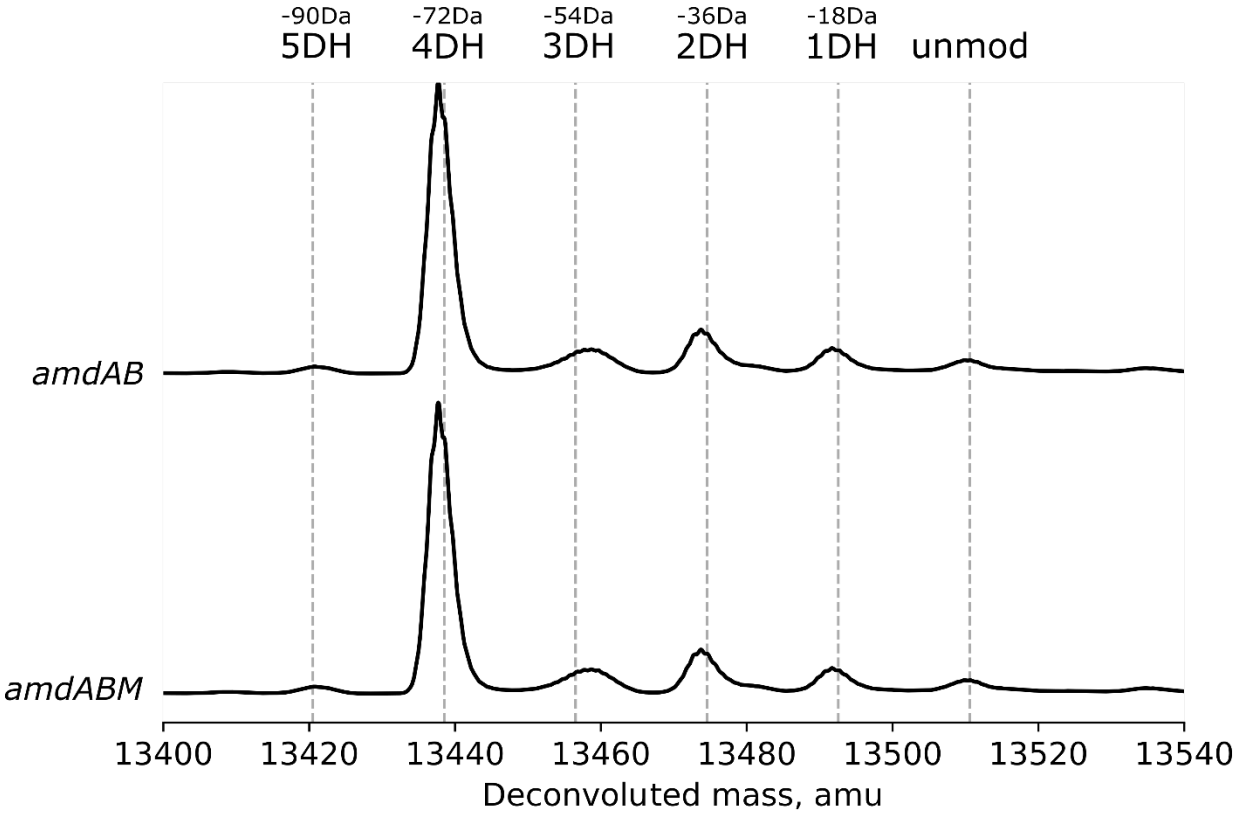

Figure S25: Co-expression of the AmdA(D14N) variant with **(A)** SUMO-AmdB and **(B)** SUMO-AmdB and AmdM. Both co-expression experiments yield four dehydrations, indicating that AmdM does not aspartimidylate the AmdA(D14N) variant.

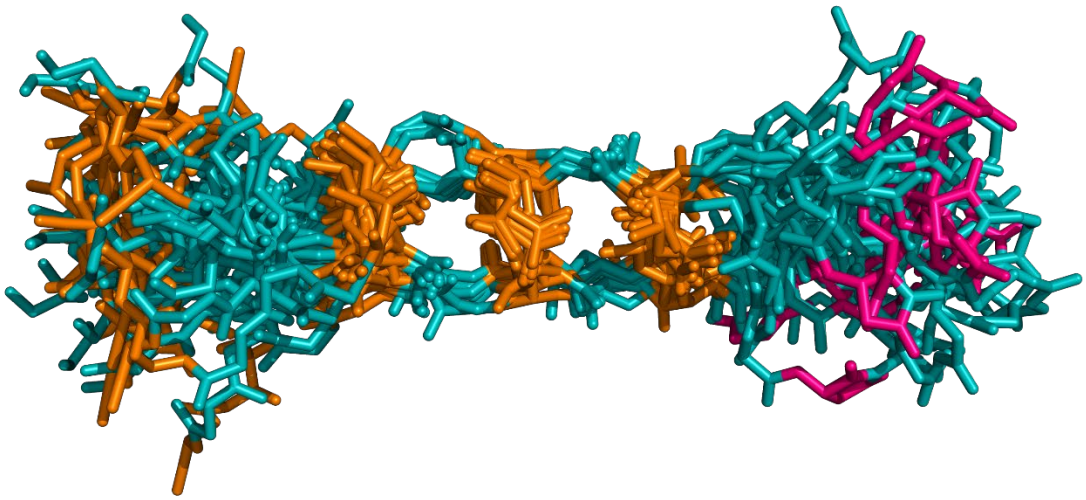

Figure S26: Alignment of the top 20 amycolimiditide NMR structures (PDB: 8DYM). Only the backbone atoms of all residues and the sidechain atoms of the ω-ester linkages and the aspartimide are shown. All atoms of the ω-ester linkages are colored orange, the aspartimide magenta, and the rest teal. The structures are aligned at the intermediate stem region, across the T10-D21, T8-D23, and T6-D25 crosslinks. The average stem length (measured as the distance between the ester carbonyl carbon of T2-D29 crosslink and the ester carbonyl carbon of T10-D21 crosslink) is 24 ± 1 Å. The average peptide length (measured as the distance between the ester carbon of T2-D29 crosslink and the sidechain carbonyl carbon of Asu-14) is 35 ± 2 Å.

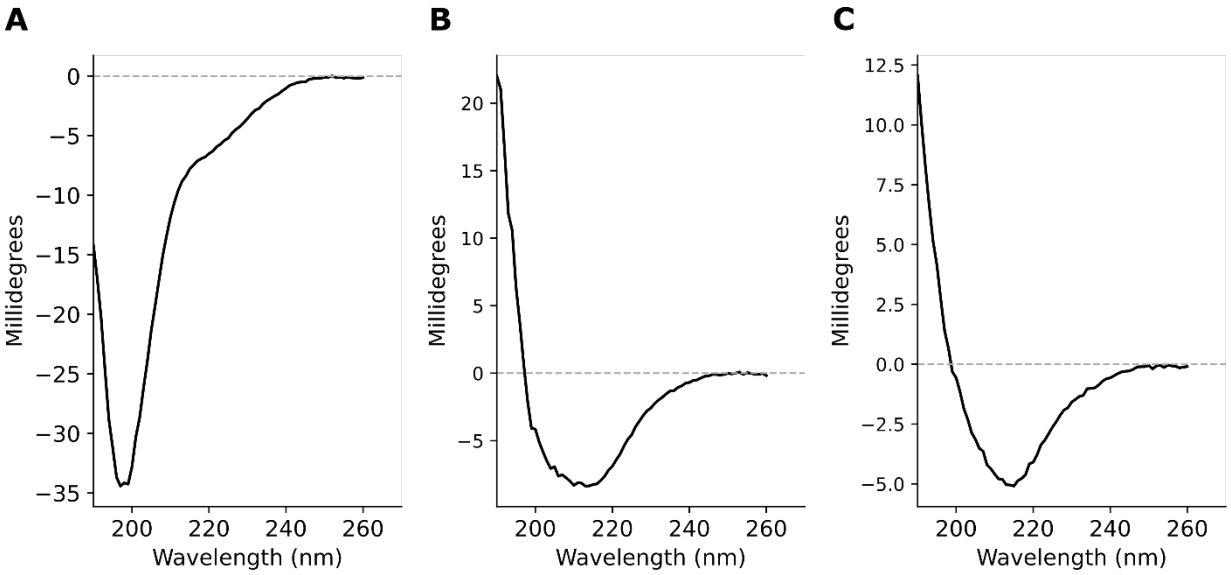

Figure S27: Circular dichroism spectroscopy on **(A)** the unmodified core peptide, **(B)** pre-amycolimiditide, and **(C)** amycolimiditide. The data suggest random coil character for the unmodified core peptide and β-strand character for pre-amycolimiditide and amycolimiditide.

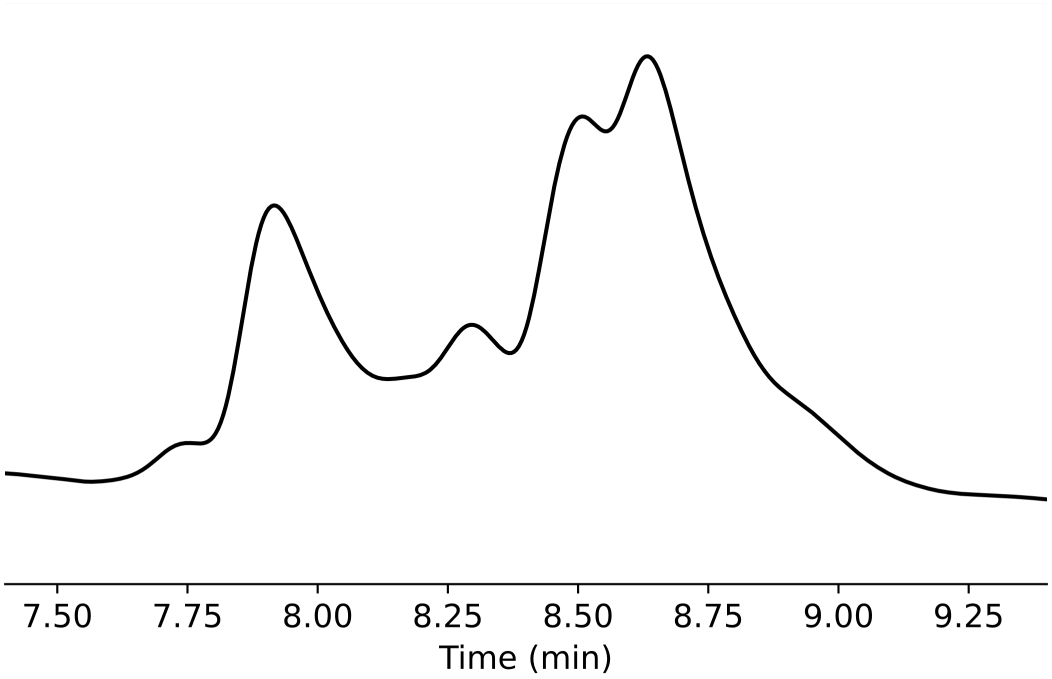

Figure S28: HPLC purification (absorbance at 215 nm) of partially-modified core peptides, obtained from the trypsin-digested His_6-AmdA modified by His_6-SUMO-AmdB for 2 h. All peaks shown here were collected together and used as a mixture.

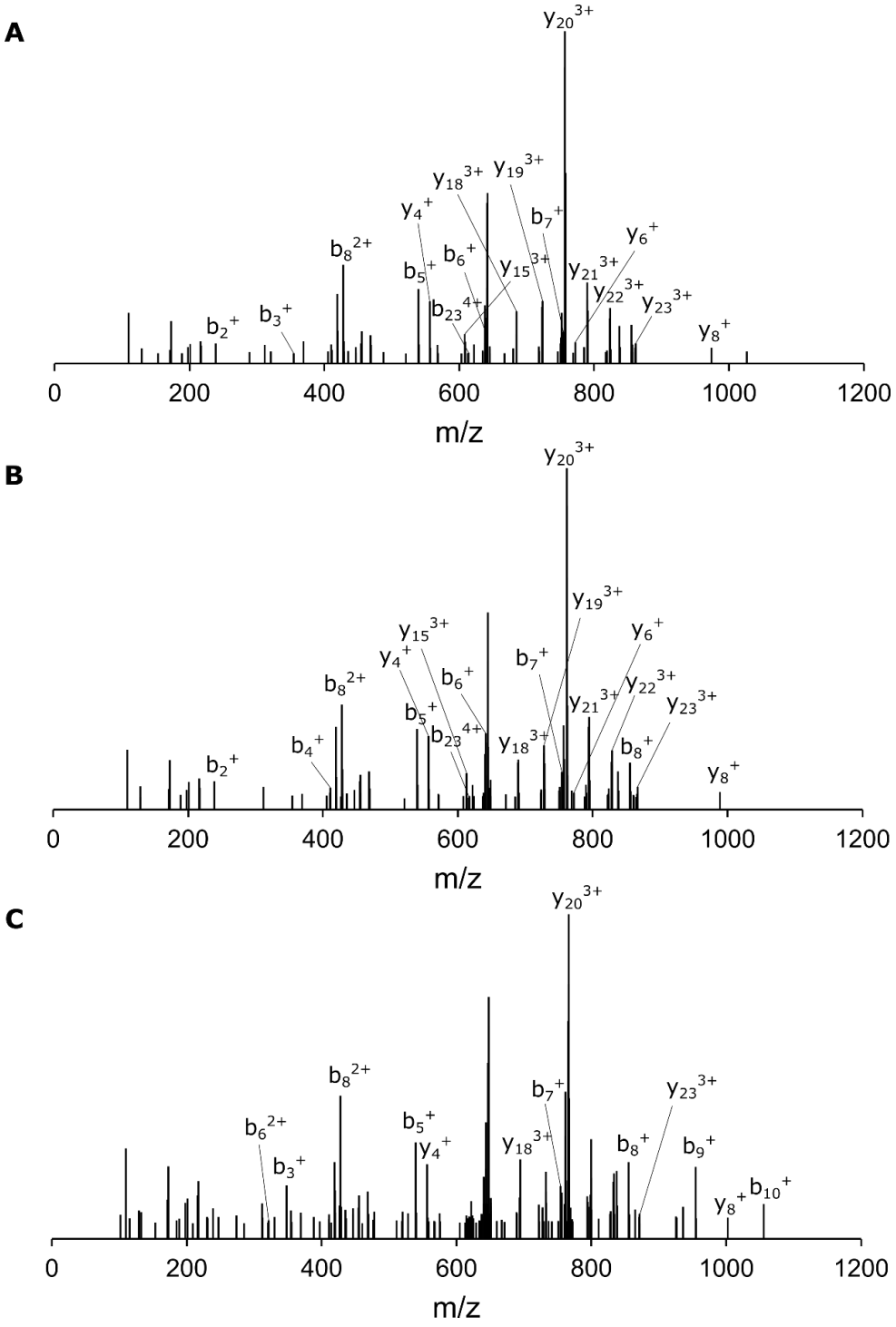

Figure S29: MS/MS spectra for pre-amycolimiditide intermediate core peptide hydrazinolyzed. **(A)** one-fold hydrazinolyzed peptide, **(B)** two-fold hydrazinolyzed peptide, **(C)** three-fold hydrazinolyzed peptide.

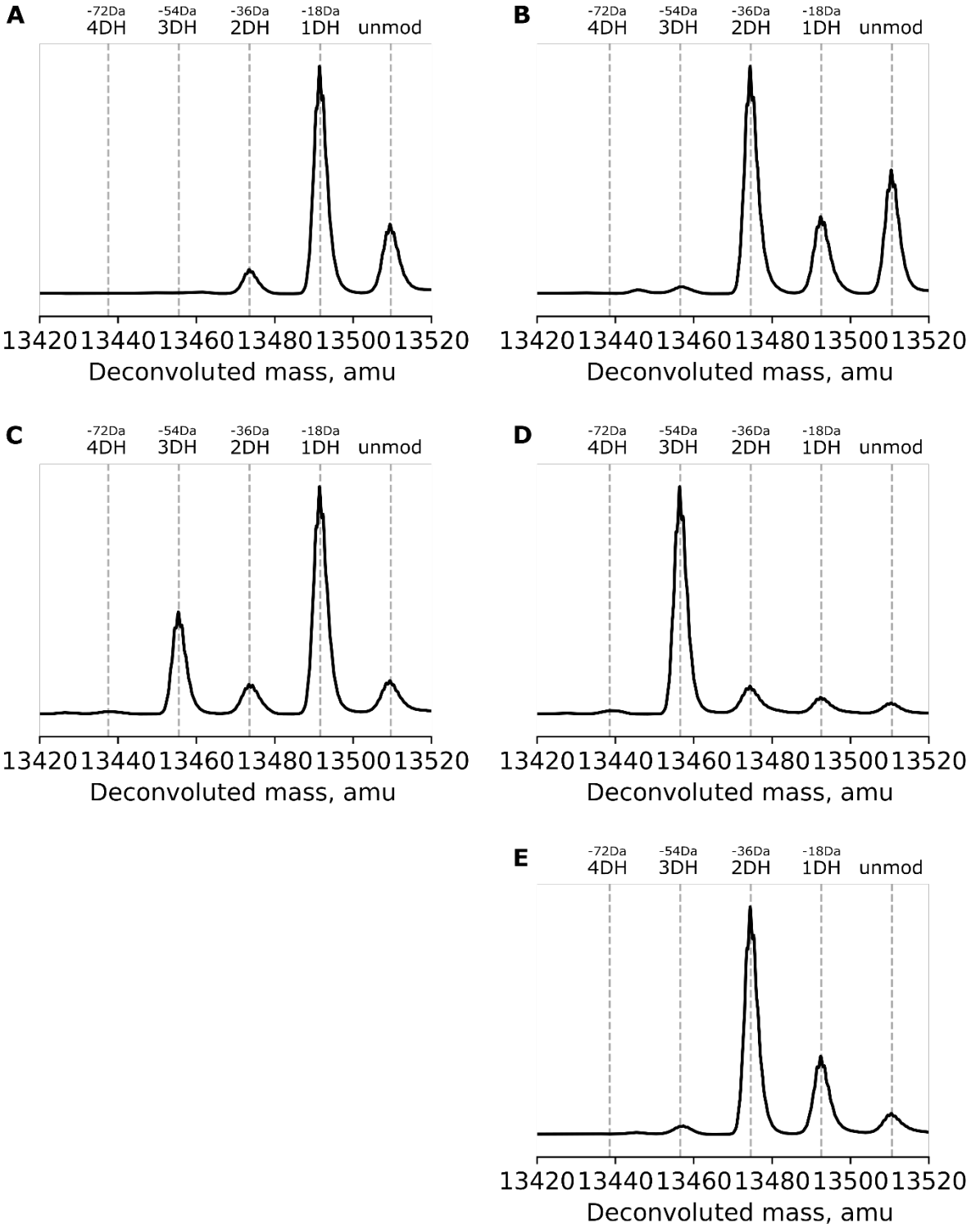

Figure S30: Deconvoluted mass spectra of AmdB-modified AmdA variants with single amino acid substitutions. **(A)** T10V and **(B)** D21N, intended to block the formation of I-ester linkage. **(C)** T8V and **(D)** D23N, intended to block the formation of II-ester linkage. **(E)** D25N, intended to block the formation of III-ester linkage.

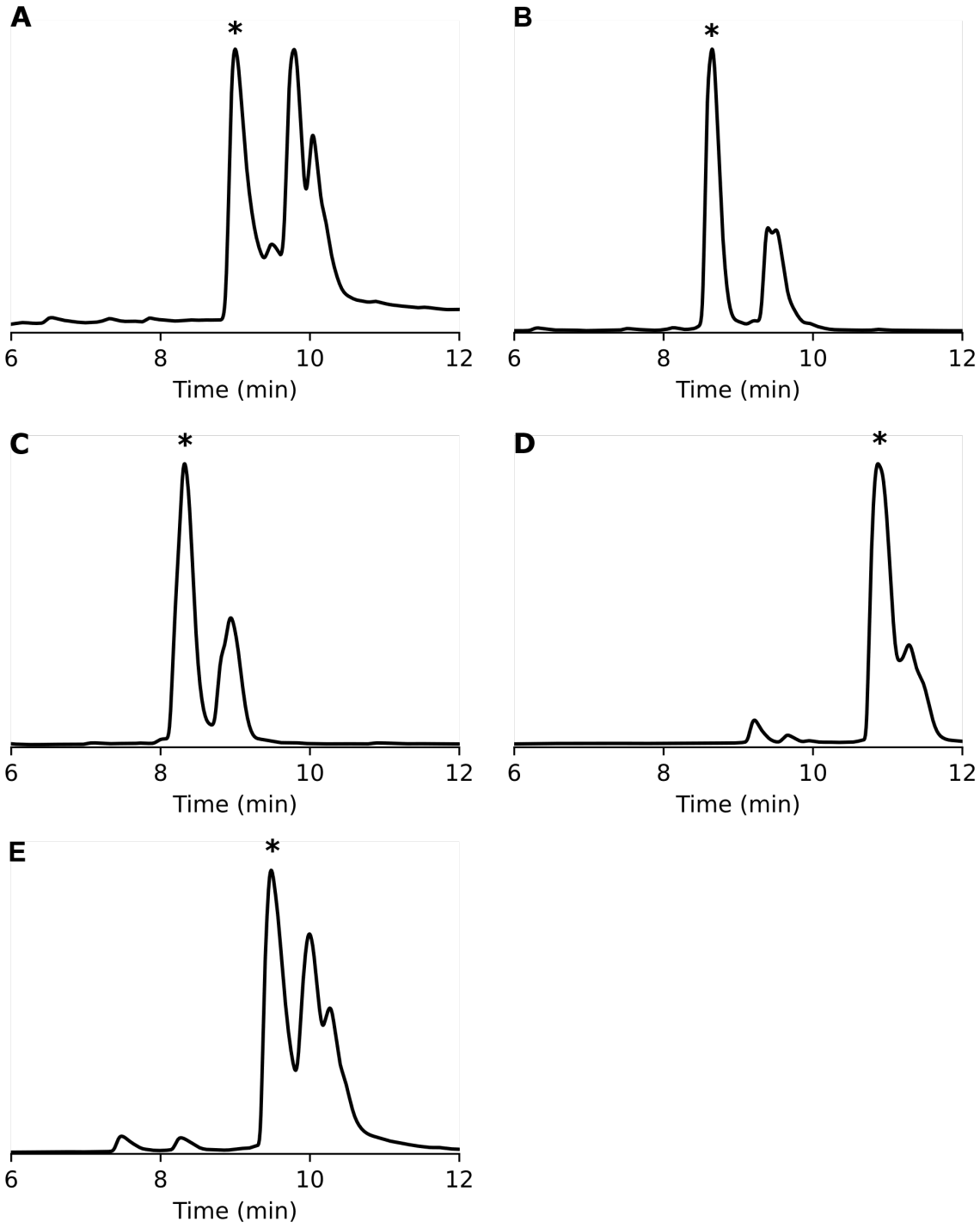

Figure S31: HPLC purification (215 nm absorbance) of the core peptides of AmdA variants with double amino acid substitutions modified by SUMO-AmdB. The purified proteins were trypsin digested prior to HPLC purification. **(A)** II-null, **(B)** III-null, **(C)** IV-null, **(D)** II,III-null, and **(E)** II,IV-null variants. The asterisks (*) indicate the peaks that were purified.

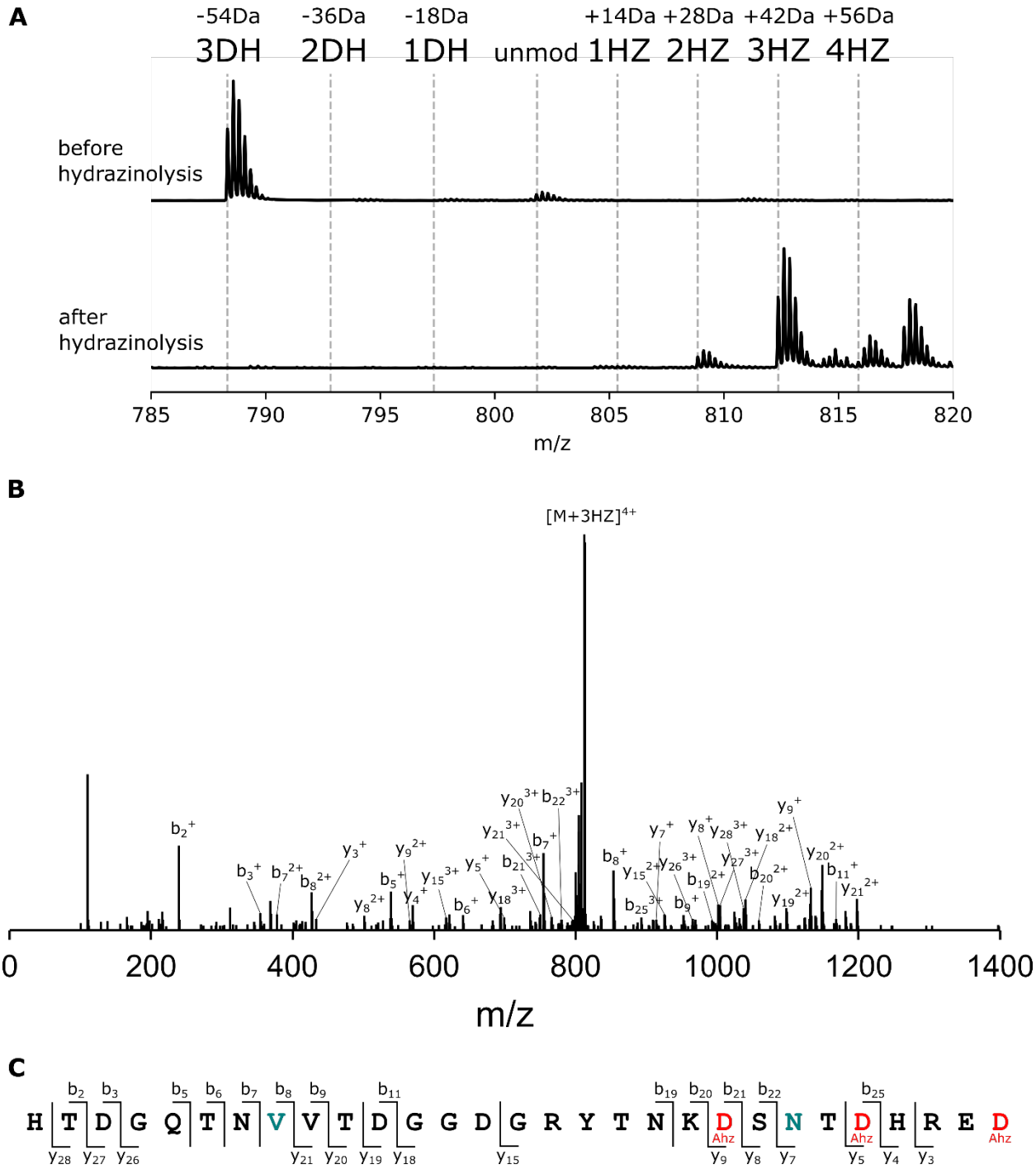

Figure S32: Determining the ω-ester linkages present in the II-null variant. **(A)** MS scan before (top) and after (bottom) hydrazinolysis. **(B)** MS/MS spectrum on the hydrazinolyzed core peptide with the identified *b* and *y* ions (**Table S12**) labelled at the corresponding peaks. The core peptide with 3 hydrazide adducts (3HZ) was selected for fragmentation (CID) at 30V, targeting m/z = 813 ± ~1.3, z = 4. **(C)** Schematics representing the MS/MS fragmentation pattern of the hydrazinolyzed core peptide.

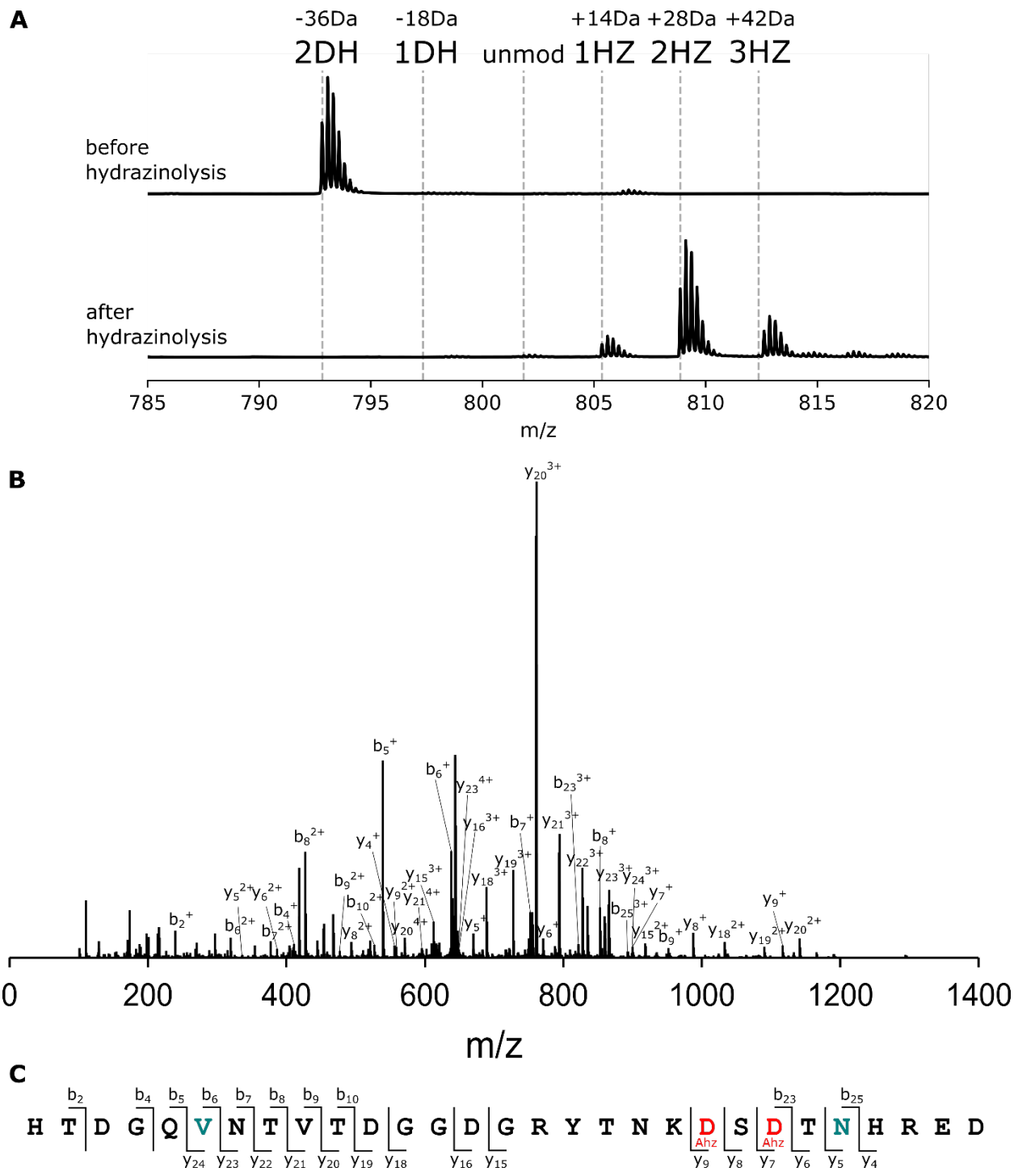

Figure S33: Determining the ω-ester linkages present in the III-null variant. **(A)** MS scan before (top) and after (bottom) hydrazinolysis. **(B)** MS/MS spectrum on the hydrazinolyzed core peptide with the identified *b* and *y* ions (**Table S13**) labelled at the corresponding peaks. The core peptide with 2 hydrazide adducts (2HZ) was selected for MS/MS fragmentation (m/z = 808 ± ~1.3). **(C)** Schematics representing the MS/MS fragmentation pattern of the hydrazinolyzed core peptide.

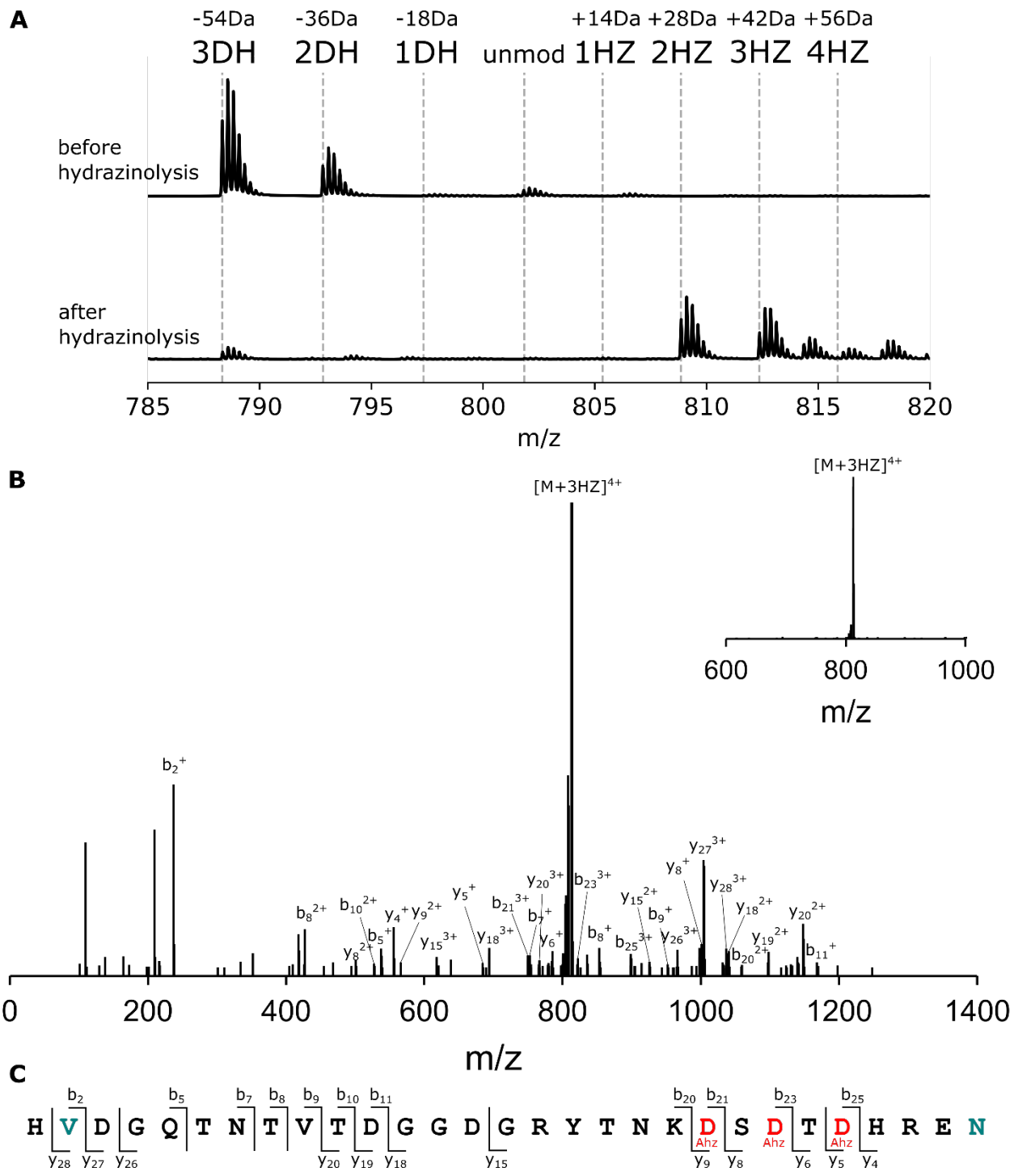

Figure S34: Determining the ω-ester linkages present in the IV-null variant. **(A)** MS scan before (top) and after (bottom) hydrazinolysis. **(B)** MS/MS spectrum on the hydrazinolyzed core peptide with the identified *b* and *y* ions (**Table S14**) labelled at the corresponding peaks. The core peptide with 3 hydrazide adducts (3HZ) was selected for MS/MS fragmentation (m/z = 813 ± ~1.3). **(C)** Schematics representing the MS/MS fragmentation pattern of the hydrazinolyzed core peptide.

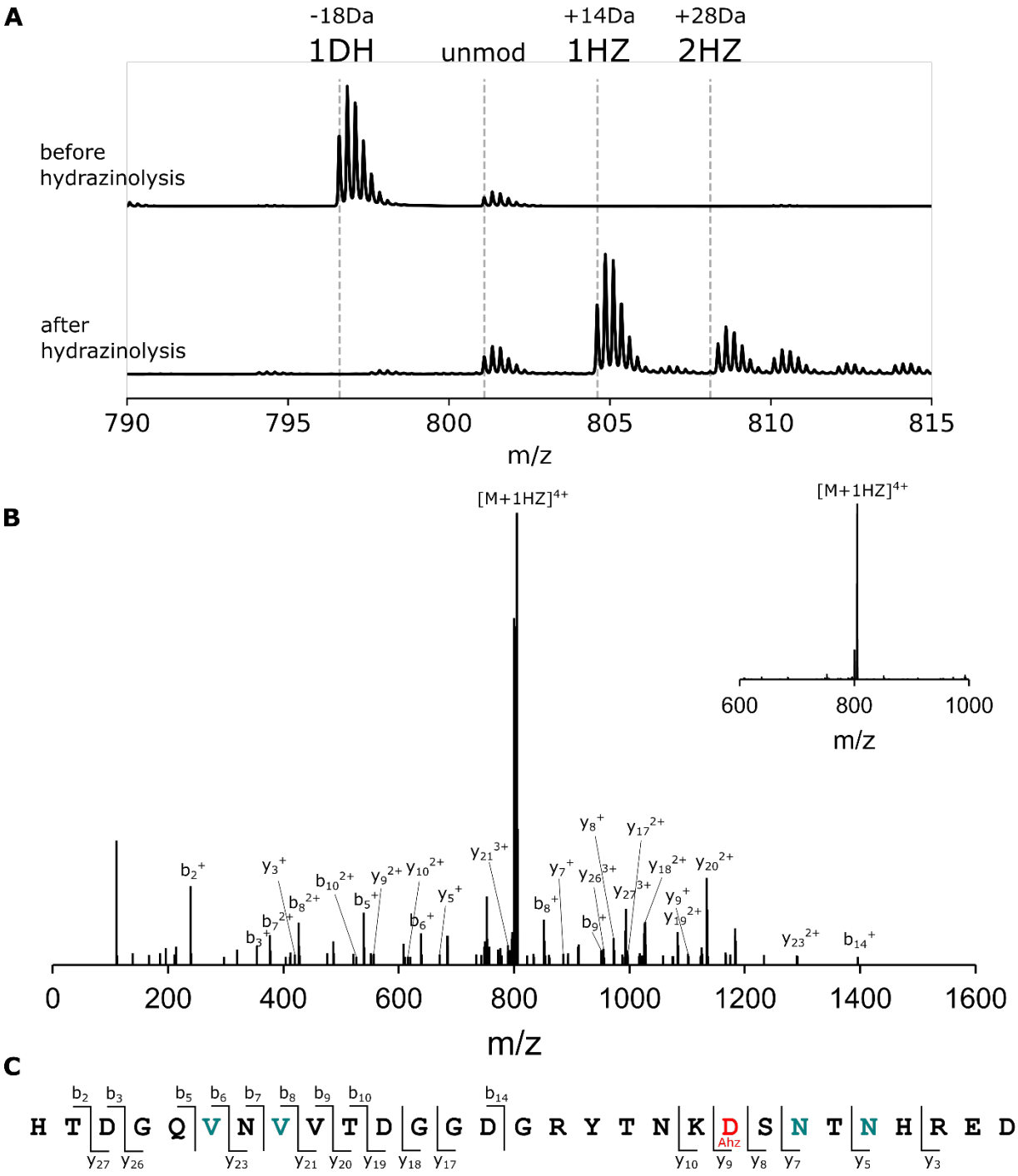

Figure S35: Determining the ω-ester linkages present in the II,III-null variant. **(A)** MS scan before (top) and after (bottom) hydrazinolysis. **(B)** MS/MS spectrum on the hydrazinolyzed core peptide with the identified *b* and *y* ions (**Table S15**) labelled at the corresponding peaks. The 1HZ peptide was selected for MS/MS fragmentation (m/z = 805 ± ~1.3). Only the bottom 20% of the y-axis is shown. (Inset) The same spectrum with the entire y-axis shown. **(C)** Schematics representing the MS/MS fragmentation pattern of the hydrazinolyzed core peptide.

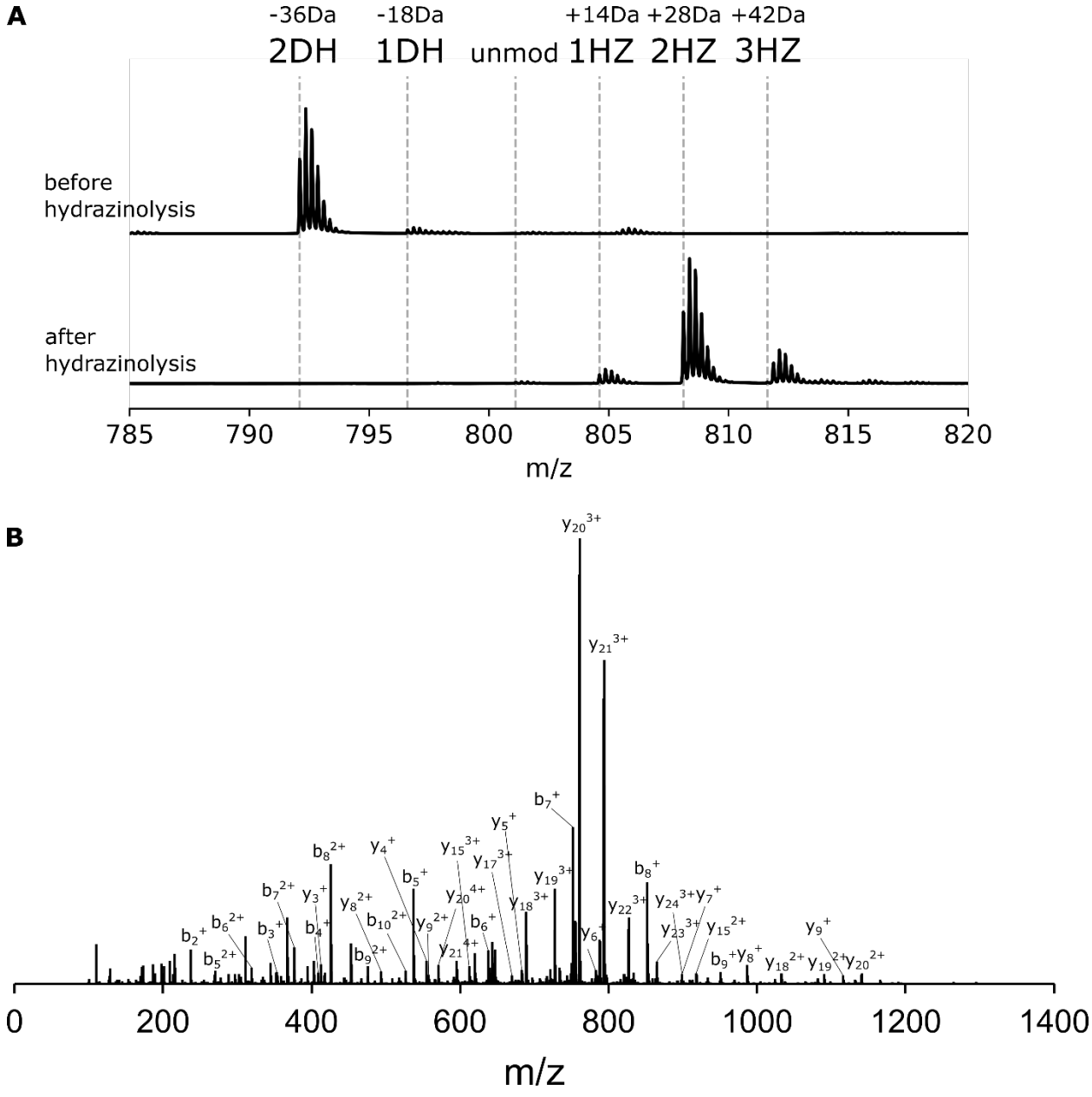

Figure S36: Determining the ω-ester linkages present in the II,IV-null variant. **(A)** MS scan (top) before and (bottom) after hydrazinolysis. **(B)** MS/MS spectrum on the hydrazinolyzed core peptide with the identified *b* and *y* ions (**Table S16**) labelled at the corresponding peaks. The core peptide with 2 hydrazide adducts (2HZ) was selected for MS/MS fragmentation (m/z = 808 ± ~1.3). **(C)** Schematics representing the MS/MS fragmentation pattern of the hydrazinolyzed core peptide.

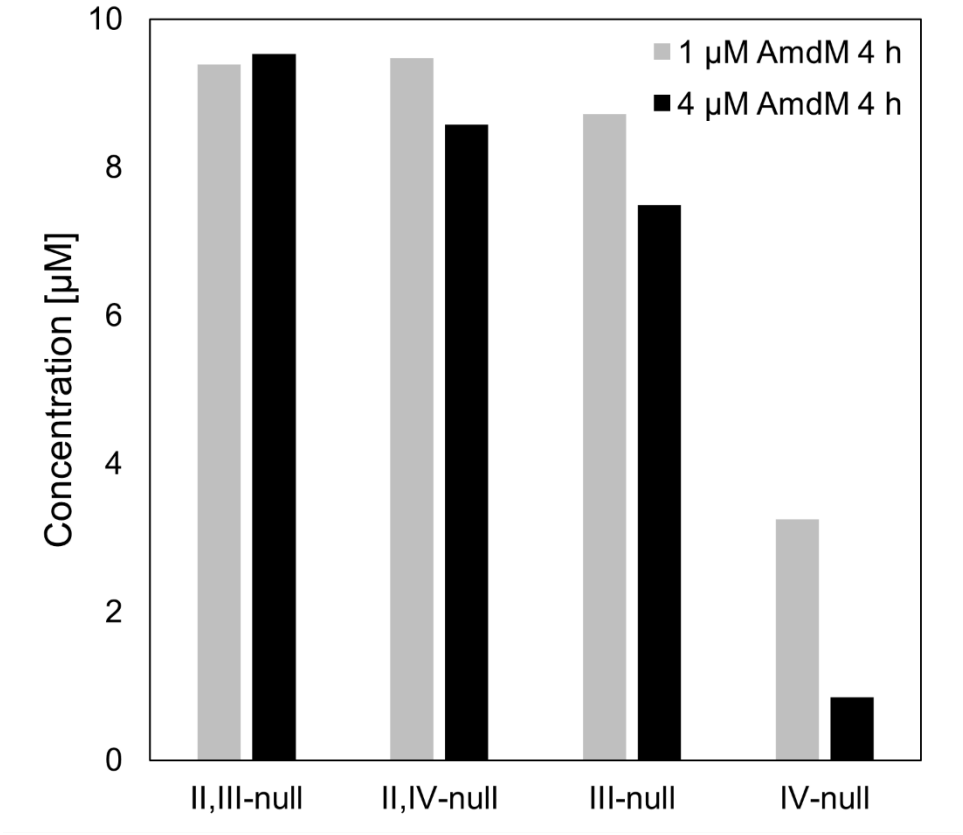

Figure S37: Comparison of *in vitro* aspartimidylation of pre-amycolimiditide variants with different concentrations of AmdM (1 μM, grey vs 4 μM, black). The y-axis values represent the concentrations of the pre-aspartimidylated species after 4 h of reaction. The data corresponding to 1 μM AmdM are identical to the data shown in Figure 5B from the main text. Increasing the enzyme concentration 4-fold improves methylation for the variants with two (II,IV-null and III-null variants) or three (IV-null variant) ester linkages, whereas no difference is observed for II,III-null variant, which has only one ester. This trend is consistent with the results of the heterologous expression experiments shown in Figure 5A from the main text.

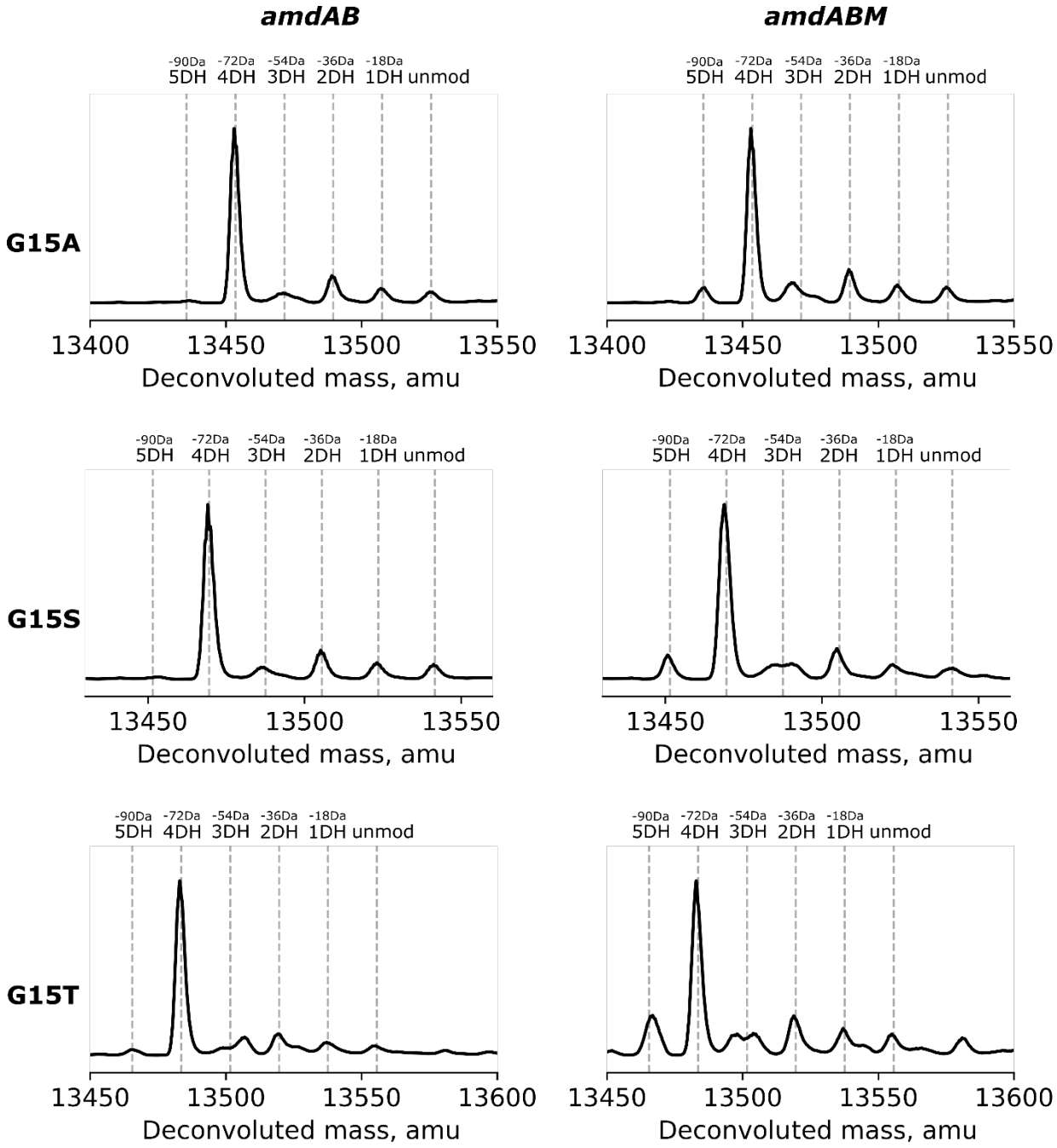

Figure S38: SUMO-AmdB and AmdM modified G15 variants. AmdA G15A (top), G15S (middle), G15T (bottom) variants co-expressed with SUMO-AmdB for 20 h (left) or SUMO-AmdB and AmdM for 24 h (right). Only small amounts of the proteins are aspartimidylated, showing that AmdM cannot modify the AmdA G15 variants efficiently.

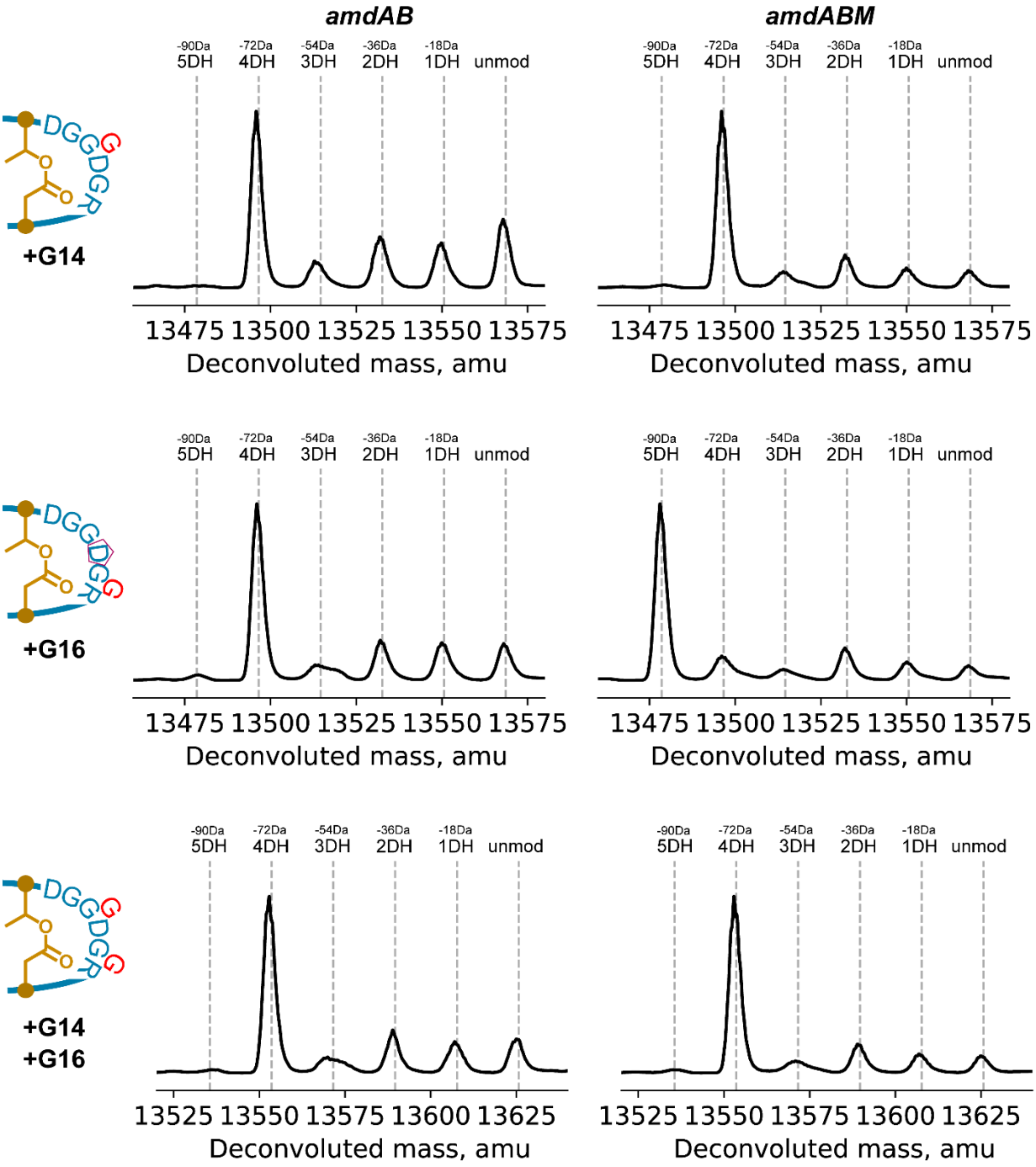

Figure S39: SUMO-AmdB and AmdM modified AmdA Gly insertion variants. AmdA +G14 (top, before the aspartimidylation site), +G16 (middle, after the aspartimidylation site), +G14+G16 (bottom) variants co-expressed with SUMO-AmdB for 20 h (left) or SUMO-AmdB and AmdM for 24 h (right). Only the +G16 variant can be aspartimidylated, showing that D14 must be the 14th residue to be aspartimidylated by AmdM.

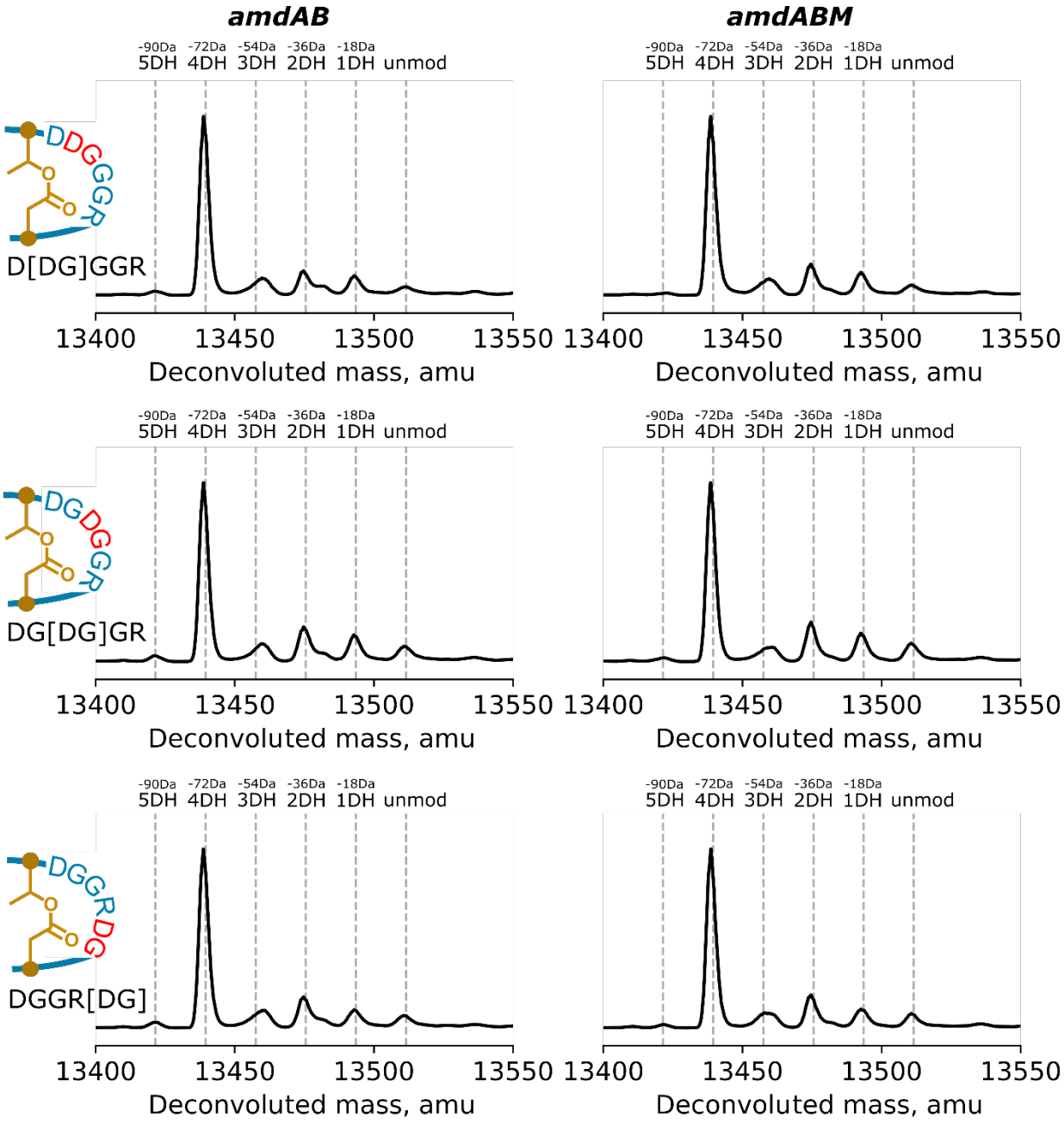

Figure S40: SUMO-AmdB and AmdM modified “DG-swap” variants. The first 6 aa in the loop of wild-type amycolimiditide are DGG[DG]R where the brackets indicate the aspartimidylation site. AmdA D[DG]GGR (top), DG[DG]GR (middle), DGGR[DG] (bottom) variants co-expressed with SUMO-AmdB for 20 h (left) or SUMO-AmdB and AmdM for 24 h (right). In these variants, the aspartimidylation site is placed at different locations on the loop. No aspartimidylation occurs for all of these variants, indicating that the location of the native aspartimidylation site is important for recognition by AmdM.

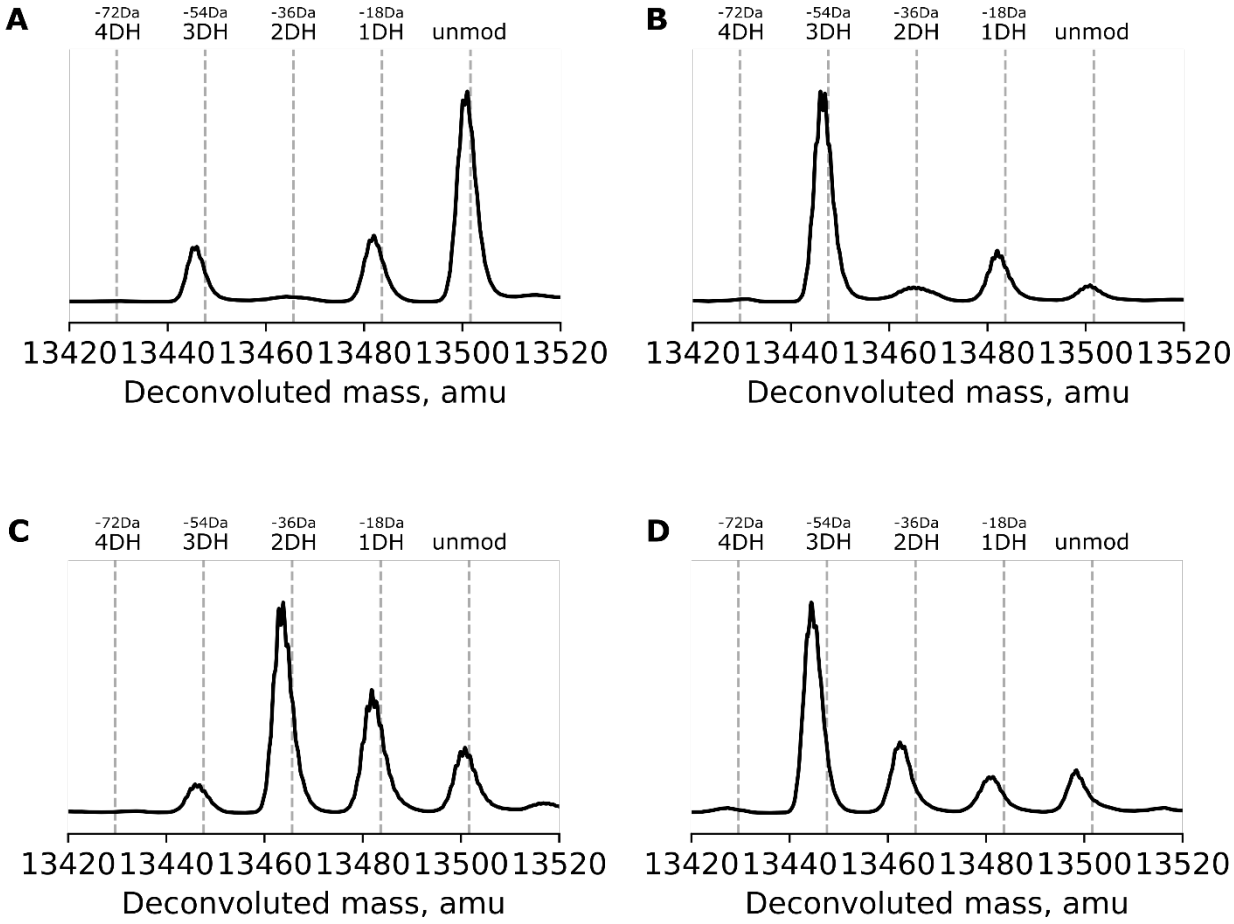

Figure S41: SUMO-AmdB modified AmdA disulfide variants. **(A)** I-disulfide, **(B)** II-disulfide, **(C)** III-disulfide, and **(D)** IV-disulfide variants co-expressed with SUMO-AmdB. The vertical dashed lines represent the calculated average masses for mAmdA^{B} with a varying number of dehydrations, without the disulfide bond formation. In *E. coli*, the disulfide variants are modified similarly to the null variants (Fig. 5A in the main text). The disulfide bonds observed in these peptides are presumed to form during protein purification rather than in the reducing *E. coli* cytoplasm.

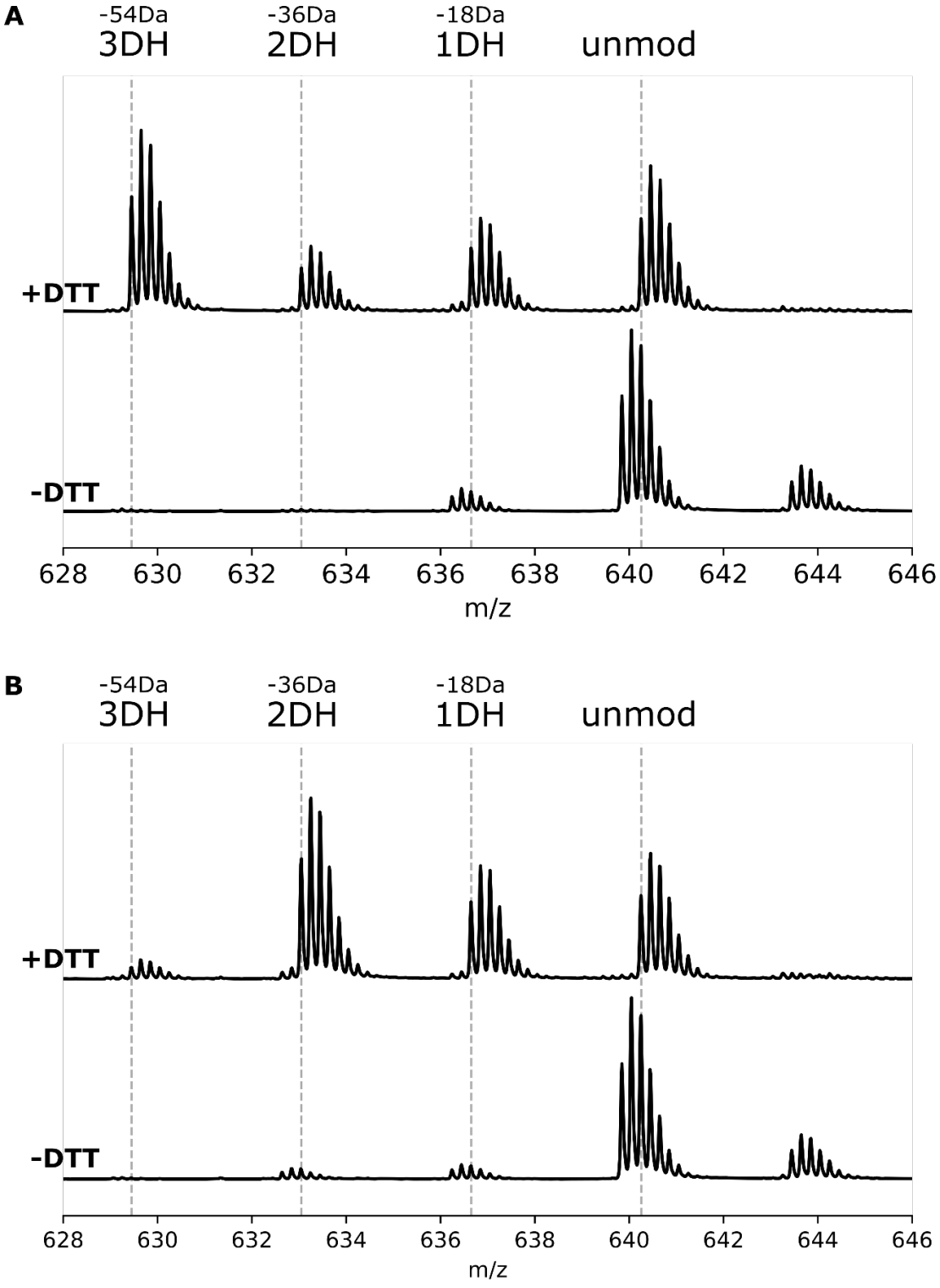

Figure S42: Trypsin digestion of AmdA **(A)** II-disulfide and **(B)** III-disulfide variants modified by His_6-SUMO-AmdB *in vitro*. These results show that DTT effectively prevents a disulfide bond from forming during the reaction. See also Fig. 6A in the main text.

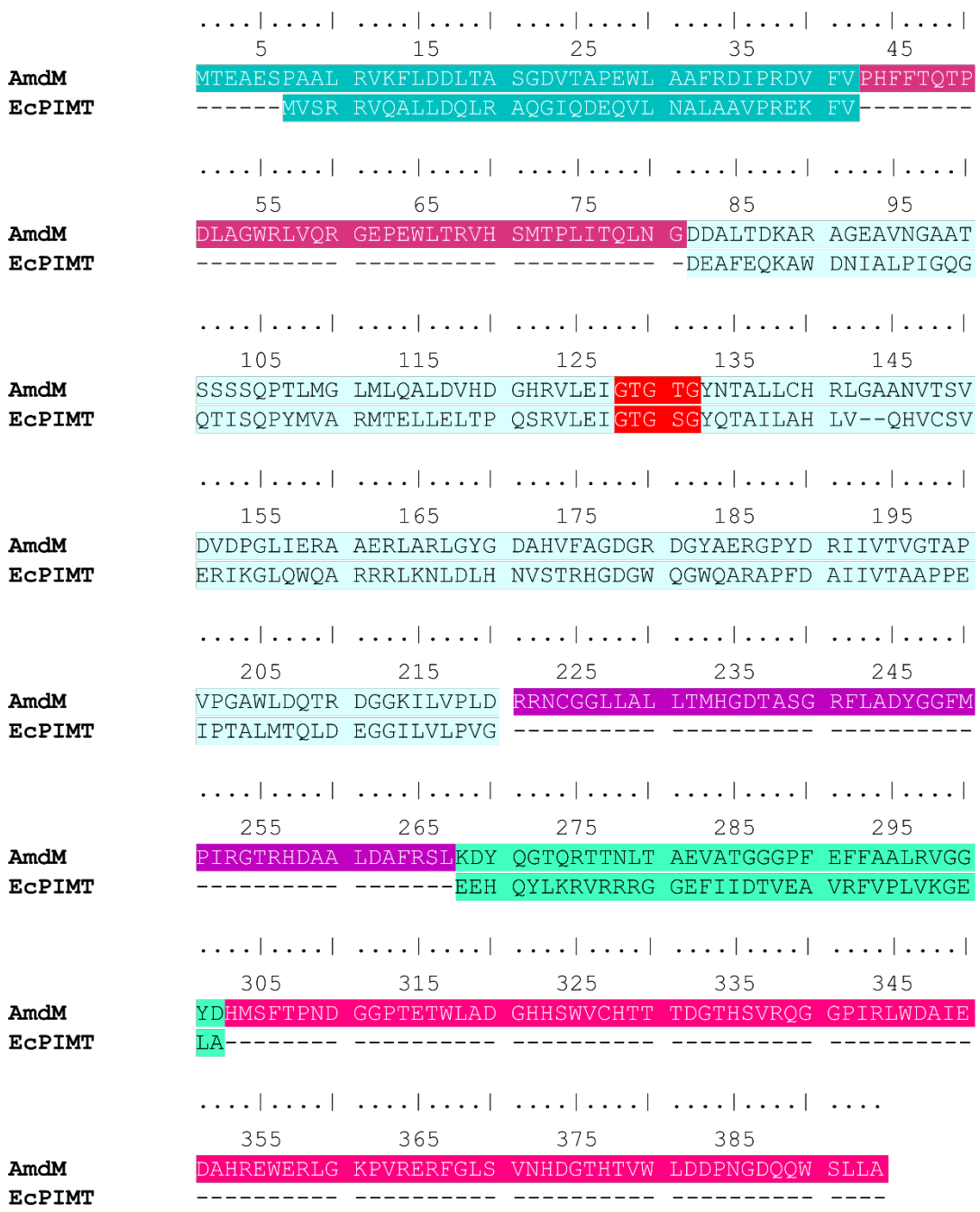

Figure S43: ClustalW sequence alignment of AmdM and EcPIMT. The background colors behind the sequences correspond to the colors of the protein structures shown in Fig. 7B (refer to the main text). In general, colors in a blue or green tone represent a segment of AmdM or EcPIMT sequence showing homology, and colors in a magenta tone represent a segment of AmdM sequence that is unique. The red GXGXG sequence is known to be a SAM binding site.

Supplementary Tables

Table S1: AmdA and its 29 homologs used for MEME.

	Accession Number	Origin	Protein Sequence
0	WP_141997876.1	Amycolatopsis cihanbeyliensis	MPVHQHERPTETGAFPSSGHFPLGRRFGMVDTAPEPASPVRPFGLTLGTRP RQVTPLNPADIGYDEDAQMGLMRDDGGQLVPMSRHTDGQTNTVTDGGDGRY TNKDSDTDHRED
1	MPZ83135.1	Actinophytocola sp.	MPLQQHERPTGAGVFPSSDHFPLGRRFGVVDATPEPASPMRPFGLTLGTRP RQVTPLNPADIGYDENAQVGLIRDDDGQLVRMGRHTDGQTGTVTDKGDGQS TNKDSDTDHRED
2	MBV9314006.1	Pseudonocardia sp.	MPVELHERRTGAGLFLSSDHFPLGRAYGHVNTTAESATLARPFGLTLAVRP RRVARLNPADLVYDEQNQVGLIRDGDELIKMGRHTDGQTNTQTNADGQNGP DSDTDWRED
3	WP_132875576.1	Tamaricihabitans halophyticus	MSIAKPEGRPGSVVFPASDQFPLGRAYGRVDSTGEPASTARPFGLTLGVRP KRVDRLNLAELSYDEEAQVGLLRHGGELVRLGRHTDGQTNTQTNSDGHQGY DSDTDHRED
4	PZS38665.1	Pseudonocardiales bacterium	MVDAAGTQRKAHHMKSREHPTGAVLCPTSDHFPLGRAYGRIDATPAPASDL RPFGLTLAVQPATSVRLDPAELGHDDVRKIGLIREGGKEMVPLSKHSDGST STLTDADGHGGRDSDTDHRED
5	MBV9010918.1	Pseudonocardiales bacterium	MSRTPLFPASDHFPLGRAYGCVQATPCPASGVRPFGLTLAVAPSAVRFDPG ELGYDDIRQVGLIRDGREMVPLARHTDGQTNTLTNADGHGGYDSDTDWRED
6	WP_207125195.1	Actinocatenispora comari	MYPTDAIDPLSTAPDQFSLGRPTALPHGDTAVSSAPRPFGATLAVEPNEVE AIDLEALSYDTERQIALIRDGSQVVPLARHTDGRTSTSTASRDGTPQDGDS DVRED
7	BCJ32534.1	Actinocatenispora thailandica	MHVTNTTDSLSTTPDQFPLGRSALPLATGIGSAACRPFGATLAVAPAETAA IELDALSYDADRQIGLIHDGDQVVPLARHTDGRTSTTTASRDGTPQDGDAD VRED
8	GID14923.1	Actinocatenispora rupis	MPATPTASAPVFRPDWLFQKEGRCAHPGSPRSEYDVHVLTPTCDPLSTVTD EFPLGRPALPLGDNEMPTAARPFGVTLAVEPTTVEPIDVNALSYDTHRQVG MIRDGEELVPLARHTDGRTSTTTASRDGTPQDGDEDTRED
9	WP_203662960.1	Actinocatenispora rupis	MFRPDWLFQKEGRCAHPGSPRSEYDVHVLTPTCDPLSTVTDEFPLGRPALP LGDNEMPTAARPFGVTLAVEPTTVEPIDVNALSYDTHRQVGMIRDGEELVP LARHTDGRTSTTTASRDGTPQDGDEDTRED
10	WP_203965230.1	Actinocatenispora thailandica	MGSAACRPFGATLAVAPAETAAIELDALSYDADRQIGLIHDGDQVVPLARH TDGRTSTTTASRDGTPQDGDADVRED
11	MBN1173025.1	Micromonosporaceae bacterium	MPTPASTADPLYPVSNQFPLGRPFGILPSGTDATLPAALPFGLRLAVTTPA ADIGDLSHYGYDHDQQIGVLHTEQGTVPLARHTTGQTRTVTHPDGHRGPDS DQDVRED
12	WP_221083949.1	Micromonospora tarapacensis	MLATTVPGRAGPADAARAPEADPLYPASGLFPLGRPFGLLPESDEVCPEEL LPFGLRRAVVGKPLPVGDLSAYGYDHDQQIGTVRDGDTVVPLMRHTTGQTS TTTNADGHKGPDSDTDHRED
13	OJF13460.1	Couchioplanes caeruleus subsp. caeruleus	MSPTAPVLSSPVTDDPLYPAAGFLPLGRPLGAVDGDDMAPTSADRRPFGLR FAVVPAHPIPVDLTTVRYDPDRQMAVDTTGAPVLGKHSTGATSTRTSDGHK SMDSDTDHTED
14	MBT8225494.1	Dactylosporangium sp.	MDTLTSPMTDPLYPTNGQFPLGRPFGIMPGGTDATPAEALPFGLRLAVTAP AADIENLDRYGYDHHRQIGVVHTHSGAVPLARHTTGQTRTVAHPDGHRGPD TDQDVRED
15	WP_211277811.1	Couchioplanes caeruleus	MTDDPLYPAAGFLPLGRPLGAVDGDDMAPTSADRRPFGLRFAVVPAHPIPV DLTTVRYDPDRQMAVDTTGAPVLGKHSTGATSTRTSDGHKSMDSDTDHTED
16	WP_018831371.1	Salinispora tropica	MTDDPLYPTAGHLPLGRPLDAVGSPDDVRPSSTDRRPFALRFATVPARPIP VNLTTVRYDPDRQMSVDPTGTPILGKHSTGATSTRTSDGHKSMDSDTDHTE D
17	WP_027661194.1	Salinispora fenicalii	MSPTSPVLSRPVTDDPLYPTAGYLPLGRPLDAVGSDDGAQPSSTDRRPFTL RFATVPARPIPVNLTTVRYDPDRQMSVDPTGTPVLGKHSTGATSTRTSDGH KSMDSDTDHTED
18	WP_028193085.1	Salinispora pacifica	MTDDPLYPTPGYLPLGRPLDAVGSDDDVQPSPTDRRPFALRFATVPARPIP VNLTTVRYDPDPQLSVDPTGTPVLGKHSTGATSTRTSDGHRSMDSDTDHTE D
19	WP_019900531.1	Salinispora arenicola	MAEDPLYPAAGYLPLGRPLDAVDSSDDVQPTSTDRRPFALRFATVPARPIP VDLTTVRYDPDRQMSVDRTGTPVLGKHSTGATSTRTSDGHKSMDADTDHTE D
20	ABP54871.1	Salinispora tropica CNB-440	MSPTSPVLSRPVTDDPLYPTAGYLPLGRPLDAVGSPDDVRPSSTDRRPFAL RFATVPARPIPVNLTTVRYDPDRQMSVDPTGTPILGKHSTGATSTRTSDGH KSMDSDTDHTED
21	WP_028565500.1	Salinispora tropica	MTDDPLYPTAGYLPLGRPLDAVGSPDDVRPSSTDRRPFALRFATVPARPIP VNLTTVRYDPDRQMSVDPTGTPILGKHSTGATSTRTSDGHKSMDSDTDHTE D

22	MPZ85240.1	Actinophytocola sp.	MSANTEALPGAHGIFPLGAYRGSTTVRDEPAARPFGLRFAAPPQPCESVPA ADFSSWDYDPDRQIAVVTEDGSRIEAAKHSTGPTQTPTNTGDGTRFERDED VTED
23	WP_018790314.1	Salinispora arenicola	MAEDPLYPAAGYLPLGRPLDAVDSSDDDAQPTSTDRRPFALRFATVPARPI PVDLTTVRYDPDRQMSVDRTGTPVLGKHSTGATSTRTSDGHKSMDADTDHT ED
24	NIL43132.1	Salinispora arenicola	MAEDPLYPAAGYLPLGRPLDAVDSSDDDAQPTSTDRRPFALRFATVPARPI PVDLTTVRYDPDRQMSVDPTGTPVLDKHSTGATSTRTSDGHKSMDADTDHT ED
25	WP_029024809.1	Salinispora arenicola	MAEDPLYPAAGYLPLGRPLDAVDSSDDDAQPTSTGRRPFALRFATVPARPI PVDLTTVRYDPDRQMSVDRTGTPVLGKHSTGATSTRTSDGHKSMDADTDHT ED
26	TQL38569.1	Salinispora arenicola	MFPTNPVLPSPMAEDPLYPAAGYLPLGRPLDAVDSSDDDAQPTSTGRRPFA LRFATVPARPIPVDLTTVRYDPDRQMSVDRTGTPVLGKHSTGATSTRTSDG HKSMDADTDHTED
27	MBI1759089.1	Actinomycetia bacterium	MGQFGLGRPFGLLPTSERVCAVEALPFGLRRAMVAATVSVGDLSAYGYDHD RQIGVIRDGDQEVPLLKHTTGQTRTTTNPDGQKGPDSDVDQRED
28	WP_038841753.1	Salinispora arenicola	MAEDPLYPAAGYLPLGRPLDAVDSSDDDAQASSTDRRPFALRFATVPARPI PVDLTTVRYDPDRQMSVDRTGTPVLGKHSTGATSTRTSDGHKSMDADTDHT ED
29	NYT94749.1	Salinispora sp. H7-4	MGEVWRCPDQPIPLGRPLDAVGSDDDVQPSPTDRRPFALRFATVPARPIPV NLTTVRYDPDRQLSVDPTGTPVLGKHSTGATSTRTSDGHESMDSDTDHTED

Table S2: Oligonucleotides used in this study.

Name	Sequence (5' -> 3')
oBC026	GCATGGTCTCTgatccCCCGTACACCAGCACG
oBC028	GCATGGTCTCTgatccGTTGGTGCAGCTCGTTCTGTGCTCGTGCTGAC
oBC029	CGATGGTCTCaagcttTCACGTCTTGTCGTATCCTTC
oBC031	CGATGGTCTCaagcttCTATGCGAGTAGGCTCCATTG
oBC032	GCATGGTCTCTaattcATTAAAGAGGAGAAATTAACTatg
oBC043	GCATcatatgCGGTGTGAAATACCGCAC
oBC044	ACGTGgttctcGCGGTATCATTGC
oBC045	GATACCGCgagaacCACGTTCACCGGCTCCAGATTTATC
oBC046	CGATggatccGTGATGGTGATG
oBC047	GCATggatccgagaccGAAAGTGAAACGTGATTTCATGC
oBC050	CGATAAGCTTgagaccTCATTTGTAGAGCTCATCCATGC
oBC054	CGATGGTCTCaagcttTCAATCCTCCCGATGGTC
oBC055	cgcacacattattaaataagatttacaaaatgttcaaaatgacgcatgaaatcacgtttc
oBC056	CTTATTTAATAATGTGTGCGgcaattcacatttaatttatgaatgttttcttaacatcgc
oBC057	ctagtagctaagatccgaacctgccgtttcttgagttgccgcgatgttaagaaaacattc
oBC058	CGGATCTTAGCTACTAGagaaagaggagaaatactagATGAGCAAAGGAGAAGAAC
oBC064	GCATGGTCTCTcatgTCGGACTCAGAAGTCAATC
oBC065	CGATGGTCTCAgtcacgtcttgtcgtatCCTTC
oBC066	CGATGGTCTCAcatgATCAATCCTCCCGATGG
oBC067	GCATGGTCTCTtgaccgaagctgaatccccg
oBC104	AATTCATTAAAGAGGAGAAATTAACTATGAGCGGATCGCATCACCATCACCATCACG
oBC105	GATCCGTGATGGTGATGGTGATGCGATCCGCTCATAGTTAATTTCTCCTCTTTAATG
oBC112	GCATGGTCTCGgatccaccgaagctgaatccccg
oBC118	GGCCGCTATCGCGGACGCTTTGGAAGGatacgacaagaca
oBC119	gtcatgtcttgtcgtatCCTTCCAAAGCGTCCGCGATAGC
oBC120	GCATaattTgagaccATTAAAGAGGAGAAATTAACTgaaagtgaaacgtgatttc
oBC121	CGATgatctgagacctataaacgc
oBC122	CGATGGTCTCaGATCCACCAATCTGTTCTC
oBC127	CGATGGTCTCaccacCACGGTGTTGGTCTG
oBC128	GCATGGTCTCggtggATGGAGGTGACGGCC
oBC129	CGATGGTCTCatattTTTGTTGGTGTACCGG
oBC130	GCATGGTCTCgaataGTGACACCGACCATC
oBC164	ggatccgagaccgaaagtgaaac
oBC165	aagcttgagacctataaacgc
oBC207	CGATggtctcaAACGTGACGACTCATCGGG
oBC208	GCATggtctcaCGTTGACGGCCAGACCAAC
oBC209	CGATggtctcaGTTCTCCCGATGGTCGG
oBC210	GCATggtctcaGAACTGATcatgTCGGACTCAG
oBC228	CGATggtctcaCATTACCTCCATCGGTCAC
oBC229	GCATggtctcaAATGGCCGGTACACCAAC
oBC230	CGATggtctcAaccaCCATCATCGGTCACGGTGTTG
oBC231	GCATggtctcAtggtGGCCGGTACACCAAC
oBC232	CGATggtctcAaccaTCACCATCGGTCACGGTGTTG
oBC233	CGATggtctcAaccaTCCCGACCTCCATCGGTCAC
oBC234	GCATggtctcAtggtTACACCAACAAAGACAGTGAC
oBC240	CGATggtctcAgagcGTCACCTCCATCGGTCAC
oBC241	GCATggtctcAgctcGGTACACCAACAAAGACAGTG
oBC255	CGATggtctcAgaccGCCGTCACCTCCATC
oBC256	GCATGGTCTCGggtcGGTACACCAACAAAGAC

oBC259	CGATggtctcAgaccgtcaccACCTCCATCGGTCAC
oBC260	CGATggtctcAgaccaccgtcaccACCTCCATCGGTCAC
oBC264	CGATggtctcAgggtGTCACCTCCATCGGTC
oBC265	GCATggtctcTacccGGTACACCAACAAAGAC
oBC266	CGATggtctcAgagaGTCACCTCCATCGGTC
oBC267	GCATggtctcTtctcGGTACACCAACAAAGAC
oBC271	GCATGGTCTCTgatccCCCGTACACC
oBC276	CGATggtctcAcgcaGTGACGACTCATCGGG
oBC277	GCATggtctcTtgcgACGGCCAGACCAAC
oBC278	CGATggtctcAagctTTCAGCACTCCCGATGGTCGGTG
oBC302	CGATGGTCTCTtaacCTGGCCGTCCGTGTG
oBC303	GCATGGTCTCTgttaACACCGTGACCGATG
oBC304	CGATGGTCTCTcaacGTTGGTCTGGCCGTC
oBC305	GCATGGTCTCTgttgTGACCGATGGAGGTG
oBC306	CGATGGTCTCTtgttACTGTCTTTGTTGGTGTACC
oBC307	GCATGGTCTCTaacaCCGACCATCGGG
oBC308	CGATGGTCTCTggttGGTGTCACTGTCTTTGTTG
oBC309	GCATGGTCTCTaaccATCGGGAGGATTGATC
oBC318	CGATGGTCTCTcacaCACGGTGTTGGTCTG
oBC319	TGTGATGGAGGTGACGGCCGGTACACCAACAAA
oBC320	TACATTTGTTGGTGTACCGGCCGTCACCTCCAT
oBC321	GCATGGTCTCTtgtaGTGACACCGACCATC
oBC326	GTTAACGTTGTGACCGATGGAGGTGACGGCCGGTACACCAACAAAGACAGTAACACC
oBC327	GGTTGGTGTTACTGTCTTTGTTGGTGTACCGGCCGTCACCTCCATCGGTCACAACGT
oBC340	CGATGGTCTCaagcttTCAATCCTCCCGATG
oBC341	CGATGGTCTCTcatgATCAGCACTCCCGATG
oBC342	CGATGGTCTCTcacaGTTGGTCTGGCCGTC
oBC343	TGTGTGACCGATGGAGGTGACGGCCGGTACACCAACAAAGACAGT
oBC344	TACAACTGTCTTTGTTGGTGTACCGGCCGTCACCTCCATCGGTCA
oBC345	GCATGGTCTCTtgtaCCGACCATCGGGAG
oBC346	CGATGGTCTCTtacaCTGGCCGTCCGTG
oBC347	TGTAACACCGTGACCGATGGAGGTGACGGCCGGTACACCAACAAAGACAGTGACACC
oBC348	GACAGGTGTCACTGTCTTTGTTGGTGTACCGGCCGTCACCTCCATCGGTCACGGTGT
oBC349	GCATGGTCTCTtgtcATCGGGAGGATTGATcatg

Table S3: Plasmids used and generated in this study.

Plasmid	Description and Purpose	Source
pQE-80	Expression vector with T5 promoter and AmpR marker	
pRSFDuet-1	Dual expression vector with T7 promoter and KanR marker, only MCS1 site used in this study	
pWC108	*panA*-LVPRGS-sfGFP-His, *panBCD* pQE-80; used in this study to amplify sfGFP	Cheung-Lee, et al. (2019)[5]
pYTK96	Yeast Toolkit (YTK) plasmid used for assembling a gene expression cassette to be integrated into the URA3 locus of *Saccharomyces cerevisiae* BY4741; used in this study to amplify PglpT-ffGFP	Lee, et al. (2015)[6]
pET-28b-SUMO	Expression vector with KanR marker for N-terminal SUMO-tag fusion of a protein	Darst Lab
pBC011	*amdABM*; His_6-mAmdA^{BM} biosynthesis; Native AmdB CDS; MRGSHHHHHHGS His_6-tag used	This study
pBC015	*amdA*; His_6-AmdA (unmodified) biosynthesis; MRGSHHHHHHGS His_6-tag used	This study
pBC016	*amdB*; His_6-AmdB expression for purification and *in vitro* reaction	This study
pBC019	*amdAB*; His_6-mAmdA^{B} biosynthesis; Native AmdB CDS; MRGSHHHHHHGS His_6-tag used	This study
pBC022	Modified pQE-80L with MCS replaced by sfGFP constitutive expression cassette flanked by *Bsa*I sites; *Bsa*I site in AmpR ablated	This study
pBC026	*amdB*; His_6-SUMO-AmdB expression for purification and *in vitro* reaction	This study
pBC031	*amdABM*; His_6-mAmdA^{BM} biosynthesis; MRGSHHHHHHGS His_6-tag used	This study
pBC032	*amdAB*; His_6-mAmdA^{B} biosynthesis; MRGSHHHHHHGS His_6-tag used	This study
pBC043	Modified pBC022 with His_6-tag modified to MSGSHHHHHHGS	This study
pBC044	*amdABM*; His_6-mAmdA^{BM} biosynthesis	This study
pBC045	*amdAB*; His_6-mAmdA^{B} biosynthesis	This study
pBC050	His_6-AmdM expression for purification and *in vitro* reaction	This study
pBC051	*amdABM*; His_6-mAmdA^{BM} biosynthesis	This study
pBC052	ffGFP-*amdBM*; Entry vector for a His_6-AmdA variant co-expression with SUMO-AmdB and AmdM	This study
pBC054	*amdA*; His_6-AmdA (unmodified) biosynthesis	This study
pBC071	*amdABM*; His_6-mAmdA(T10V)^{BM} biosynthesis	This study
pBC072	*amdABM*; His_6-mAmdA(D21N)^{BM} biosynthesis	This study
pBC108	Modified pQE-80 with MCS replaced by ffGFP constitutive expression cassette flanked by *Bsa*I sites; *Bsa*I recognition sequence in AmpR ablated; 6XHis-tag modified to MSGSHHHHHHGS	This study
pBC123	His_6-AmdA(T2V) in *amdABM*, for cloning His_6-mAmdA(T2V, D29N)	This study
pBC133	ffGFP-amdB; Entry vector for His_6-AmdA variant co-expression with SUMO-AmdB; 6XHis-tag: MSGSHHHHHHGS	This study
pBC135	*amdAB*; His_6-mAmdA(D14N)^{B} biosynthesis	This study
pBC136	*amdABM*; His_6-mAmdA(D14N)^{BM} biosynthesis	This study
pBC137	*amdABM*; His_6-mAmdA(G12D, D14G)^{BM} biosynthesis	This study
pBC138	*amdABM*; His_6-mAmdA(G13D, D14G)^{BM} biosynthesis	This study
pBC139	*amdABM*; His_6-mAmdA(D14R, G15D, R16G)^{BM} biosynthesis	This study
pBC140	*amdAB*; His_6-mAmdA(G12D, D14G)^{B} biosynthesis	This study
pBC141	*amdAB*; His_6-mAmdA(G13D, D14G)^{B} biosynthesis	This study
pBC142	*amdAB*; His_6-mAmdA(D14R, G15D, R16G)^{B} biosynthesis	This study
pBC147	*amdABM*; His_6-mAmdA(G15A)^{BM} biosynthesis	This study
pBC148	*amdAB*; His_6-mAmdA(G15A)^{B} biosynthesis	This study
pBC156	*amdA*; His_6-AmdA(T2C, D29C) expression	This study

pBC163	*amdABM*; His_6-mAmdA(+G16)^{BM} biosynthesis	This study
pBC167	*amdAB*; His_6-mAmdA(+G16)^{B} biosynthesis	This study
pBC169	*amdABM*; His_6-mAmdA(+G14)^{BM} biosynthesis	This study
pBC170	*amdABM*; His_6-mAmdA(+G14+G16)^{BM} biosynthesis	This study
pBC172	*amdABM*; His_6-mAmdA(G15T)^{BM} biosynthesis	This study
pBC173	*amdABM*; His_6-mAmdA(G15S)^{BM} biosynthesis	This study
pBC174	*amdAB*; His_6-mAmdA(G15T)^{B} biosynthesis	This study
pBC175	*amdAB*; His_6-mAmdA(G15S)^{B} biosynthesis	This study
pBC201	His_6-mAmdA(T6V) in *amdAB*, for cloning AmdA(T6V, D25N)	This study
pBC202	*amdAB*; His_6-mAmdA(T8V)^{B} biosynthesis	This study
pBC203	*amdAB*; His_6-mAmdA(T10V)^{B} biosynthesis	This study
pBC204	*amdAB*; His_6-mAmdA(D21N)^{B} biosynthesis	This study
pBC205	*amdAB*; His_6-mAmdA(D23N)^{B} biosynthesis	This study
pBC206	*amdAB*; His_6-mAmdA(D25N)^{B} biosynthesis	This study
pBC208	*amdABM*; His_6-mAmdA(T8V)^{BM} biosynthesis	This study
pBC209	*amdABM*; His_6-mAmdA(D23N)^{BM} biosynthesis	This study
pBC210	*amdABM*; His_6-mAmdA(D25N)^{BM} biosynthesis	This study
pBC215	*amdAB*; His_6-mAmdA(T10C, D21C)^{B} biosynthesis	This study
pBC216	*amdAB*; His_6-mAmdA(T10V, D21N)^{B} biosynthesis	This study
pBC217	*amdAB*; His_6-mAmdA(T8V, D23N)^{B} biosynthesis	This study
pBC218	*amdAB*; His_6-mAmdA(T6V, D25N)^{B} biosynthesis	This study
pBC219	*amdAB*; His_6-mAmdA(T2V, D29N)^{B} biosynthesis	This study
pBC220	*amdABM*; His_6-mAmdA(T10V, D21N)^{BM} biosynthesis	This study
pBC221	*amdABM*; His_6-mAmdA(T8V, D23N)^{BM} biosynthesis	This study
pBC222	*amdABM*; His_6-mAmdA(T6V, D25N)^{BM} biosynthesis	This study
pBC223	*amdABM*; His_6-mAmdA(T2V, D29N)^{BM} biosynthesis	This study
pBC226	*amdAB*; His_6-mAmdA(T6V, T8V, D23N, D25N)^{B} biosynthesis	This study
pBC231	*amdABM*; His_6-mAmdA(T6V, T8V, D23N, D25N)^{BM} biosynthesis	This study
pBC238	*amdAB*; His_6-mAmdA(T2V, T8V, D23N, D29N)^{B} biosynthesis	This study
pBC239	*amdABM*; His_6-mAmdA(T2V, T8V, D23N, D29N)^{BM} biosynthesis	This study
pBC242	*amdA*; His_6-mAmdA(T10C, D21C) expression	This study
pBC243	*amdAB*; His_6-mAmdA(T8C, D23C)^{B} biosynthesis	This study
pBC244	*amdAB*; His_6-mAmdA(T6C, D25C)^{B} biosynthesis	This study
pBC245	*amdA*; His_6-mAmdA(T8C, D23C) expression	This study
pBC246	*amdA*; His_6-mAmdA(T6C, D25C) expression	This study
pBC247	*amdAB*; His_6-mAmdA(T2C, D29C)^{B} biosynthesis	This study
pBC248	*amdAB*; His_6-mAmdA(+G14)^{B} biosynthesis	This study
pBC249	*amdAB*; His_6-mAmdA(+G14+G16)^{B} biosynthesis	This study

Table S4: Plasmids used in this study and their construction methodology.

Plasmid	Preparation Method for the Insert(s)	Vector	Assembly Method
pBC011	Insert 11-1: PCR on *A. cihanbeyliensis* DSM 45679 genomic DNA (German Collection of Microorganisms and Cell Cultures, DSMZ) using oBC026 and oBC031	pQE-80	Golden Gate Assembly (GGA) (pQE-80L pre-digested with *Bam*HI and *Hin*dIII)
pBC015	Insert 15-1: PCR on pBC011 using oBC026 and oBC054	pQE-80	Restriction digestion and ligation using *Bam*HI and *Hin*dIII
pBC016	Insert 16-1: PCR on pBC011 using oBC028 and oBC029	pQE-80	GGA (pQE-80L pre-digested with *Bam*HI and *Hin*dIII)
pBC019	Insert 19-1: PCR on pBC011 using oBC026 and oBC029	pQE-80	GGA (pQE-80L pre-digested with *Bam*HI and *Hin*dIII)
pBC022	Refer to pages 4-5 of this document	pQE-80	Refer to pages 4-5 of this document
pBC026	Insert 26-1: PCR on pBC011 using oBC028 and oBC029	pET-28b-SUMO	Restriction digestion and ligation using *Bam*HI and *Hin*dIII
pBC031	Insert 31-1: PCR on pBC020 using oBC026 and oBC066 Insert 31-2: PCR on pBC026 using oBC064 and oBC065 Insert 31-3: PCR on pBC020 using oBC067 and oBC031	pBC022	GGA
pBC032	Insert 32-1: PCR on pBC020 using oBC026 and oBC066 Insert 32-2: PCR on pBC026 using oBC064 and oBC029	pBC022	GGA
pBC043	Insert 43-1: oBC104 and oBC105 annealed	pBC022	Restriction digestion and ligation using *Bam*HI and *Eco*RI
pBC044	Insert 44-1: PCR on pBC031 using oBC026 and oBC031	pBC043	GGA
pBC045	Insert 45-1: PCR on pBC031 using oBC026 and oBC029	pBC043	GGA
pBC050	Insert 50-1: PCR on pBC011 using oBC112 and oBC031	pBC043	GGA
pBC051	Insert 51-1: PCR on pBC011 using oBC067 and oBC031 Insert 51-2: oBC118 and oBC119 annealed	pBC044	GGA (pBC044 pre-digested with *Not*I and *Hin*dIII)
pBC052	Insert 52-1: PCR on pYTK96[1] using oBC120 and oBC121	pBC051	GGA (pBC051 pre-digested with *Bam*HI and *Eco*RI)
pBC054	Insert 54-1: oBC104 and oBC105 annealed	pBC015	Restriction digestion and ligation using *Bam*HI and *Eco*RI
pBC071	Insert 71-1: PCR on pBC044 using oBC032 and oBC127 Insert 71-2: PCR on pBC044 using oBC128 and oBC122	pBC052	GGA
pBC072	Insert 72-1: PCR on pBC044 using oBC032 and oBC129 Insert 72-2: PCR on pBC044 using oBC130 and oBC122	pBC052	GGA
pBC108	Insert 108-1: PCR on pYTK96[1] using oBC164 and oBC165	pBC043	GGA (pBC043 pre-digested with *Bam*HI and *Hin*dIII)
pBC123	Insert 123-1: PCR on pBC044 using oBC032 and oBC207 Insert 123-2: PCR on pBC044 using oBC208 and oBC122	pBC052	GGA
pBC133	Insert 133-1: PCR on pYTK96[1] using oBC120 and oBC121	pBC045	GGA (pBC045 pre-digested with *Bam*HI and *Hin*dIII)
pBC135	Insert 135-1: PCR on pBC051 using oBC032 and oBC228 Insert 135-2: PCR on pBC051 using oBC229 and oBC122	pBC133	GGA
pBC136	Insert 136-1: PCR on pBC051 using oBC032 and oBC228 Insert 136-2: PCR on pBC051 using oBC229 and oBC122	pBC052	GGA
pBC137	Insert 137-1: PCR on pBC051 using oBC032 and oBC230 Insert 137-2: PCR on pBC051 using oBC231 and oBC122	pBC052	GGA
pBC138	Insert 138-1: PCR on pBC051 using oBC032 and oBC232 Insert 138-2: PCR on pBC051 using oBC231 and oBC122	pBC052	GGA
pBC139	Insert 139-1: PCR on pBC051 using oBC032 and oBC233 Insert 139-2: PCR on pBC051 using oBC234 and oBC122	pBC052	GGA
pBC140	Insert 140-1: PCR on pBC051 using oBC032 and oBC230 Insert 140-2: PCR on pBC051 using oBC231 and oBC122	pBC133	GGA
pBC141	Insert 141-1: PCR on pBC051 using oBC032 and oBC232 Insert 141-2: PCR on pBC051 using oBC231 and oBC122	pBC133	GGA
pBC142	Insert 142-1: PCR on pBC051 using oBC032 and oBC233 Insert 142-2: PCR on pBC051 using oBC234 and oBC122	pBC133	GGA
pBC147	Insert 147-1: PCR on pBC051 using oBC032 and oBC240 Insert 147-2: PCR on pBC051 using oBC241 and oBC122	pBC052	GGA
pBC148	Insert 148-1: PCR on pBC051 using oBC032 and oBC240	pBC133	GGA

	Insert 148-2: PCR on pBC051 using oBC241 and oBC122		
pBC156	Insert 156-1: PCR on pBC051 using oBC271 and oBC276 Insert 156-2: PCR on pBC051 using oBC277 and oBC278	pBC108	GGA
pBC163	Insert 163-1: PCR on pBC051 using oBC032 and oBC255 Insert 163-2: PCR on pBC051 using oBC256 and oBC122	pBC052	GGA
pBC167	Insert 167-1: PCR on pBC051 using oBC032 and oBC255 Insert 167-2: PCR on pBC051 using oBC256 and oBC122	pBC133	GGA
pBC169	Insert 169-1: PCR on pBC051 using oBC032 and oBC259 Insert 169-2: PCR on pBC051 using oBC256 and oBC122	pBC052	GGA
pBC170	Insert 170-1: PCR on pBC051 using oBC032 and oBC260 Insert 170-2: PCR on pBC051 using oBC256 and oBC122	pBC052	GGA
pBC172	Insert 172-1: PCR on pBC051 using oBC261 and oBC264 Insert 172-2: PCR on pBC051 using oBC265 and oBC122	pBC052	GGA
pBC173	Insert 173-1: PCR on pBC051 using oBC032 and oBC266 Insert 173-2: PCR on pBC051 using oBC267 and oBC122	pBC052	GGA
pBC174	Insert 174-1: PCR on pBC172 using oBC032 and oBC122	pBC133	GGA
pBC175	Insert 175-1: PCR on pBC173 using oBC032 and oBC122	pBC133	GGA
pBC201	Insert 201-1: PCR on pBC051 using oBC032 and oBC302 Insert 201-2: PCR on pBC051 using oBC303 and oBC122	pBC133	GGA
pBC202	Insert 202-1: PCR on pBC051 using oBC032 and oBC304 Insert 202-2: PCR on pBC051 using oBC305 and oBC122	pBC133	GGA
pBC203	Insert 203-1: PCR on pBC051 using oBC032 and oBC127 Insert 203-2: PCR on pBC051 using oBC128 and oBC122	pBC133	GGA
pBC204	Insert 204-1: PCR on pBC051 using oBC032 and oBC129 Insert 204-2: PCR on pBC051 using oBC130 and oBC122	pBC133	GGA
pBC205	Insert 205-1: PCR on pBC051 using oBC032 and oBC306 Insert 205-2: PCR on pBC051 using oBC307 and oBC122	pBC133	GGA
pBC206	Insert 206-1: PCR on pBC051 using oBC032 and oBC308 Insert 206-2: PCR on pBC051 using oBC309 and oBC122	pBC133	GGA
pBC208	Insert 208-1: PCR on pBC051 using oBC032 and oBC304 Insert 208-2: PCR on pBC051 using oBC305 and oBC122	pBC052	GGA
pBC209	Insert 209-1: PCR on pBC051 using oBC032 and oBC306 Insert 209-2: PCR on pBC051 using oBC307 and oBC122	pBC052	GGA
pBC210	Insert 210-1: PCR on pBC051 using oBC032 and oBC308 Insert 210-2: PCR on pBC051 using oBC309 and oBC122	pBC052	GGA
pBC215	Insert 215-1: PCR on pBC051 using oBC032 and oBC318 Insert 215-2: PCR on pBC051 using oBC321 and oBC122 Insert 215-3: oBC319 and oBC320 annealed	pBC133	GGA
pBC216	Insert 216-1: PCR on pBC203 using oBC032 and oBC129 Insert 216-2: PCR on pBC203 using oBC130 and oBC122	pBC133	GGA
pBC217	Insert 217-1: PCR on pBC202 using oBC032 and oBC306 Insert 217-2: PCR on pBC202 using oBC307 and oBC122	pBC133	GGA
pBC218	Insert 218-1: PCR on pBC201 using oBC032 and oBC308 Insert 218-2: PCR on pBC201 using oBC309 and oBC122	pBC133	GGA
pBC219	Insert 219-1: PCR on pBC123 using oBC032 and oBC209 Insert 219-2: PCR on pBC123 using oBC210 and oBC122	pBC133	GGA
pBC220	Insert 220-1: PCR on pBC203 using oBC032 and oBC129 Insert 220-2: PCR on pBC203 using oBC130 and oBC122	pBC052	GGA
pBC221	Insert 221-1: PCR on pBC202 using oBC032 and oBC306 Insert 221-2: PCR on pBC202 using oBC307 and oBC122	pBC052	GGA
pBC222	Insert 222-1: PCR on pBC201 using oBC032 and oBC308 Insert 222-2: PCR on pBC201 using oBC309 and oBC122	pBC052	GGA
pBC223	Insert 223-1: PCR on pBC123 using oBC032 and oBC209 Insert 223-2: PCR on pBC123 using oBC210 and oBC122	pBC052	GGA
pBC226	Insert 226-1: PCR on pBC051 using oBC032 and oBC302 Insert 226-2: PCR on pBC051 using oBC309 and oBC122 Insert 226-3: oBC326 and oBC327 annealed	pBC133	GGA
pBC231	Insert 231-1: PCR on pBC051 using oBC032 and oBC302 Insert 231-2: PCR on pBC051 using oBC309 and oBC122 Insert 231-3: oBC326 and oBC327 annealed	pBC052	GGA
pBC238	Insert 238-1: PCR on pBC217 using oBC032 and oBC207 Insert 238-2: PCR on pBC217 using oBC208 and oBC209	pBC133	GGA
pBC239	Insert 239-1: PCR on pBC217 using oBC032 and oBC207 Insert 239-2: PCR on pBC217 using oBC208 and oBC209	pBC052	GGA
pBC242	Insert 242-1: PCR on pBC215 using oBC026 and oBC054	pBC108	GGA
pBC243	Insert 243-1: PCR on pBC051 using oBC032 and oBC342 Insert 243-2: PCR on pBC051 using oBC345 and oBC122	pBC133	GGA

	Insert 243-3: oBC343 and oBC344 annealed		
pBC244	Insert 244-1: PCR on pBC051 using oBC032 and oBC346 Insert 244-2: PCR on pBC051 using oBC349 and oBC122 Insert 244-3: oBC347 and oBC348 annealed	pBC133	GGA
pBC245	Insert 245-1: PCR on pBC243 using oBC271 and oBC340	pBC108	GGA
pBC246	Insert 246-1: PCR on pBC244 using oBC271 and oBC340	pBC108	GGA
pBC247	Insert 247-1: PCR on pBC156 using oBC032 and oBC341 Insert 247-2: PCR on pBC051 using oBC64 and oBC122	pBC133	GGA
pBC248	Insert 248-1: PCR on pBC169 using oBC032 and oBC122	pBC133	GGA
pBC249	Insert 249-1: PCR on pBC170 using oBC032 and oBC122	pBC133	GGA

Table S5: Amycolimiditide variant core sequences.

Name	AA Substitutions	Core Sequence
WT		HTDGQTNTVTDGGDGRYTNKDSDTDHRED
I-null	T10V, D21N	HTDGQTNTVVDGGDGRYTNKNSDTDHRED
II-null	T8V, D23N	HTDGQTNVVTDGGDGRYTNKDSNTDHRED
III-null	T6V, D25N	HTDGQVNTVTDGGDGRYTNKDSDTNHRED
IV-null	T2V, D29N	HVDGQTNTVTDGGDGRYTNKDSDTDHRENN
II,III-null	T6V, T8V, D23N, D25N	HTDGQVNVVTDGGDGRYTNKDSNTNHRED
II,IV-null	T2V, T8V, D23N, D29N	HVDGQTNVVTDGGDGRYTNKDSNTDHRENN
	T8V	HTDGQTNVVTDGGDGRYTNKDSDTDHRED
	T10V	HTDGQTNTVVDGGDGRYTNKDSDTDHRED
	D21N	HTDGQTNTVTDGGDGRYTNKNSDTDHRED
	D23N	HTDGQTNTVTDGGDGRYTNKDSNTDHRED
	D25N	HTDGQTNTVTDGGDGRYTNKDSDTNHRED
I-disulfide	T10C, D21C	HTDGQTNTVCDGGDGRYTNKCSDTDHRED
II-disulfide	T8C, D23C	HTDGQTNCVTDGGDGRYTNKDSCTDHRED
III-disulfide	T6C, D25C	HTDGQCNTVTDGGDGRYTNKDSDTCHRED
IV-disulfide	T2C, D29C	HCDGQTNTVTDGGDGRYTNKDSDTDHRECC
	D14N	HTDGQTNTVTDGGNGRYTNKDSDTDHRED
D[DG]GGR	G12D, D14G	HTDGQTNTVTDDGGGGRYTNKDSDTDHRED
DG[DG]GR	G13D, D14G	HTDGQTNTVTDGDGGGRYTNKDSDTDHRED
DGGR[DG]	D14R, G15D, R16G	HTDGQTNTVTDGGRDGGYTNKDSDTDHRED
	G15A	HTDGQTNTVTDGGDARYTNKDSDTDHRED
	G15T	HTDGQTNTVTDGGDTRYTNKDSDTDHRED
	G15S	HTDGQTNTVTDGGDSRYTNKDSDTDHRED
	+G16	HTDGQTNTVTDGGDGGRYTNKDSDTDHRED
	+G14	HTDGQTNTVTDGGGDGRYTNKDSDTDHRED
	+G14+G16	HTDGQTNTVTDGGGDGGRYTNKDSDTDHRED

Table S6: Chemical shift assignments for amycolimiditide.

RESIDUE	^{1}H ATOM	CHEMICAL SHIFT (PPM)	^{13}C ATOM	CHEMICAL SHIFT (PPM)
HIS1	H	7.345		
HIS1	HA	4.507	CA	49.864
HIS1	HB2	3.471	CB	26.381
HIS1	HB3	3.373		
THR2	H	8.453		
THR2	HA	4.683	CA	unresolved
THR2	HB	5.280	CB	72.762
THR2	QG2	1.163	CG	16.358
ASP3	H	8.850		
ASP3	HA	4.996	CA	50.060
ASP3	HB2	2.806	CB	36.557
ASP3	HB3	2.649		
GLY4	H	8.374		
GLY4	HA2	4.233	CA	42.428
GLY4	HA3	3.686		
GLN5	H	8.635		
GLN5	HA	4.585	CA	unresolved
GLN5	QB	1.984	CB	27.751
GLN5	QG	2.258	CG	32.052
THR6	H	8.092		
THR6	HA	4.664	CA	unresolved
THR6	HB	5.137	CB	72.955
THR6	QG2	0.928	CG	16.206
ASN7	H	8.993		
ASN7	HA	5.192	CA	50.255
ASN7	HB2	2.728	CB	38.123
ASN7	HB3	2.591		
THR8	H	8.120		
THR8	HA	4.742	CA	unresolved
THR8	HB	5.172	CB	72.892
THR8	QG2	0.850	CG	18.378
VAL9	H	8.854		
VAL9	HA	4.468	CA	58.866
VAL9	HB	1.848	CB	31.469
VAL9	QQG	0.870	CG	16.206
THR10	H	7.996		
THR10	HA	4.644	CA	unresolved
THR10	HB	5.236	CB	72.368
THR10	QG2	0.889	CG	18.554
ASP11	H	8.873		
ASP11	HA	4.664	CA	unresolved

ASP11	HB2	2.771	CB	35.773
ASP11	HB3	2.757		
GLY12	H	8.178		
GLY12	HA2	3.901	CA	42.819
GLY12	HA3	3.764		
GLY13	H	8.126	C	171.484
GLY13	QA	3.862	CA	42.036
ASP14	H	8.572	C	177.257
ASP14	HA	4.583	CA	49.081
ASP14	HB2	3.138	CB	34.600
ASP14	HB3	2.747	CO	176.866
GLY15	HA2	4.238	C	168.745
GLY15	HA3	4.205	CA	41.058
ARG16	H	8.436		
ARG16	HA	4.018	CA	54.560
ARG16	HB2	1.495	CB	27.360
ARG16	HB3	1.451		
ARG16	QG	1.163	CG	23.837
ARG16	QD	2.943	CD	40.471
ARG16	HE	6.935		
TYR17	H	7.836		
TYR17	HA	4.527	CA	54.952
TYR17	HB2	3.119	CB	35.579
TYR17	HB3	2.825		
TYR17	QD	7.042	CD	130.490
TYR17	QE	6.737	CE	115.421
THR18	H	7.597		
THR18	HA	4.214	CA	58.866
THR18	HB	4.077	CB	67.085
THR18	QG2	1.026	CG	18.750
ASN19	H	8.218		
ASN19	HA	4.644	CA	unresolved
ASN19	HB2	2.720	CB	36.557
ASN19	HB3	2.630		
LYS20	H	8.141		
LYS20	HA	4.468	CA	53.386
LYS20	QB	1.652	CB	31.078
LYS20	QG	1.359	CG	22.272
LYS20	HD2	1.574	CD	26.376
LYS20	HD3	1.535		
LYS20	QE	1.828		
ASP21	H	8.395		
ASP21	HA	4.898	CA	48.103

ASP21	HB2	3.256	CB	39.101
ASP21	HB3	2.767	CG	168.940
SER22	H	8.640		
SER22	HA	5.250	CA	54.365
SER22	QB	3.784	CB	63.366
ASP23	H	8.315		
ASP23	HA	4.820	CA	48.298
ASP23	HB2	3.197	CB	39.297
ASP23	HB3	2.627	CG	168.256
THR24	H	8.534		
THR24	HA	5.113	CA	58.279
THR24	HB	3.979	CB	69.237
THR24	QG2	1.124	CG	19.141
ASP25	H	8.532		
ASP25	HA	4.742	CA	unresolved
ASP25	HB2	3.175	CB	39.297
ASP25	HB3	2.571	CG	168.060
HIS26	H	8.558		
HIS26	HA	5.270	CA	52.799
HIS26	HB2	3.164	CB	28.730
HIS26	HB3	2.884		
ARG27	H	8.671		
ARG27	HA	4.507	CA	52.212
ARG27	QB	1.476	CB	30.099
ARG27	HG2	1.261	CG	23.904
ARG27	HG3	1.320		
ARG27	QD	3.001	CD	40.462
ARG27	HE	7.013		
GLU28	H	8.580		
GLU28	HA	4.585	CA	53.191
GLU28	HB2	1.887	CB	26.381
GLU28	HB3	1.945		
GLU28	QG	2.395	CG	30.099
ASP29	H	8.293		
ASP29	HA	4.527	CA	54.952
ASP29	HB2	3.119	CB	38.318
ASP29	HB3	2.610	CG	169.918

Table S7: Key proton chemical shifts of ω-ester linkages of other graspetides.

	Asp β or Glu γ protons			Ser or Thr β protons		
Fuscimiditide[7]	ASP-18	2.734	3.165	THR-3	5.271	
	ASP-22	2.518	3.067	THR-7	5.096	
Marinostatin[8]	ASP-9	3.03		THR-3	5.57	
	ASP-11	2.69	2.76	SER-8	4.31	4.97
Microviridin 1777[9]	ASP-10	2.63	2.77	THR-4	5.33	
	GLU-12	1.33	2.08	SER-9	4.2	4.54
Marinomonasin[10]	ASP-14	2.88	3.29	THR-4	5.34	
Microviridin J[11]	ASP-10	2.59	2.68	THR-4	5.34	
	GLU-12	1.3	2.05	SER-9	4.12	
Thatisin[12]	ASP-13	2.61	2.68	THR-5	5.05	
	ASP-17	2.78	3.16	THR-8	4.42	
BMRB average*	ASP	2.666	2.716	SER	3.844	3.868
	GLU	2.246	2.264	THR	4.169	

* The average chemical shift values reported in BMRB, Jul. 7, 2022

Table S8: Vicinal amide-alpha proton $^{3}J_{HN\alpha}$ coupling constants

Residue	**$^{3}J_{HN\alpha}$ (Hz)**
ASP-3	7.71
THR-6	9.67
ASN-7	8.80
VAL-9	7.84
THR-10	9.79
ASP-11	7.60
ARG-16	5.09
TYR-17	7.71
THR-18	7.34
ASN-19	6.96
ASP-21	9.15
ASP-23	8.21
THR-24	7.65
ARG-27	8.38
ASP-29	8.51

Table S9: MS/MS on the hydrazinolyzed core peptide with one hydrazide adduct

ions	error (ppm)	charge	number of hydrazide adducts
b_2	-7.5	1	0
b_3	-0.2	1	0
b_5	1.7	1	0
b_6	-2.1	1	0
b_7	-1.2	1	0
b_8	6.5	2	0
b_{23}	4.7	4	1
y_{23}	0.6	3	1
y_{22}	0.2	3	1
y_{21}	-1.6	3	1
y_{20}	-1.2	3	1
y_{19}	0.4	3	1
y_{18}	-2.7	3	1
y_{15}	-5.1	3	1
y_8	-4.0	1	0
y_6	-0.5	1	0
y_4	-3.6	1	0

Table S10: MS/MS on the hydrazinolyzed core peptide with two hydrazide adducts

ions	error (ppm)	charge	number of hydrazide adducts
b_2	-4.2	1	0
b_4	2.6	1	0
b_5	-1.0	1	0
b_6	-1.7	1	0
b_7	-1.1	1	0
b_8	-0.8	1	0
b_8	1.4	2	0
b_{23}	-1.5	4	2
y_{23}	-3.3	3	2
y_{22}	-4.1	3	2
y_{21}	-3.3	3	2
y_{20}	0.3	3	2
y_{19}	-5.0	3	2
y_{18}	-2.6	3	2
y_{15}	1.0	3	2
y_8	0.1	1	1
y_6	-1.3	1	0
y_4	0.0	1	0

Table S11: MS/MS on the hydrazinolyzed core peptide with three hydrazide adducts

ions	error (ppm)	charge	number of hydrazide adducts
b_3	-2	1	0
b_5	-5.4	1	0
b_6	-6.4	2	0
b_7	-12.9	1	0
b_8	-9.9	1	0
b_8	2.1	2	0
b_9	0.2	1	0
b_{10}	10.2	1	0
y_{23}	-6.1	3	3
y_{20}	-5.5	3	3
y_{18}	-3.4	3	3
y_8	0.9	1	2
y_4	-4.8	1	0

Table S12: MS/MS on the hydrazinolyzed II-null variant core peptide

ions	error (ppm)	charge	number of hydrazide adducts
b_2	-7.1	1	0
b_3	-10.8	1	0
b_5	-3.7	1	0
b_6	-5.5	1	0
b_7	-6.0	1	0
b_7	-8.9	2	0
b_8	-6.2	1	0
b_8	-4.4	2	0
b_9	-7.7	1	0
b_{11}	-8.6	1	0
b_{19}	-1.5	2	0
b_{20}	-6.4	2	0
b_{21}	-6.6	3	1
b_{22}	1.4	3	1
b_{25}	0.6	3	2
y_{28}	-8.1	3	3
y_{27}	-8.0	3	3
y_{26}	-12.6	3	3
y_{21}	-6.1	2	3
y_{21}	-5.9	3	3
y_{20}	-6.1	2	3
y_{20}	-8.3	3	3
y_{19}	-8.3	2	3
y_{18}	-8.8	2	3
y_{18}	-6.0	3	3
y_{15}	-7.8	2	3
y_{15}	-6.2	3	3
y_9	-7.5	1	3
y_9	-11.4	2	3
y_8	-7.9	1	2
y_8	-5.9	2	2
y_7	-11.9	1	2
y_5	-11.0	1	2
y_4	-6.4	1	1
y_3	-10.6	1	1

Table S13: MS/MS on the hydrazinolyzed III-null variant core peptide

ions	error (ppm)	charge	number of hydrazide adducts
b_2	-4.7	1	0
b_4	-1.0	1	0
b_5	-2.2	1	0
b_6	-2.6	1	0
b_6	-2.9	2	0
b_7	-2.7	1	0
b_7	-2.5	2	0
b_8	-2.5	1	0
b_8	-0.9	2	0
b_9	-5.2	1	0
b_9	-8.4	2	0
b_{10}	-0.7	2	0
b_{23}	-12.2	3	2
b_{25}	2.5	3	2
y_{24}	-7.3	3	2
y_{23}	-2.1	3	2
y_{23}	-7.0	4	2
y_{22}	-1.9	3	2
y_{21}	-1.7	3	2
y_{21}	-4.1	4	2
y_{20}	-3.9	2	2
y_{20}	-1.5	3	2
y_{20}	-1.1	4	2
y_{19}	-4.3	2	2
y_{19}	-1.5	3	2
y_{18}	-2.7	2	2
y_{18}	-1.1	3	2
y_{16}	3.6	3	2
y_{15}	-3.7	2	2
y_{15}	0.2	3	2
y_9	-4.6	1	2
y_9	-1.7	2	2
y_8	-2.9	1	1
y_8	-4.7	2	1
y_7	-3.9	1	1
y_6	-2.5	1	0
y_6	-1.1	2	0
y_5	11.3	1	0
y_5	-10.7	2	0
y_4	-3.9	1	0

Table S14: MS/MS on the hydrazinolyzed IV-null variant core peptide

ions	error (ppm)	charge	number of hydrazide adducts
b_2	-3.5	1	0
b_5	-0.7	1	0
b_7	-5.5	1	0
b_8	-0.4	1	0
b_8	-2.5	2	0
b_9	-0.9	1	0
b_{10}	-5.0	2	0
b_{11}	-8.3	1	0
b_{20}	-8.6	2	0
b_{21}	-5.5	3	1
b_{23}	5.5	3	2
b_{25}	-3.3	3	3
y_{28}	1.4	3	3
y_{27}	-2.4	3	3
y_{26}	11.4	3	3
y_{20}	-0.9	2	3
y_{20}	-8.1	3	3
y_{19}	-3.7	2	3
y_{18}	-6.7	2	3
y_{18}	-1.5	3	3
y_{15}	-2.9	2	3
y_{15}	-5.6	3	3
y_9	-14.7	2	3
y_8	-2.9	1	2
y_8	-1.5	2	2
y_6	-6.7	1	1
y_5	-4.0	1	1
y_4	-1.2	1	0

Table S15: MS/MS on the hydrazinolyzed II,III-null variant core peptide

ions	error (ppm)	charge	number of hydrazide adducts
b_2	-11.8	1	0
b_3	-1.8	1	0
b_5	-11.9	1	0
b_6	-13.8	1	0
b_7	-11.5	2	0
b_8	-11.5	1	0
b_8	-14.5	2	0
b_9	-13.5	1	0
b_{10}	-5.3	2	0
b_{14}	-12.8	1	0
y_{27}	-11.2	3	1
y_{26}	-12.4	3	1
y_{23}	-12.8	2	1
y_{21}	-10.1	3	1
y_{20}	-14.9	2	1
y_{19}	-10.3	2	1
y_{18}	-13.6	2	1
y_{17}	-12.6	2	1
y_{10}	-11.5	2	1
y_9	-9.8	1	1
y_9	-10.4	2	1
y_8	-11.6	1	0
y_7	-12.0	1	0
y_5	-12.0	1	0
y_3	-13.8	1	0

Table S16: MS/MS on the hydrazinolyzed II,IV-null variant core peptide

ions	error (ppm)	charge	number of hydrazide adducts
b_2	-1.8	1	0
b_3	-0.9	1	0
b_4	-2.1	1	0
b_5	-0.9	1	0
b_5	-6.2	2	0
b_6	-1.7	1	0
b_6	-1.5	2	0
b_7	-0.9	1	0
b_7	-0.6	2	0
b_8	-0.8	1	0
b_8	3.0	2	0
b_9	-4.9	1	0
b_9	-0.9	2	0
b_{10}	-2.1	2	0
y_{24}	-3.6	3	2
y_{23}	-1.4	3	2
y_{22}	-2.7	3	2
y_{21}	-1.6	3	2
y_{21}	-0.5	4	2
y_{20}	-3.5	2	2
y_{20}	-1.9	3	2
y_{20}	-3.4	4	2
y_{19}	-1.7	2	2
y_{19}	-2.4	3	2
y_{18}	-1.7	2	2
y_{18}	-1.6	3	2
y_{17}	-2.9	3	2
y_{15}	-3.1	2	2
y_{15}	-3.6	3	2
y_9	-2.5	1	2
y_9	-5.7	2	2
y_8	-2.4	1	1
y_8	0.3	2	1
y_7	0.5	1	1
y_6	-3.7	1	1
y_5	-5.5	1	1
y_4	-2.2	1	0
y_3	-7.1	1	0

References for Supplemental Information

1. Crooks, G. E.; Hon, G.; Chandonia, J. M.; Brenner, S. E., WebLogo: a sequence logo generator. *Genome Res* **2004,** *14* (6), 1188-90.
2. Apostol, I.; Aitken, J.; Levine, J.; Lippincott, J.; Davidson, J. S.; Abbott-Brown, D., Recombinant protein sequences can trigger methylation of N-terminal amino acids in Escherichia coli. *Protein Sci* **1995,** *4* (12), 2616-8.
3. Butt, T. R.; Edavettal, S. C.; Hall, J. P.; Mattern, M. R., SUMO fusion technology for difficult-to-express proteins. *Protein Expr Purif* **2005,** *43* (1), 1-9.
4. Hirel, P. H.; Schmitter, M. J.; Dessen, P.; Fayat, G.; Blanquet, S., Extent of N-terminal methionine excision from Escherichia coli proteins is governed by the side-chain length of the penultimate amino acid. *Proc Natl Acad Sci U S A* **1989,** *86* (21), 8247-51.
5. Cheung-Lee, W. L.; Cao, L.; Link, A. J., Pandonodin: A Proteobacterial Lasso Peptide with an Exceptionally Long C-Terminal Tail. *ACS Chem Biol* **2019,** *14* (12), 2783-2792.
6. Lee, M. E.; DeLoache, W. C.; Cervantes, B.; Dueber, J. E., A Highly Characterized Yeast Toolkit for Modular, Multipart Assembly. *ACS Synth Biol* **2015,** *4* (9), 975-86.
7. Elashal, H. E.; Koos, J. D.; Cheung-Lee, W. L.; Choi, B.; Cao, L.; Richardson, M. A.; White, H. L.; Link, A. J., Update CITATION. **2021**.
8. Kanaori, K.; Kamei, K.; Taniguchi, M.; Koyama, T.; Yasui, T.; Takano, R.; Imada, C.; Tajima, K.; Hara, S., Solution structure of marinostatin, a natural ester-linked protein protease inhibitor. *Biochemistry* **2005,** *44* (7), 2462-8.
9. Sieber, S.; Grendelmeier, S. M.; Harris, L. A.; Mitchell, D. A.; Gademann, K., Microviridin 1777: A Toxic Chymotrypsin Inhibitor Discovered by a Metabologenomic Approach. *J Nat Prod* **2020,** *83* (2), 438-446.
10. Kaweewan, I.; Nakagawa, H.; Kodani, S., Heterologous expression of a cryptic gene cluster from Marinomonas fungiae affords a novel tricyclic peptide marinomonasin. *Appl Microbiol Biotechnol* **2021,** *105* (19), 7241-7250.
11. Rohrlack, T.; Christoffersen, K.; Hansen, P. E.; Zhang, W.; Czarnecki, O.; Henning, M.; Fastner, J.; Erhard, M.; Neilan, B. A.; Kaebernick, M., Isolation, characterization, and quantitative analysis of Microviridin J, a new Microcystis metabolite toxic to Daphnia. *J Chem Ecol* **2003,** *29* (8), 1757-70.
12. Ramesh, S.; Guo, X.; DiCaprio, A. J.; De Lio, A. M.; Harris, L. A.; Kille, B. L.; Pogorelov, T. V.; Mitchell, D. A., Bioinformatics-Guided Expansion and Discovery of Graspetides. *ACS Chem Biol* **2021,** *16* (12), 2787-2797.